Impacts of Coherent Crosstalk on the Performance and Scalability of WDM AONs

by

Can Emre Koksal

B.S., Middle East Technical University (1996)

Submitted to the Department of Electrical Engineering and Computer Science
in partial fulfillment of the requirements for the degree of

Master of Science in Electrical Engineering and Computer Science

at the

MASSACHUSETTS INSTITUTE OF TECHNOLOGY

May 1998

Signature of Author .....
Department of Electrical Engineering and Computer Science
May 13, 1998

Certified by .....
Dr. Richard A. Barry
MIT Lincoln Laboratory
Thesis Supervisor

Accepted by .....
Professor Arthur C. Smith
Chairman, Department Committee on Graduate Students

Impacts of Coherent Crosstalk on the Performance and Scalability of WDM AONs

by

Can Emre Koksal

Submitted to the Department of Electrical Engineering and Computer Science
on May 13, 1998, in partial fulfillment of the
requirements for the degree of
Master of Science in Electrical Engineering and Computer Science

Abstract

The scalability of Wavelength Division Multiplexed All Optical Networks (WDM AONs) is intimately linked to the way optical signals interact with the physical network and the overall network architecture and protocols. The physical interaction can lead to degradation of signal quality. There are multiple causes of signal degradation that occur as optical signals propagate between two users in a WDM-AON, an important one of which is crosstalk. In previous research, the analysis of crosstalk was developed employing Gaussian and worst case assumptions for the interference portion of the detected signal. Furthermore, the crosstalk-crosstalk beat which occurs due to the square-law nature of the optical detector was neglected and the interferers were assumed to be at the same rate and synchronous with the signal. This thesis presents rigorous crosstalk analysis techniques starting from a worst case approach for one interferer, to more general cases which account for the rate differences of the signal and the crosstalk, the asynchronousness of their bit slots and the randomnesses of their phases and polarizations. In each step, the error probability of the optimum detector is evaluated. The impact of the AC-coupled decision thresholding on the performance is also investigated for some cases. Finally, an accurate analysis is performed for multiple crosstalk sources employing an MMSE estimation for the crosstalk-crosstalk beat terms and the tightest Chernoff bound for the error probability. The error probability curves for three practical examples are illustrated, including a system using a Lucent Waveguide Grating Router (WGR) whose specifications were experimentally determined. Furthermore, the validity of the Gaussian approximation and the neglection of crosstalk-crosstalk beat terms are argued and the regions of system parameters which make these assumptions valid are illustrated.

Thesis Supervisor: Dr. Richard A. Barry
Title: Staff, MIT Lincoln Laboratory

Acknowledgments

I feel very fortunate to have Dr. Rick Barry as my thesis advisor. I am deeply thankful to him for his incredible guidance, support and patience throughout this work. His clarity of thought, deep knowledge, enthusiasm for his work and his commitment to excellence was a great inspiration and will always set an example for me throughout my life.

I am also grateful to Professor Robert Gallager for providing invaluable help and advice. This work would be impossible without his support, teachings and intellectual inspiration.

I would like to thank Dr. Roe Hemenway for letting me use the AON Laboratory and his invaluable help and advice on the experimental part of this work. I also thank Lori Jeromin and Mark Stevens for many stimulating, helpful discussions and Paul Green for letting me use his images.

I greatly appreciate the support I have received from the U.S. Government, through U.S. Army Research Office of Sponsored Research grant DAAH04-95-1-0103.

Finally, I am deeply grateful to my lovely wife Asu, for always being there for me, her patient support and encouragement. I would like to thank all my family members for their support, love and for always believing in me.

Contents

List of Figures

List of Tables

Chapter 1

Introduction

The explosive growth of telecommunications and computer communications has placed increasing demand on the global communications infrastructure. A global research effort is currently underway to determine if Wavelength Division Multiplexed All-Optical Fiber Optic Networks (WDM-AONs) can meet these needs.

Wavelength division multiplexing (WDM) allows multiple users to share a fiber optic link or network in a manner similar to radio communications. WDM takes advantage of the tremendous bandwidth of optical fibers, which is on the order of 25,000 GHz. In practice, the usable bandwidth in a fiber link or network is lower than 25 THz and is determined by a complex interplay between the components and devices and the link or network architecture. In a WDM transmission link, different wavelengths (λ_1, λ_2, . . ., λ_N) are combined at the input of an optical fiber and separated at the fiber output, with each wavelength carrying different information. Wavelengths are combined and separated using wavelength division multiplexers/demultiplexers. An important quality of a WDM link is that multiple optical channels are transmitted together and amplified simultaneously and are then converted to electronic signals only at the link output.

WDM-AONs establish communication paths between different users and each path appears as a point-to-point WDM link without optoelectronic regeneration at the nodes. The term "all-optical" comes from the fact that the transmitted data remains as an

optical signal throughout the network. Access to the network and connections within the network are achieved by "adding," "dropping" and "routing" wavelengths at each node.

The scalability of a WDM-AON is intimately linked to the way optical signals interact with the physical network and the overall network architecture and protocols. The physical interaction can lead to degradation of signal quality. There are multiple causes of signal degradation that occur as optical signals propagate between two users in a WDM-AON including signal attenuation, crosstalk, signal distortion and noise accumulation. These effects reduce the signal-to-noise ratio (SNR) at a photoreceiver, resulting in bit errors in digital systems or distortion in analog systems.

The rest of this chapter contains four sections. Basic definitions on crosstalk, the mechanisms of it and the network structure is presented together with a practical example of a wavelength router in Background section. The following section illustrates the possible models for crosstalk and the receiver which will be used throughout the thesis. The third section reviews the past work on crosstalk analysis and discusses their weaknesses which motivate this work. In the final section, the following chapters are briefly introduced.

1.1 Background

1.1.1 Crosstalk Mechanism

Crosstalk is the leakage of light from one received wavelength channel to another. It is especially important in WDM-AONs due to the cascading of multiple fiber links, optical amplifiers and network nodes over any given path. Crosstalk can be classified as linear and nonlinear depending on how it is generated.

Linear crosstalk can be caused by leakage of unwanted optical power from same or adjacent wavelengths through an optical filter, multiplexer/demultiplexer, photonic switch, or an add/drop element. Intersymbol interference is another kind of linear crosstalk which occurs between time slots in digital systems due to fiber dispersion.

Nonlinear crosstalk can occur between multiple wavelength channels through optical nonlinearities in optical fiber or in optical amplifiers since new optical frequencies can be generated that coincide with the desired signal wavelength. Nonlinear crosstalk is much worse in cascaded fiber/amplifier chains.

Crosstalk can be further classified as coherent or incoherent, depending on its wavelength relative to that of the desired signal. If linearly or non-linearly generated interference is at the same wavelength with the signal, this is referred to as coherent crosstalk; if it does not coincide with that of the desired signal, this is referred to as incoherent crosstalk.

Once the signal is detected at the photoreceiver, power from wavelengths at or other than the desired channel that pass through the optical filter will be converted to an electrical crosstalk signal which is then filtered electrically. Typically, the receiver electrical bandwidth is much narrower than the spacing between the desired channel and neighboring channels, only a little portion of which remains at the output of the optical filter (-30 - 35 dB for a typical optical filter). Thus, the signal-incoherent crosstalk beating is filtered out. However, the electrical filter cannot reject the interference components which are at the same wavelength as the desired channel since the signal-coherent crosstalk beating is within the electrical bandwidth. Therefore, coherent crosstalk can be much more severe than incoherent crosstalk because it beats with the strong signal. We will deal with the impacts of coherent crosstalk throughout the thesis. Note that, in practice the lasers that transmit at the same channel may have a difference between their resonant frequencies. Furthermore, lasers have non-zero linewidths. The signal and crosstalk spectrum has a bandwidth of the order of sum of the laser linewidths and modulation bandwidth. In this thesis, we assume that the bandwidth of the electrical receive filter is much wider than the frequency difference of the lasers which transmit on the same channel.

To make the definitions clear, an illustration is given in Figure 1.1. There are three channels. The desired channel is at optical frequency f_c. The other two channels are at $f_{incoh,1}$ and $f_{incoh,2}$ where the subscripts stand for incoherent. There are three lasers

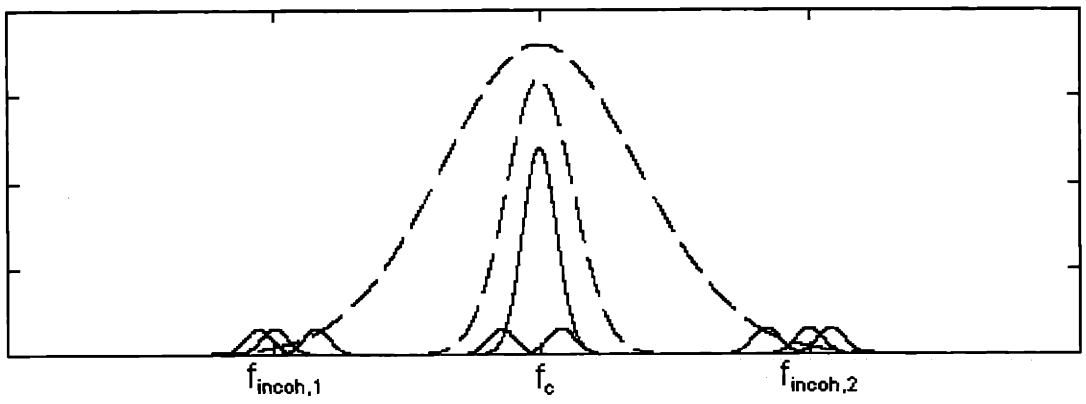

Figure 1-1: The detected frequency spectrum is shown by the solid curves. The wide and the narrow dashed curves illustrate the optical and the electrical filters respectively. The big solid curve centered at f_c is the communication signal and the other solid curves are the crosstalk components. Note that the difference between the center frequency of a signal and a coherent component is less than the electrical bandwidth whereas, that between the signal and an incoherent component is much wider than the electrical bandwidth.

transmitting at each wavelength. The optical filter at the receiver input rejects most of the incoherent crosstalk, and the signal-incoherent crosstalk beat is centered at a frequency which is outside the electrical baseband. There is a difference between the center frequencies of the lasers that transmit on the same channel and the lasers have non-zero linewidths. Most of the coherent crosstalk cannot be rejected by the electrical filter though, because for a high speed transmission, the filter should have a bandwidth large enough to cover the signal-crosstalk beat frequencies.

There may be nonlinearly generated interference components due to the nonlinearities in the fiber, optical amplifiers, etc. Nonlinear crosstalk might be severe if its center frequency is close to that of the signal (i.e., the signal-nonlinear crosstalk beating is in the electrical baseband). Such a case is illustrated in figure 1.2 where the non-linearly generated components are centered at $f_{n,1}$ and $f_{n,2}$.

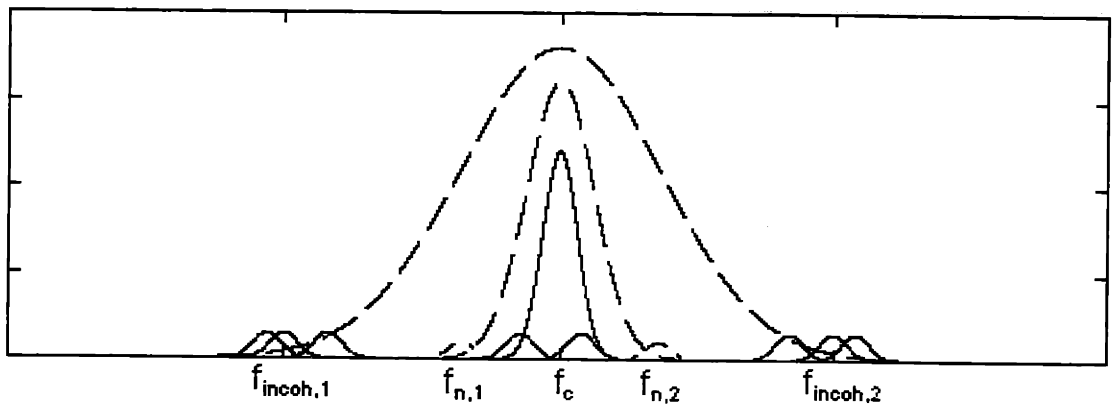

Figure 1-2: There are nonlinear components (small dashed curves located near the tails of the electrical filter) located at frequencies $f_{n,1}$ and $f_{n,2}$.

1.1.2 Network Crosstalk

Network Structure

In a WDM-AON there may be more than two nodes communicating using the same wavelength. This is called wavelength reuse and Figure 1.3 illustrates such a network.

Each node has N transmitters and N receivers that are tuned to different wavelengths (i.e., $\lambda_1, \lambda_2, \ldots, \lambda_N$). Communication between a transmitter and a receiver is handled by the Network Router which has N^2 internal connections to connect N input ports to N output ports. Thus there are N^2 distinct transmission functions one can observe corresponding to all input-output port pairs. The peak locations of the functions are shown on the routing table of the router. A typical routing table is shown in Table 1.1 and Figure 1.4 illustrates the paths that a signal at λ_1 follows when it is inserted from different input ports.

Every node has a multi-wavelength transmitter (N light sources and a multiplexer) and the corresponding receiver (a demultiplexer and N detectors) as shown in Figure 1.5.

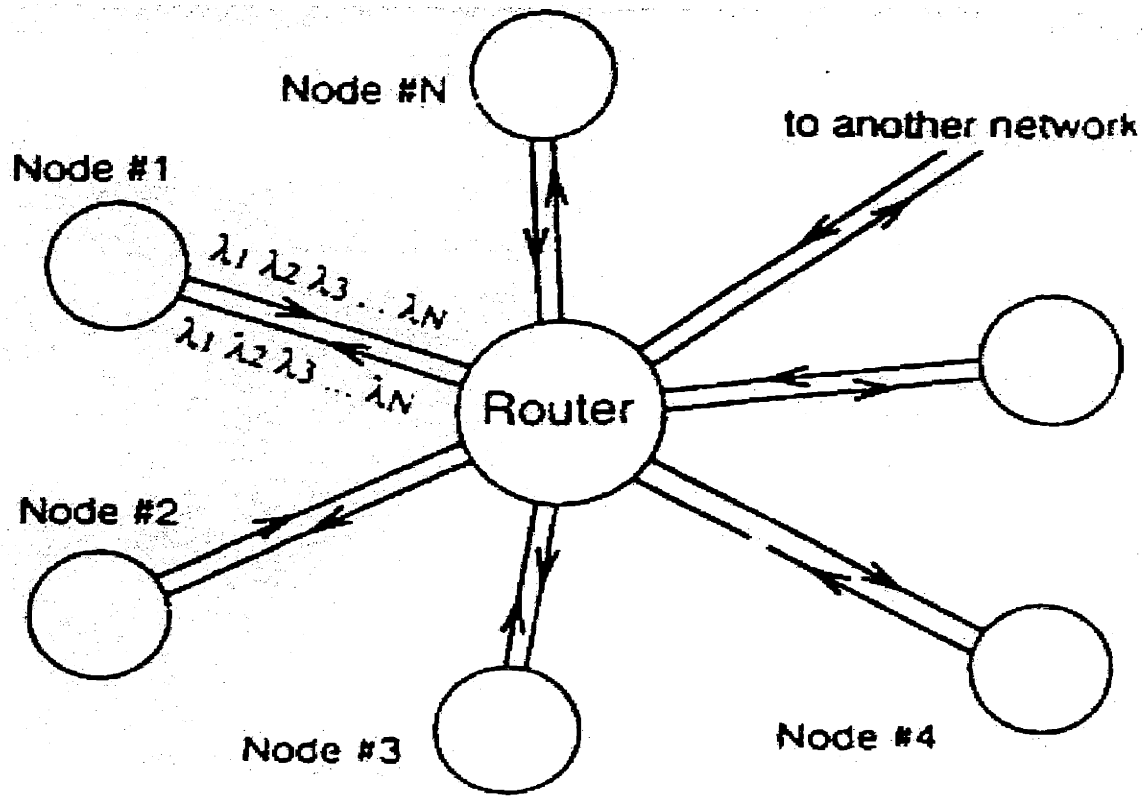

Figure 1-3: A WDM-AON with N nodes

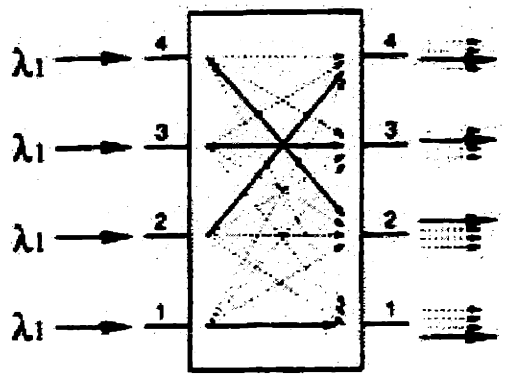

Figure 1-4: Signal on the first channel is routed differently depending on which input port it is inserted.

↓Output / Input→	1	2	3	4	. . .	N-1	N
1	λ_1	λ_2	λ_3	λ_4	. . .	λ_{N-1}	λ_N
2	λ_2	λ_3	λ_4	λ_5	. . .	λ_N	λ_1
3	λ_3	λ_4	λ_5	λ_6	. . .	λ_1	λ_2
4	λ_4	λ_5	λ_6	λ_7	. . .	λ_2	λ_3
⋮	⋮	⋮	⋮	⋮	⋱	⋮	⋮
N-1	λ_{N-1}	λ_N	λ_1	λ_2	. . .	λ_{N-3}	λ_{N-2}
N	λ_N	λ_1	λ_2	λ_3	. . .	λ_{N-2}	λ_{N-1}

Table 1.1: Routing table of a wavelength router. The entry i, j represents the wavelength at which j^{th} input port communicates with the i^{th} output port.

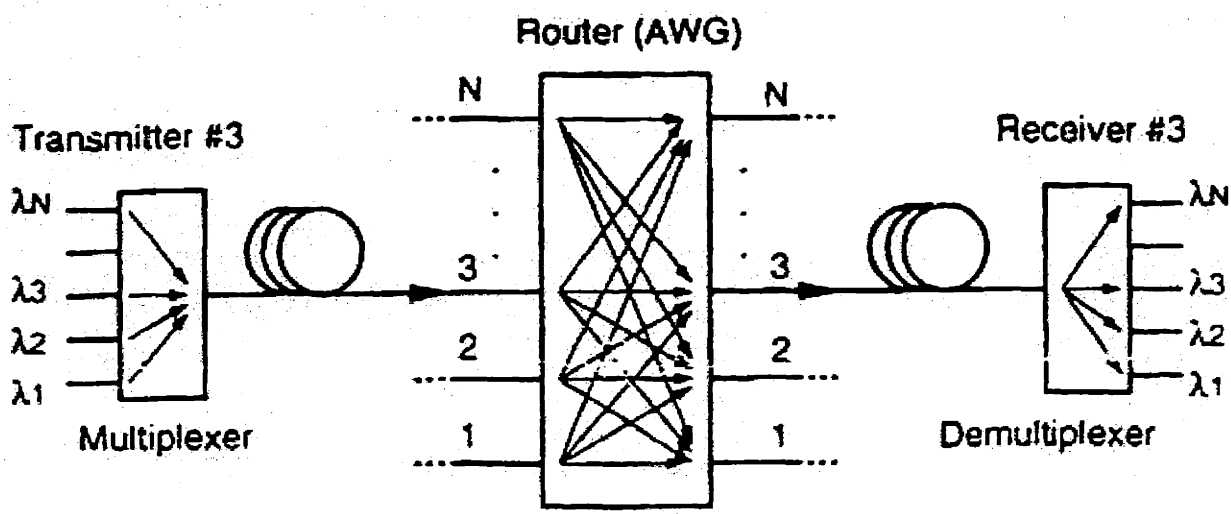

Figure 1-5: Every node has N trancievers tuned to N different channels.

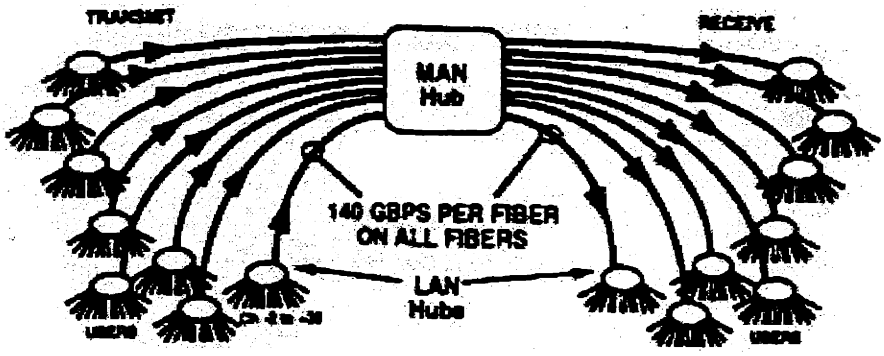

Figure 1-6: AON LAN and MAN hierarchy. Odd numbered channels remain local to each LAN, and are re-used in every LAN domain. Even numbered channel interconnect LANs at the MAN hub. MAN frequencies are re-used 8 times within the MAN domain.

The ATT/DEC/MIT AON test-bed [3] uses two levels of passive wavelength routing to partition the networks into multiple area domains which are local area subnetworks (L-0's) and metro-area networks (L-1's) [1], [2]. It is illustrated in Figure 1.6.

Standard AON channels are separated by 50 GHz and enumerated with integers starting from 0 at 1561.5 nm, increasing by 1 with increasing frequency.

In the L-0 hubs, the odd numbered channels are confined to the L-0 domain, so that they can be re-used within other L-0 domains. L-0's communicate with each other by means of the L-1 hub using even numbered channels which are spaced by 100 GHz. There, a second level of wavelength routing takes place utilizing an $N \times N$ Arrayed Waveguide Grating Router. This allows frequencies to be re-used within the L-1 hub up to N times.

Arrayed Waveguide Grating Router (AWGR)

This section will evolve to crosstalk in WGRs starting from the WGR operation. Although WGR's are not the only crosstalk source in AONs, it is useful to understand the crosstalk in WGR to figure out the mechanism of crosstalk.

AWGR Operation Waveguide Grating Router is a key component for multi-wavelength cross-connects. The operation of the router [3] is illustrated schematically in Figure 1.7.

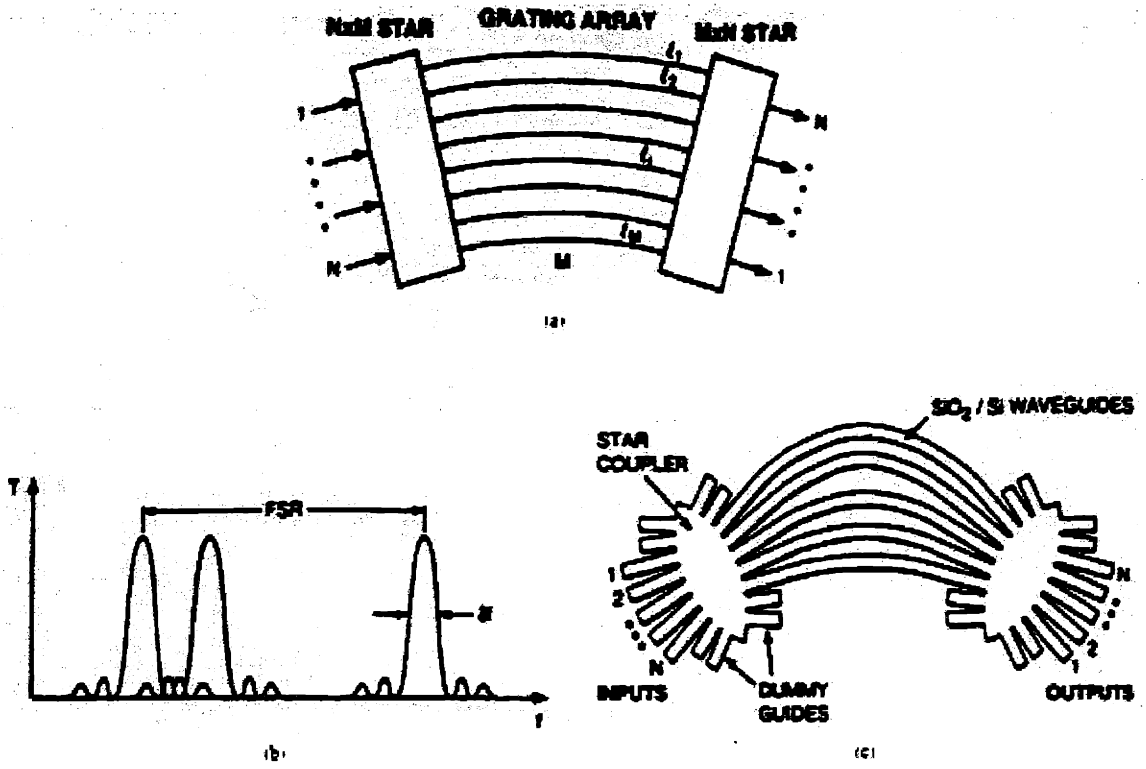

Figure 1-7: Waveguide Grating Router (a) schematic and (b) transmission through adjacent inputs and (c) mask pattern

There are two identical $M \times M$ star couplers which are connected by M waveguides. N input optical waveguides enter the first star coupler, where $M \geq N$ so that a fraction of the inputs may not be connected. The signal from any of the N input ports is diffracted and distributed over the M outputs of the first star coupler and hence to the M waveguides, whose lengths progressively decrease by a fixed amount ($\Delta l = l_i - l_{i+1}$). Thus there occurs a progressive phase delay between adjacent waveguides, $\Delta\phi = \frac{2\pi f \cdot \Delta l \cdot n}{c}$. Therefore, as f increases by $\frac{c}{\Delta l \cdot n}$, ϕ increases by 2π which means that the same response is observed every $\frac{c}{\Delta l \cdot n}$ Hz. This period is called free spectral range (FSR).

$$FSR = \frac{c}{\Delta l \cdot n} \tag{1.1}$$

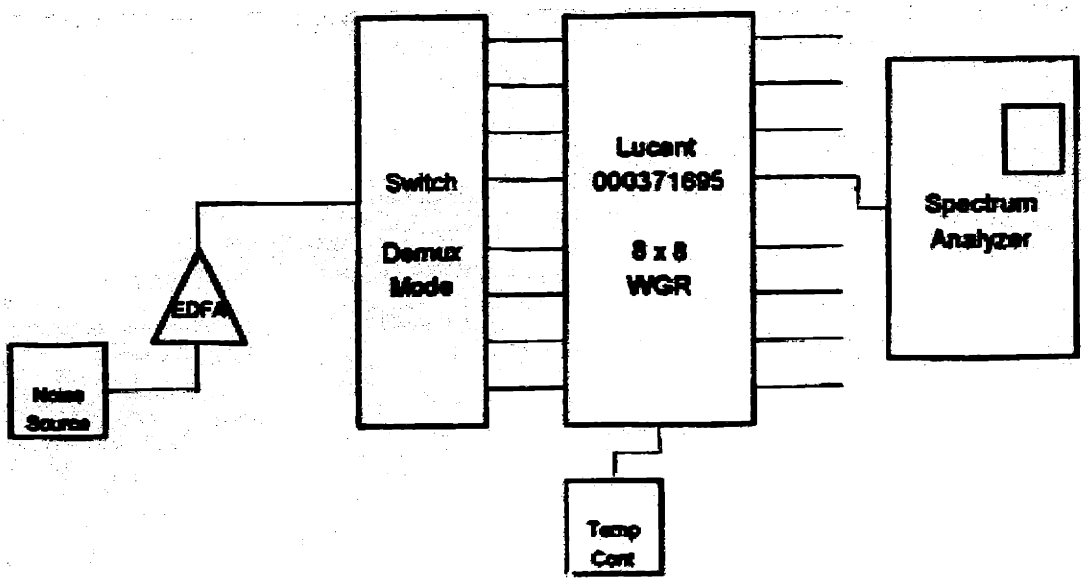

Figure 1-8: This setup is constructed to calculate the transmission function of the router for the selected input and output ports.

The refractive index of the silica substrate is dependent on the temperature, thus so are the free spectral range and transmission peaks.

Lucent 000371695 WGR The Lucent 000371695 is an 8x8 wavelength router. We constructed some experimental setups with Lucent 000371695 to find its specifications and the amount of crosstalk introduced by it.

First, we evaluate the transmission function of the router for some input output couples. We used a white light source to stimulate the entire spectrum and an Erbium Doped Fiber Amplifier to amplify the source to emit sufficient power. The rest of the connections are as shown in Figure 1.8.

We observed a 5 dB lower response than we had with the same setup when the router is disconnected. Therefore the insertion loss of the router is 5 dB.

Some typical responses are as shown in Figures 1.9, 1.10. The data correspond to input port 2, output port 4 as labelled on the graphs. We can observe from Figure 1.10

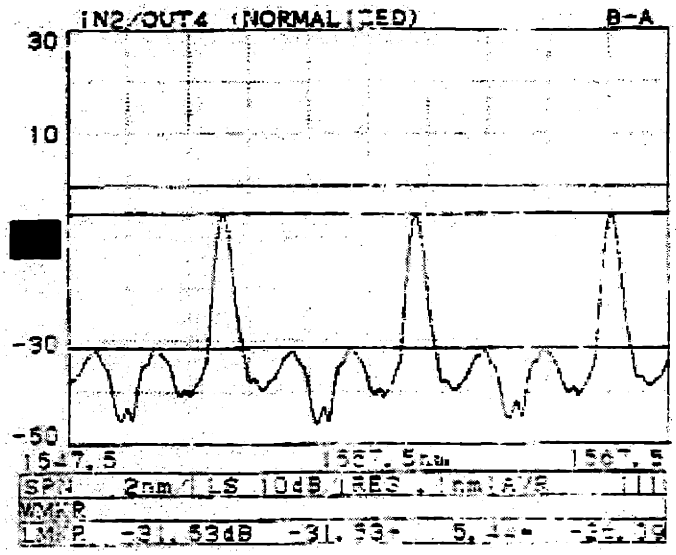

Figure 1-9: Input port 2 and output port 4 is connected. The main peaks are 26.09 dB higher than the neighbor peaks.

that the router supports many free spectral ranges. The FSR is 800 GHz. When carefully examined, it can be observed that there are seven peaks in between the two main peaks which are separated by 100 GHz. These peaks are the even numbered standard AON channels. The routing table at 92.5°C is given in table 2 where the entries indicate the standard AON channel that the input-output port pair supports.

↓ Output/Input →	1	2	3	4	5	6	7	8
1	18, 2	16, 0	14, -2	12, -4	10, -6	8, 24	6, 22	4, 20
2	4, 20	18, 2	16, 0	14, -2	12, -4	10, -6	8, 24	6, 22
3	6, 22	4, 20	18, 2	16, 0	14, -2	12, -4	10, -6	8, 24
4	8, 24	6, 22	4, 20	18, 2	16, 0	14, -2	12, -4	10, -6
5	10, -6	8, 24	6, 22	4, 20	18, 2	16, 0	14, -2	12, -4
6	12, -4	10, -6	8, 24	6, 22	4, 20	18, 2	16, 0	14, -2
7	14, -2	12, -4	10, -6	8, 24	6, 22	4, 20	18, 2	16, 0
8	16, 0	14, -2	12, -4	10, -6	8, 24	6, 22	4, 20	18, 2

Table 1.2: The routing table of the Lucent 000371695 WGR at the specified conditions.

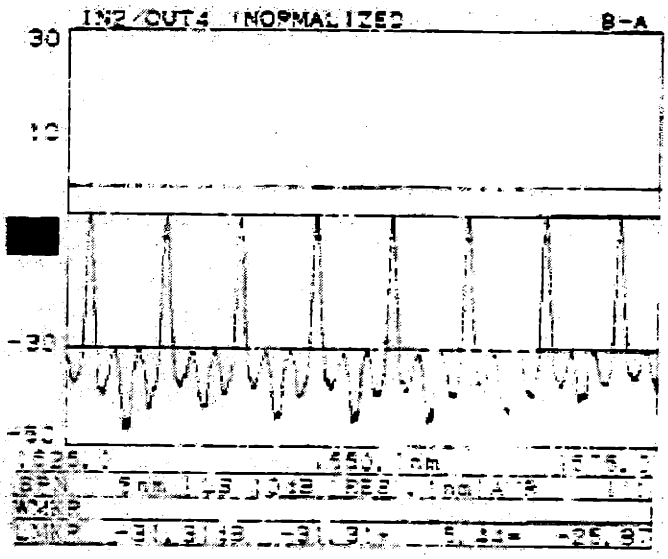

Figure 1-10: Input port 2 and output port 4 is connected. This time a larger frequency span is adjusted. Many FSRs are supported.

Crosstalk in AWGRs As explained in section 2.1, there occurs an N-fold frequency re-use within the L-1 hub by the help of the WGR. For instance for Lucent 000371695, at 92.5°C, the connection between input port 3 and output port 5 is achieved at channel 6. The same router handles the communication between nodes 2 and 4 at the same channel, and nodes 2 and 3 at the neighboring wavelength 4. However 100% of the input port power could not be coupled to the output port due to the insertion loss and leakage of the signal to other output ports. We defined this as coherent or incoherent crosstalk depending on the channel of the leakage.

It is important to know what percent of the input power leaks to the other ports in a router. To find out, we constructed the experimental setup shown in Figure 1.11.

Having the laser adjusted to the required channel, we choose the input port by means of the demultiplexer. After that, we connect the spectrum analyzer to the output port whose crosstalk is to be investigated. On the same graph, we sketch the observed spectrum at the output port as we connect the same channel to different input ports. Figures 1.12 and 1.13 are the observed responses for different output ports at channel 12. The

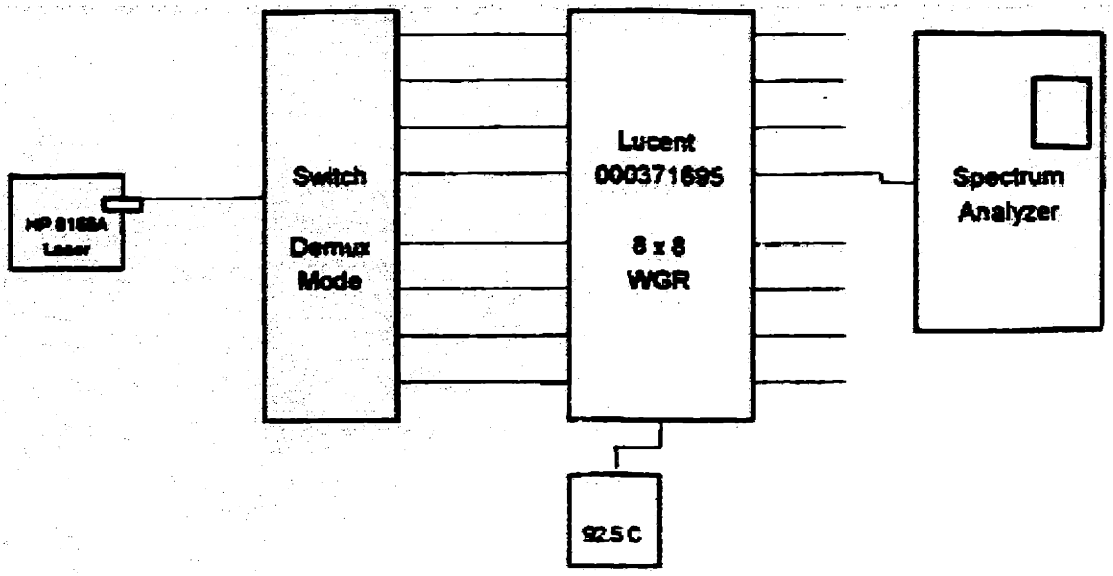

Figure 1-11: This setup is constructed to simulate the coherent crosstalk. All the input ports are switched one by one and all the outputs are sketched on one graph.

output port and the channel are labelled on the graphs.

These figures illustrate the coherent crosstalk. The main peak is the desired communication signal. There are 7 other peaks under the main peak which are the signals at the same channel that leak from other input ports. As there are 8 input ports, there are 7 such signals and the strongest one is 27 dB lower than the main communication signal on the average. This quantity is labelled at the bottom of the graphs on the right. The peak communication signal power can be seen on the left. These 7 interference signals have an aggregate average power of 23 dB lower than the communication signal.

Finally, keeping the same setup, we changed the laser wavelength for an input port, output port pair. All the data is sketched on the same graph so that we can observe the incoherent crosstalk as shown in Figure 1.14. From the figure, the peak incoherent interference is about -26 dB; therefore we can conclude that the incoherent crosstalk is as severe as the coherent at the output of the router.

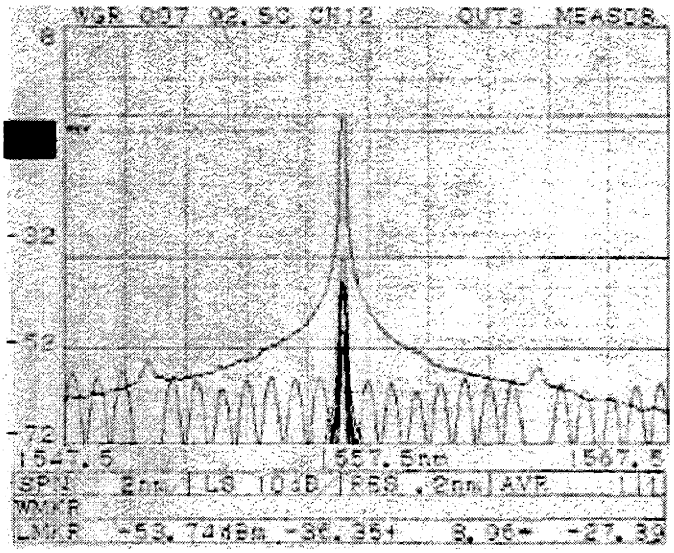

Figure 1-12: Output port 3 is connected. At channel 12, the peak coherent crosstalk is -27.39 dB.

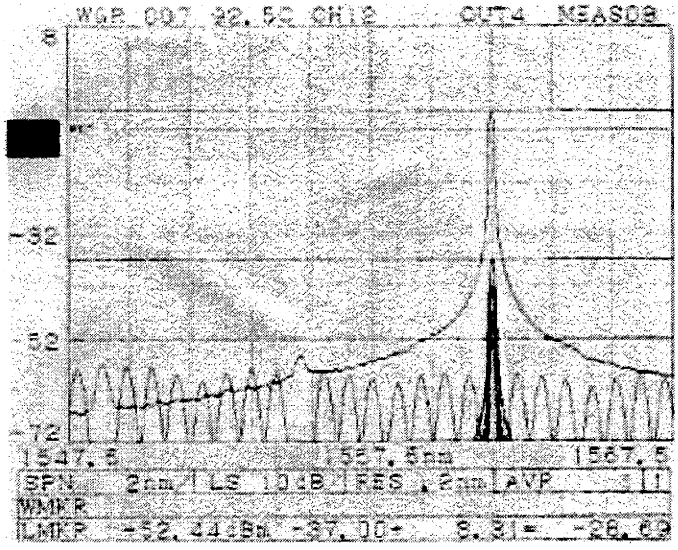

Figure 1-13: Output port 4 is connected. At channel 12, the peak coherent crosstalk is -28.69 dB.

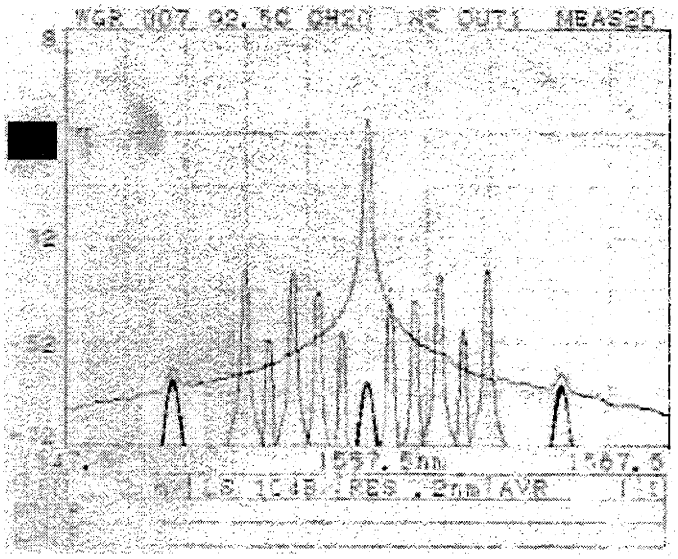

Figure 1-14: The incoherent crosstalk peaks are 27 lower than the signal on the average.

1.2 System Model

1.2.1 Crosstalk Model

In an AON, an optical signal is converted to electronics only at the link output. It remains optical (i.e., electromagnetic wave) until it is detected; therefore, we have to focus on the electric field at the input of the detector. This field is composed of both the desired signal and the signals that coherently or incoherently couple to it. Our model shall contain only the coherent crosstalk since its effects are more severe.

Definition 1 *If there are $N-1$ coherent intruders at the channel centered at the optical frequency f_c, the detected field will be*

$$\mathbf{E}_{\text{det}} = E_s(t) \begin{bmatrix} \cos[\theta_s(t)] \cos[2\pi f_c t + \phi_s(t)] \\ \sin[\theta_s(t)] \cos[2\pi f_c t + \phi_s(t) + \Psi_s(t)] \end{bmatrix}$$

$$+\sum_{i=1}^{N-1} E_{xi}(t) \begin{bmatrix} \cos\left[\theta_{xi}(t)\right] \cos\left[2\pi f_c t + \phi_{xi}(t)\right] \\ \sin\left[\theta_{xi}(t)\right] \cos\left[2\pi f_c t + \phi_{xi}(t) + \Psi_{xi}(t)\right] \end{bmatrix} \tag{1.2}$$

where $E_s(t)$ and $E_{xi}(t)$ are the amplitudes and $\phi_s(t)$, $\phi_{xi}(t)$ are the optical phases of the signal field and i^{th} crosstalk component field respectively [9]. The optical phases are assumed random and uniformly distributed in $(0, 2\pi)$ with fluctuations that are rapid ($\sim$MHz) compared with the slow ($\sim$Hz) fluctuation in the polarization states of the signal and crosstalk which are specified by $\Psi_s(t)$, $\theta_s(t)$ and $\Psi_{xi}(t)$, $\theta_{xi}(t)$ respectively. However even a fluctuation of the order of MHz is small compared to the bit rate, thus one can assume phases and polarizations remain constant within a bit time. Ψ and θ are uniformly distributed in $(0, 2\pi)$ as well. Some insight in these polarization parameters can be obtained by considering some special cases.

For example when $\Psi_s(t)$ and $\Psi_{xi}(t) = 0$ or $\pm\pi$, signal and i^{th} crosstalk component field are linearly polarized. When $\Psi_s(t) = \frac{\pi}{2}$ and $\theta_s(t) = \frac{\pi}{4}$, the signal is circularly polarized. If we assume aligned polarizations for all the $N-1$ coherent intruders and the signal (i.e., $\Psi_s(t) = \Psi_{xi}(t)$ and $\theta_s(t) = \theta_{xi}(t)$ for all i), the direction of the signal and crosstalk fields will be the same and we can drop the vector notation. In this case, the detected electric field can be written as [4]-[8]

$$E_{\text{det}}(t) = E_s(t) \cos\left(2\pi f_c t + \phi_s(t)\right) + \sum_{i=1}^{N-1} E_{xi}(t) \cos\left(2\pi f_c t + \phi_{xi}(t)\right) \tag{1.3}$$

$E_s(t)$ and $E_{xi}(t)$ are OOK modulated, thus they attain two values randomly (0 or $E_{s,1}$ for the signal, 0 or $E_{xi,1}$ for the crosstalk where $E_{s,1}$ and $E_{xi,1}$ are the amplitudes of the signal and crosstalk respectively) at instants separated by a bit period which may be different for signal and crosstalk.

Using definition 1, leads to an expression for the detected current [9] as follows.

Definition 2 *The current at the output of the detector at an instant t is proportional to the square of the magnitude of the electric field vector at that instant.*

$$i_{\text{det}}(t) = \Re E_{\text{det}}^{T}(t)\, E_{\text{det}}(t) \tag{1.4}$$

$$= \Re P_s(t) + 2\Re\sqrt{P_s(t)} \sum_{i=1}^{N-1} \left\{ \sqrt{P_{xi}(t)} \cos\left[\phi_s(t) - \phi_{xi}(t) + \gamma_{s,i}\right] \right. \tag{1.5}$$

$$\left. \cdot f\left(\theta_s, \theta_{xi}, \Psi_s, \Psi_{xi}\right) \right\}$$

$$+\Re \sum_{i=1}^{N-1} \sum_{j=i+1}^{N} \sqrt{P_{xi}(t)}\sqrt{P_{xj}(t)} \cos\left[\phi_{xj}(t) - \phi_{xi}(t) + \gamma_{i,j}\right] f\left(\theta_{xj}, \theta_{xi}, \Psi_{xj}, \Psi_{xi}\right)$$

where

$$\begin{aligned} f\left(\theta_s, \theta_{xi}, \Psi_s, \Psi_s\right) &= \frac{1}{2}\left\{2 + \cos\left[2\left(\theta_s - \theta_{xi}\right)\right]\left[1 + \cos\left(\Psi_s - \Psi_{xi}\right)\right]\right. \\ &\quad \left. + \cos\left[2\left(\theta_s + \theta_{xi}\right)\right]\left[1 - \cos\left(\Psi_s - \Psi_{xi}\right)\right]\right\}^{1/2} \end{aligned} \tag{1.6}$$

$$\gamma_{s,i} = \tan^{-1}\left(\frac{\sin\left(\theta_s\right)\sin\left(\theta_{xi}\right)\sin\left(\Psi_s - \Psi_{xi}\right)}{\cos\left(\theta_s\right)\cos\left(\theta_{xi}\right) + \sin\left(\theta_s\right)\sin\left(\theta_{xi}\right)\sin\left(\Psi_s - \Psi_{xi}\right)}\right) \tag{1.7}$$

and

$$\gamma_{i,j} = \tan^{-1}\left(\frac{\sin\left(\theta_{xi}\right)\sin\left(\theta_{xj}\right)\sin\left(\Psi_{xi} - \Psi_{xj}\right)}{\cos\left(\theta_{xi}\right)\cos\left(\theta_{xj}\right) + \sin\left(\theta_{xi}\right)\sin\left(\theta_{xj}\right)\sin\left(\Psi_{xi} - \Psi_{xj}\right)}\right) \tag{1.8}$$

Here $\Re$ is the detector's responsivity, $P_s(t) = \frac{1}{2}\left[E_s(t)\right]^2$, $P_{xi}(t) = \frac{1}{2}\left[E_{xi}(t)\right]^2$ are the instantaneous optical powers of the signal and i^{th} crosstalk component respectively. The polarization-dependent quantities $\gamma_{s,i}$ and $\gamma_{i,j}$ have no significance, since they are independent of the optical phases $\phi_s(t)$, $\phi_{xi}(t)$ which are uniformly distributed in $[0, 2\pi]$. Therefore $\cos\left(\phi_s(t) - \phi_{xi}(t) + \gamma_{s,i}\right)$ and $\cos\left(\phi_{xj}(t) - \phi_{xi}(t) + \gamma_{i,j}\right)$ have the same distribution as $\cos\left(\phi_s(t) - \phi_{xi}(t)\right)$ and $\cos\left(\phi_{xj}(t) - \phi_{xi}(t)\right)$ respectively. Definition 1 will be explained in more detail and Relations 1.5 through 1.8 will be derived later in Chapter 4.

There are some simulated detected currents for different number of intruders in Figures 1.15 and 1.16. The amplitude of the signal is normalized to 1 in each case. Each intruder is at the same rate with the signal, however they all are asynchronous with a

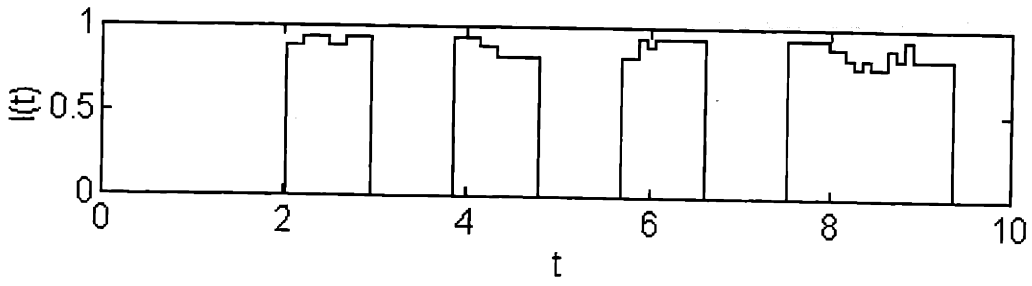

Figure 1-15: Detected Current for $N = 11$

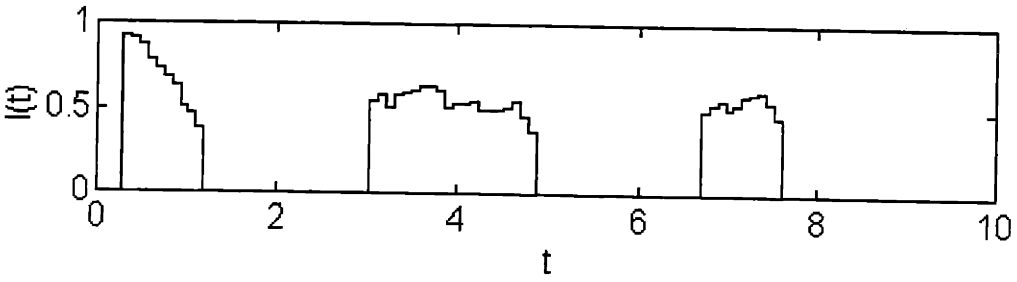

Figure 1-16: Detected Current for $N = 101$

random amount of time which is uniformly distributed in a bit period. The power of each component is 28 dB lower than that of the signal. One can observe that when the number of intruders increase, the fluctuations become more frequent and have greater amplitude.

1.2.2 Receiver Model

Our receiver is modeled as an optical detector followed by a matched filter demodulator as shown in Figure 1.17.The optical detector is modeled as a polarization insensitive device where the current at the output of such a device is proportional to the square of the electric field intensity it is illuminated with (i.e., $\Re \mathbf{E}^T \mathbf{E}$). The optimum filter in the absence of crosstalk is the cross-correlation type which is equivalent to the matched filter demodulator [13].

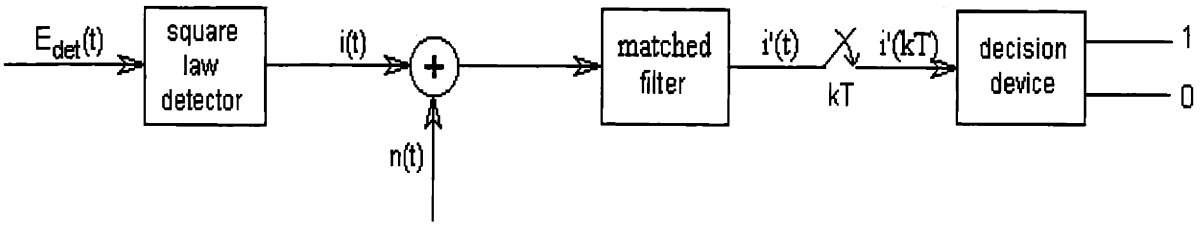

Figure 1-17: The receiver model.

The electrical filter in the demodulator is matched to rectangular pulse shape because our system uses OOK signalling. Such a filter is equivalent to an integrator whose integrating interval is a pulse length. Perfect timing recovery is assumed to be achieved by means of a sampler which samples the output of the integrator every T seconds where T is the pulse length. The decision device is a simple comparator whose reference is a threshold which is constant or varying depending on whether the device is DC or AC coupled respectively. In the DC coupled case, we assume that the threshold is optimized minimizing bit errors. An AC coupled decision circuit basically filters out the DC component of the signal (so that the average of the signal at the output is 0) at its input and sets the threshold to 0. The performance of every AC coupled decision circuit is upper and lower bounded with a best and a worst curve which will be dealt with in Chapter 3. We will mainly focus on DC coupled decisions. We will deal with the AC coupled decision systems in a separate section in Chapter 3 in a detailed manner and prove that they perform no better than DC coupled decision systems if the system parameters are static.

In optical communication, there are two main noise sources depending on the generation mechanism: fiber generated and receiver generated. Examples to fiber generated noises are the shot noise (or quantum noise) which is due to the Poisson nature of the photon arrivals, and the dark current noise which results from the generation of photons at room temperature even if there is no input. The noise generated in the receiver is

the thermal noise. The shot noise is a white Poisson process and the dark current and the thermal noises are white Gaussian. Under room conditions thermal noise dominates, i.e., the fiber generated noises are negligible compared to thermal noise. However, if the optical signal is amplified by means of an APD, then the fiber generated processes are amplified (i.e., their variances are increased by a factor of the square of the gain of the amplifier, the shot noise becomes a bulky Poisson process, where every photon at the input of the amplifier stimulates other photons and the output is the amplified process) and they start to become dominant. Also, if there are in line optical amplifiers another noise is generated at the amplifier due to Amplified Spontaneous Emission (ASE) which is white Gaussian. We only consider thermal noise in this thesis (hence the optical detector is a pin diode).

1.3 Impacts of Coherent Crosstalk on Receiver Performance

Coherent Crosstalk is extremely detrimental to the performance of the receiver, especially if the scale of the network is large. The amount of degradation in performance can be calculated in terms of a "power penalty". The power penalty is basically the factor by which the detected optical power should be increased to achieve the bit error rate performance of the crosstalk-free system.

The signals emitted by an OOK optical transmitter (i.e., Intensity Modulation System) can be modelled as a Bernoulli Process. As defined before, the detected current is proportional to the square of the electric field intensity (power density), it is illuminated with $(\mathbf{E}_{\text{det}}^T \mathbf{E}_{\text{det}})$ and it involves three terms: signal term, signal-crosstalk beat term and crosstalk-crosstalk beat term. Crosstalk-crosstalk beat power is very small compared to signal crosstalk beat power; however for $N-1$ crosstalk components interfering, signal-crosstalk beat power is composed of $N-1$ terms, while crosstalk-crosstalk beat power involves $\frac{N(N-1)}{2}$. Therefore for large numbers of network nodes communicating, that

term may dominate. This phenomena will be examined in Chapter 5.

As N increases, the signal-crosstalk and crosstalk-crosstalk beat power terms become the sum of a large number of correlated discrete random variables which makes them hard to deal with. Thus, two common techniques have been used to analyze them: Gaussian [4], [6], [7], [9]-[12] and worst case [5], [6], [16].

1.3.1 Gaussian Approximation

Gaussian approximation is a common technique for analysis of the sum of IID random variables. It is based on the celebrated Central Limit Theorem which analytically can be stated as follows [14].

Theorem 3 *Let S_n be the sum of n IID random variables $X_1, \ldots, X_n$ whose mean and variance are $\overline{X}$ and $\sigma^2 < \infty$ respectively. Then,*

$$\lim_{n\to\infty} P\left(\left(\frac{S_n - n\overline{X}}{\sqrt{n}\sigma}\right) \leq y\right) = 1 - Q(y) \tag{1.9}$$

Gaussian approximation is used in most papers on coherent crosstalk [4], [6], [7], [9]-[12]. In these papers, the crosstalk-crosstalk terms are ignored and the sum of the signal-crosstalk beat terms is modeled as Gaussian. The problem with doing this can be stated as follows.

The Gaussian approximation is valid only if the number of crosstalk sources is large (i.e., $N - 1 \gg 1$). However, as the network size gets larger, the crosstalk-crosstalk beat terms start to become dominant since there are $O(N^2)$ such terms (it will be considered in Chapter 5 in a more detailed manner). Thus ignoring crosstalk-crosstalk terms and Gaussian approximation cannot be reasonable at the same time. If crosstalk-crosstalk terms are not ignored, there are two main problems with using Gaussian approximation.

The Gaussian approximation is valid for the sum of independent random variables. However, the crosstalk-crosstalk beat terms are not a sum of independent random variables. Besides, the terms that signal-crosstalk beat power is composed of, are not in-

dependent of those of crosstalk-crosstalk beat power. The negligible crosstalk-crosstalk beat power assumption is doubtful as well, because the Central Limit Theorem is reasonable for large N, whereas the crosstalk-crosstalk beat power is negligible for small N.

Furthermore, for large values of y, Theorem 3 does not yield a very good approximation for reasonable values of n. It is for this reason that the word central appears in the name "Central Limit Theorem". That is, the Gaussian Approximation is not an accurate approximation in the tails of the Gaussian function. As we deal with the error probabilities of $\sim 10^{-10}$, this approximation may not give accurate results.

As a result, Gaussian approximation may not be suitable for this work.

1.3.2 Worst Case Analysis

Worst Case Analyses give us an idea about the performance of systems, when every parameter in the corresponding model is assigned their worst possible value to deteriorate the system performance [5], [6], [16]. The worst case crosstalk for our model occurs when all the crosstalk components interfere with the signal with aligned polarization and out of phase with π rads. The worst case bit sequence depends on the decision device. It will be defined in Chapter 2 for DC-coupled decision device and Chapter 3 for AC-coupled decision device. The theoretical performance under worst case crosstalk is a function of threshold. The power penalty versus the crosstalk is given in Figure 1.18 for various thresholds and analysis techniques [6].

1.3.3 Improving System Performance Under Crosstalk

Coherent crosstalk is extremely detrimental to WDM-AONs and becomes a serious issue especially when the network scale is large. Therefore methods to improve the system performance under crosstalk should be sought.

Up to date, not too much work on communication theory has been done to eliminate

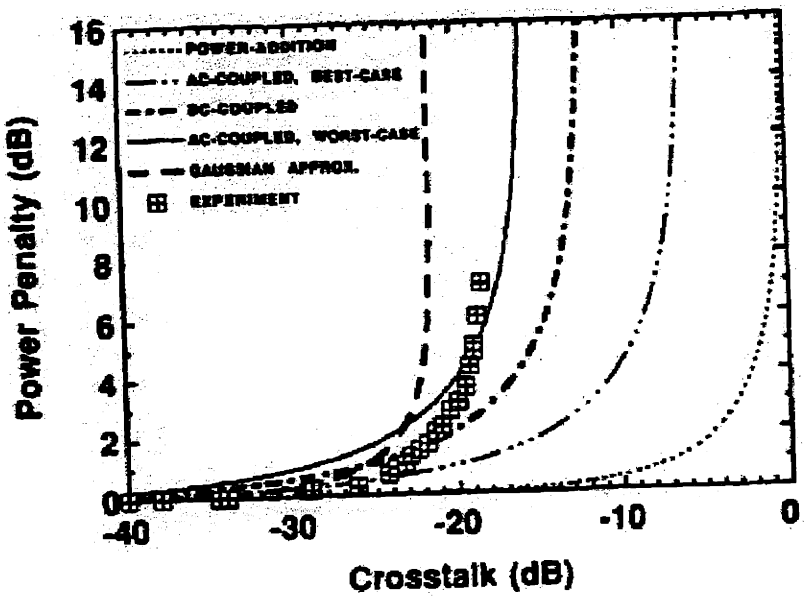

Figure 1-18: Power Penalty versus Crosstalk for Various Thresholds [6]

crosstalk in WDM optical networks. The current approaches to this issue are not based on modulation, demodulation or coding, but protocol design and networking instead. For instance the approach in [18] is ensuring that a switch is not used by two connections simultaneously. The cost of eliminating the crosstalk is a decrease in the capacity of the communications (e.g., a smaller bit rate, less circuit allocation duration).

The problem, analogous to crosstalk in wireless communications is "cochannel interference" which limits the performance of a multiple access communication link [19], [20]. There are communication theory based approaches to suppress cochannel interference. They are mostly based on system theory (i.e., in terms of special pre, post-filters) [21] and coding.

1.4 Outline of the Thesis

We will begin our work by analyzing the error performance of the receiver shown in Figure 1.17. The thesis work will begin with a worst case analysis for single crosstalk

Analysis steps	# of interferers	C.talk bits	Polarization,Phase
Case 1	1	all 1's	aligned, out of phase (π)
Case 2	1	random	aligned, out of phase (π)
Case 3	1	random	random, random
Case 4	$N > 1$	random	random,random

Table 1.3: The steps of the analysis.

source. Step 2 extends the analysis to random crosstalk bit sequence, step 3 analyzes the performance when the phase and the polarization state of the crosstalk is random, step 4 generalizes the analysis to multiple crosstalk sources. It is important to note that the notion of the random bit sequence covers the random bit rate case as well; thus the analysis is general in the sense that all the sources have the freedom to transmit pulses at the any rate (e.g., the error performance curve of a 622 Mb/s channel can be found under the interference of 3 other channels at 155 Mb/s, 2.488 Gb/s and 9.95 Gb/s). The optimum threshold will be calculated in every step. These steps are summarized in Table 1.3.

The remainder of the thesis is organized as follows. Chapter 2 initiates the analysis with discussing the crosstalk-free and worst cases, and Chapter 3 extends it to the case of random crosstalk bit sequence. Chapter 4 evaluates the error performance when the phase and the polarization of the detected signal are random. Chapter 5 generalizes the analysis to cover the network performance where more than one crosstalk source is active. Chapter 6 presents the conclusions drawn from the thesis and the future work.

Chapter 2

Baseline and Worst Case Performances

In this chapter, we will present an introduction to the analysis methods we will employ in the thesis by analyzing the two extreme cases, crosstalk-free (baseline) and the worst cases. In the latter case, the crosstalk field is assumed to be pointing in the same direction (or the opposite) as that of the signal. Thus, we will drop the vector notation and use Equation 1.3 for the electric field at the input of the receiver.

The remainder of the chapter is organized as follows. Section 2.1 deals with the case where there is no crosstalk and introduces two different methods which will lead to the error probability as a function of E_b/N_0, the signal energy per bit / one sided power spectrum of the noise. Section 2.2 gives an introductory crosstalk analysis by evaluating the error probability of the worst case. Finally, the important conclusions deduced from the chapter are presented and similarities and differences with other works are discussed.

2.1 Crosstalk-free Performance Curve (Baseline)

Let us recall Equation 1.3.

$$E_{\text{det}}(t) = E_s(t)\cos\left(2\pi f_c t + \phi_s(t)\right) + \sum_{i=1}^{N-1} E_{xi}(t)\cos\left(2\pi f_c t + \phi_{xi}(t)\right)$$

In this section, we will assume $E_{xi} = 0$ for all i. In the following two subsections, an expression for the error probability will be derived using two different methods.

2.1.1 First Method

Since the detector is assumed to be polarization independent, it is useful to drop the vector notation. After that the detected field becomes,

$$E_{\text{det}}(t) = E_s(t)\cos\left(2\pi f_c t + \phi_s(t)\right) \tag{2.1}$$

therefore the signal square is,

$$[E_{\text{det}}(t)]^2 = [E_s(t)]^2\left[\frac{1}{2} + \frac{1}{2}\cos\left(4\pi f_c t + 2\phi_s(t)\right)\right] \tag{2.2}$$

The double frequency term is rejected by the detector. The baseband DC component of the detected signal can be written as follows.

$$P_s(t) = \frac{1}{2}[E_s(t)]^2 \tag{2.3}$$

and the detected photocurrent can be found as

$$i_s(t) \triangleq \Re P_s(t) \tag{2.4}$$

For OOK signals, $i_s(t)$ is constant at $i_{s,1}$ given that the signal is a mark, and constant at 0 given that the signal is a space.

The noise $n(t)$ is assumed to be additive, white and Gaussian with two-sided power

spectral density of $N(f) = \frac{N_o}{2}\ Amp^2/Hz$[1]. The power spectrum ($N(f)$) at the output of the matched filter becomes,

$$\begin{aligned} N'(f) &= |H(f)|^2 N(f) \\ &= |H(f)|^2 \frac{N_o}{2} Amp^2/Hz \end{aligned} \tag{2.5}$$

Thus, the variance of $n'(t)$ is

$$\begin{aligned} \sigma^2_{n'(t)} &= \int_{-\infty}^{\infty} N'(f)df \\ &= \frac{N_o}{2} \int_{-\infty}^{\infty} |H(f)|^2 df \end{aligned} \tag{2.6}$$

Using Parseval's relation, the variance can be written as follows.

$$\sigma^2_{n'(t)} = \frac{N_o}{2} \int_{-\infty}^{\infty} |h(t)|^2 dt \tag{2.7}$$

where $h(t)$ is matched to rectangular pulse as shown in Figure 3.1 where T is the period of a pulse.

Thus, Equation 2.7 simplifies to

$$\begin{aligned} \sigma^2_{n'(t)} &= \frac{N_o}{2} \int_{0}^{T} |h(t)|^2 dt \\ &= \frac{N_o}{2} T \end{aligned} \tag{2.8}$$

[1]The thermal noise for the optical receiver is assumed to be white, Gaussian with two sided power spectral density $\frac{N_0}{2} = \frac{2k_B T}{R_L}$ where k_B is the Boltzmann constant, T is the absolute temperature and R_L is the load resistance seen at the output of the receiver [23].

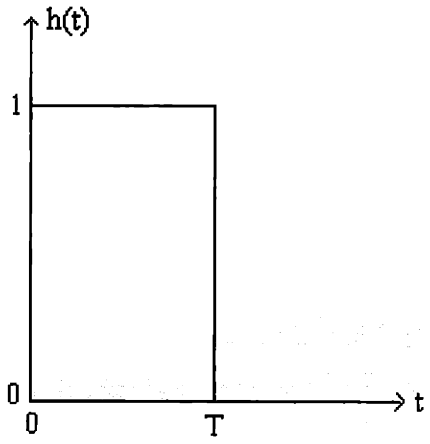

Figure 2-1: Impulse Response of the Matched Filter

The detected current at the output of the sampler $i'(kT)$ is (the input of the sampler is the integral of $i_s(t)$ within the interval equal to the length of a pulse) given in the following expression.

$$i'(kT) = \begin{cases} Ti_{s,1} + n'(kT) & \text{when signal bit is a 1} \\ n'(kT) & \text{when signal bit is a 0} \end{cases}$$

The probability density of the detected current conditioned on the transmitted pulse is given in Figure 3.2.

When the threshold is set to $T\frac{i_{s,1}}{2}$, the error probability becomes

$$\begin{aligned} P(E) &= Q\left(\frac{Ti_{s,1}}{2\sigma_{n'(t)}}\right) \\ &= Q\left(\sqrt{\frac{\frac{1}{2}Ti_{s,1}^2}{N_0}}\right) \end{aligned} \tag{2.9}$$

Let the average energy per symbol be E_s and the average power per symbol be P_s. They

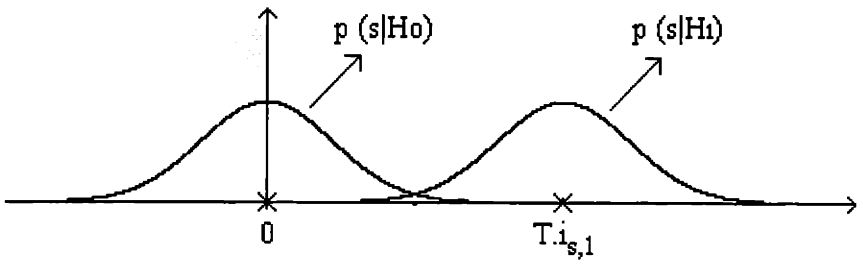

Figure 2-2: The Density of the Detected Current Conditioned on the Signal

are equivalent to average electrical energy per bit E_b and P_b respectively because the rate of transmission is 1 bit/symbol.

$$\begin{aligned} P_b &= \frac{1}{2}i_{s,1}^2 + \frac{1}{2}0^2 \\ &= \frac{1}{2}i_{s,1}^2 \end{aligned} \tag{2.10}$$

Therefore, the energy per bit becomes

$$E_b = \int_0^T P_b dt = \frac{1}{2}Ti_{s,1}^2 \tag{2.11}$$

As a result, the error probability can be written as

$$P(E) = Q\left(\sqrt{\frac{E_b}{N_0}}\right) \tag{2.12}$$

Probability of error is illustrated in Figure 2.3.

From now on this will be our baseline. We will evaluate power penalties, using this curve as a reference.

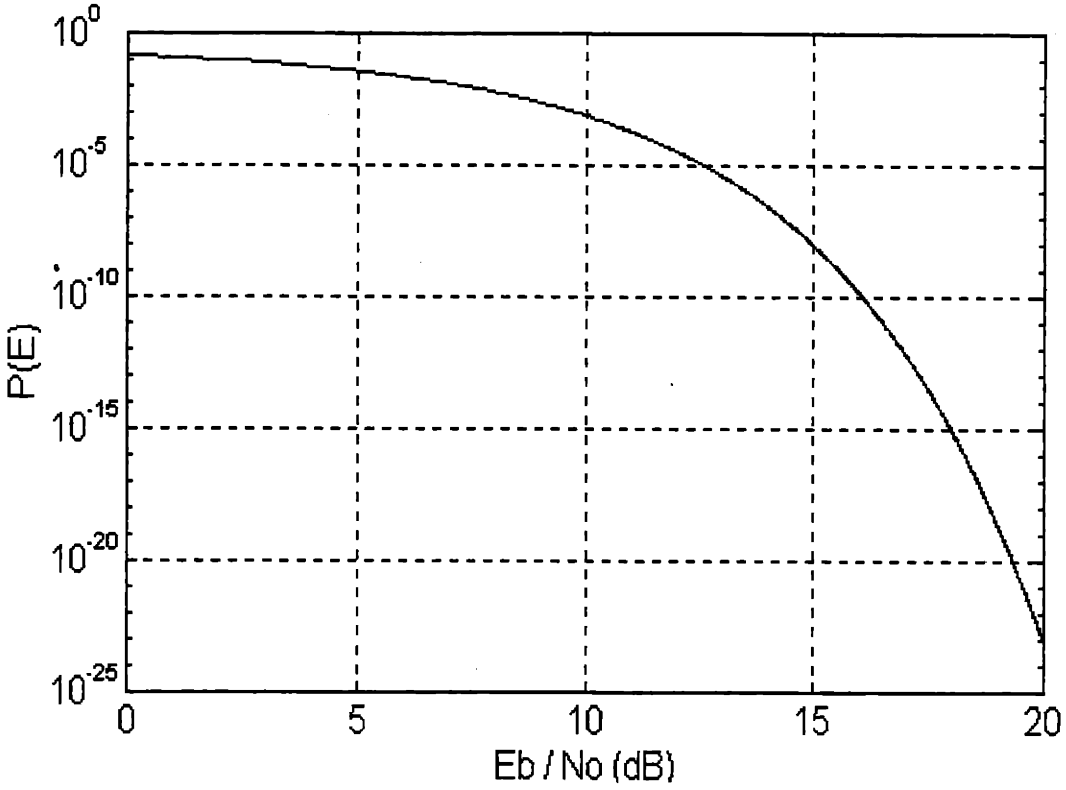

Figure 2-3: Error Performance Curve of the Crosstalk-free System

2.1.2 Second Method

The following analysis presents another way of getting the same curve. This section is useful in the sense that it gives intuition on the basics of crosstalk analysis of optical CDMA networks. It can be a reference for the interested reader and might be skipped otherwise, since the results derived in this section will not be used later in this thesis. The fundamentals of the analysis are presented in [24].

Parameters of the Signal Space

Let the signal space $W(S)$ be composed of M signals.

$$S = \{s_k, 1 \leqslant k \leqslant M\}$$

The following items are the parameters of the signal space.

1. The actual **dimension** of the signal space S,

$$N = \dim\{W(S)\} \tag{2.13}$$

2. The **rate** of the signal space,

$$r = \log_2 M \text{ bits/symbol} \tag{2.14}$$

3. The average energy per symbol,

$$\begin{aligned} E_s &= E\left[\|s\|^2\right] \\ &= \frac{1}{M}\sum_{k=1}^{M}\|s_k\|^2 \text{ joules/symbol} \end{aligned} \tag{2.15}$$

where $\|s_k\|^2$is the magnitude of the k^{th} signal in the space and the average energy per bit is

$$\begin{aligned} E_b &= \frac{E_s \text{ joules/symbol}}{r \text{ bits/symbol}} \\ &= \frac{E_s}{r} \text{ joules/bit} \end{aligned} \tag{2.16}$$

4. The **minimum squared distance** of the space $W(S)$,

$$d^2_{\min}(S) = \min_{s \neq s'} \|s - s'\|^2 \tag{2.17}$$

and for each $s \in S$, the number of nearest neighbors $K_{\min}(S)$ is the number of $s' \in S$ such that $\|s - s'\|^2 = d^2_{\min}(S)$ and the average number of nearest neighbors can be found as

$$\begin{aligned} K_{\min}(S) &= E\left[K_{\min}(s)\right] \\ &= \frac{1}{M} \sum_{k=1}^{M} K_{\min}(s_k) \end{aligned} \tag{2.18}$$

5. The two sided **noise power spectrum** is $\frac{N_0}{2}$ joules/sec/Hz. We have to reflect this quantity onto the space spanned by the signals and find the variance of noise per dimension.

$$\begin{aligned} \sigma^2 &= \frac{N_0}{2} \text{ joules/sec/Hz } x \text{ } 2W \text{ Hz} \\ &= N_0 W \text{ joules/sec} \end{aligned} \tag{2.19}$$

where W is the bandwidth of the channel. The quantity found in Equation 2.19 is the power (energy per second) of white noise after it is filtered. We have to convert it to energy per symbol and energy per dimension consequently. The maximum symbol rate

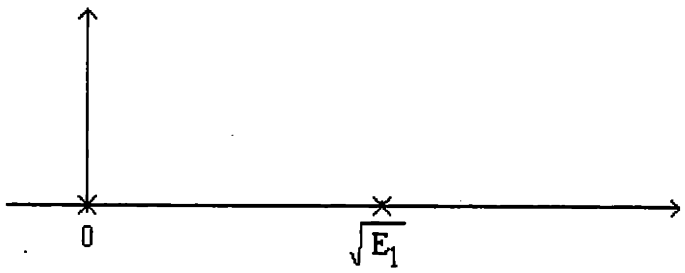

Figure 2-4: OOK symbols: Mark with energy E_1, space with energy 0.

achieved by a channel with bandwidth W Hz is $2W$ real symbols per second (i.e., $2W$ 1D/sec) in the absence of ISI. Hence, the noise variance per dimension becomes,

$$\begin{aligned} \sigma^2_{per-D} &= \frac{N_0 W \text{ j/sec}}{2W \text{ 1D/sec}} \\ &= \frac{N_0}{2} \text{ j/1D} \end{aligned} \tag{2.20}$$

Performance of an OOK System

The signal constellation of an OOK system is illustrated in Figure 3.4. The energy levels are mark and space. The energy mark is E_1 and that of a space is 0. Let us evaluate the pre-defined parameters going over the following steps.

1. The signal space is 1 dimensional ($N = 1$).
2. The rate is $r = \log_2 2 = 1$ bits/symbol.
3. The average energy per symbol is $E_s = \frac{E_1}{2}$, and the energy per bit is $E_b = \frac{E_s}{r} = \frac{E_1}{2}$ joules/bit.
4. The minimum squared distance of the signal space is $d^2_{\min} = E_1 = 2E_s = 2E_b$, and $K_{\min}(S) = 1$.

The probability density curves of the detected signal conditioned on a mark and a space bit are illustrated in Figure 2.5. The variance of the Gaussian curves are σ^2_{per-D} because the signal space is 1 dimensional. The probability of error when the threshold is

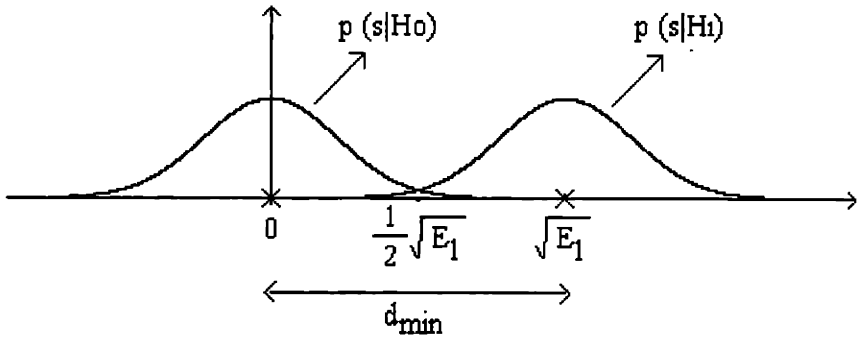

Figure 2-5: The pdf of the detected current conditioned on the signal

set at $\frac{1}{2}\sqrt{E_1}$ can be found as follows.

$$\begin{aligned} P(E) &= Q\left(\frac{d_{\min}}{2\sigma_{per-D}}\right) \\ &= Q\left(\sqrt{\frac{d_{\min}^2}{4\sigma_{per-D}^2}}\right) \\ &= Q\left(\sqrt{\frac{E_b}{N_0}}\right) \end{aligned} \tag{2.21}$$

Using this result leads to BER expression of other signal spaces.

$$\begin{aligned} P(E) &= K_{\min}(S)Q\left(\sqrt{\frac{d_{\min}^2}{4\sigma_{per-D}^2}}\right) \\ &= K_{\min}(S)Q\left(\sqrt{\frac{d_{\min}^2}{2N_0}}\right) \end{aligned} \tag{2.22}$$

for any signal space. The above relation can be written as

$$P(E) = K_{\min}(S)Q\left[\sqrt{\left(\frac{d^2_{\min}}{2E_b}\right)\left(\frac{E_b}{N_0}\right)}\right] \tag{2.23}$$

$\gamma_c \triangleq \frac{d^2_{\min}}{2E_b}$ will be called the coding gain and the BER expression can be rewritten as

$$P(E) = K_{\min}(S)Q\left[\sqrt{\gamma_c\left(\frac{E_b}{N_0}\right)}\right] \tag{2.24}$$

Writing the error probability expression in this form helps us compare the error probability of systems with different crosstalk statistics.

2.2 Worst Case Crosstalk Performance Curve

To analyze the worst case performance, we have to define what the worst case is and when it occurs for our system. In this section we will only deal with the single crosstalk source case. The detected electric field is composed of two components, the signal and the crosstalk. They add to each other as vectors. The sum of two vectors is minimum when they are in opposite directions. Thus, a necessary condition for the worst case to occur is that the crosstalk field points in the opposite direction of the signal field. For this condition to be satisfied, the phase and polarization parameters should be as follows. The signal and crosstalk fields should be either out of phase with π rads and have the same state of polarization or vice versa (actually, both are different definitions of the same thing). Another necessary condition for the worst case crosstalk is that the crosstalk component is a mark all the times since we make the analysis for DC coupled decision threshold. Note that the worst case bit sequence for an optical system is different from that of a non-optical system in the following sense. In a non-optical system a constant interferer has no impact on the performance since it is deterministic and independent of the signal. However, in an optical system the signal at the output of the detector is proportional to the square of the electric field strength at its input. Thus, the interference portion of the current becomes a function the communication signal due to the signal-

interference beat terms. It takes on different values depending on whether the signal bit is a 1 or a 0. Therefore, even though we know everything about the crosstalk in the fiber, we cannot do anything to cancel the interference at the receiver.

With the assumption of phase and polarization being constant within the transmission, the received field can be written as follows.

$$E_{\text{det}}(t) = E_s(t)\cos\left(2\pi f_c t + \phi_s(t)\right) + E_c(t)\cos\left(2\pi f_c t + \phi_c(t)\right) \tag{2.25}$$

where $\phi_s(t) = \phi_c(t) + \pi$. Therefore the detected current becomes

$$E_{\text{det}}(t) = \left[E_s(t) - E_c(t)\right]\cos\left(2\pi f_c t\right) \tag{2.26}$$

and the square of the baseband component of the detected field is

$$E^2_{\text{det}-DC}(t) = \frac{1}{2}E_s^2(t) - E_s(t)E_c(t) + \frac{1}{2}E_c^2(t) \tag{2.27}$$

Using $P_s(t) = \frac{1}{2}E_s^2(t)$ and $P_c(t) = \frac{1}{2}E_c^2(t)$, the detected optical power and the detected current can be expressed as

$$P_{\text{det}}(t) = P_s(t) - 2\sqrt{P_s(t)P_c(t)} + P_c(t) \text{ watts} \tag{2.28}$$

and

$$i_{\text{det}}(t) = \Re P_{\text{det}}(t) = \Re P_s(t) - 2\Re\sqrt{P_s(t)P_c(t)} + \Re P_c(t) \text{ Amps} \tag{2.29}$$

respectively. Let $i_s(t) \triangleq \Re P_s(t)$ and $i_c(t) \triangleq \Re P_c(t)$. With these two definitions, the detected current becomes

$$i_{\text{det}}(t) = i_s(t) - 2\sqrt{i_s(t)i_c(t)} + i_c(t) \text{ Amps} \tag{2.30}$$

$i_s(t)$ is constant at $i_{s,1}$ given that the signal is a mark and 0 given that the signal is a space. The amplitude of the crosstalk signal is constant all the times at $i_{c,1}$ given the

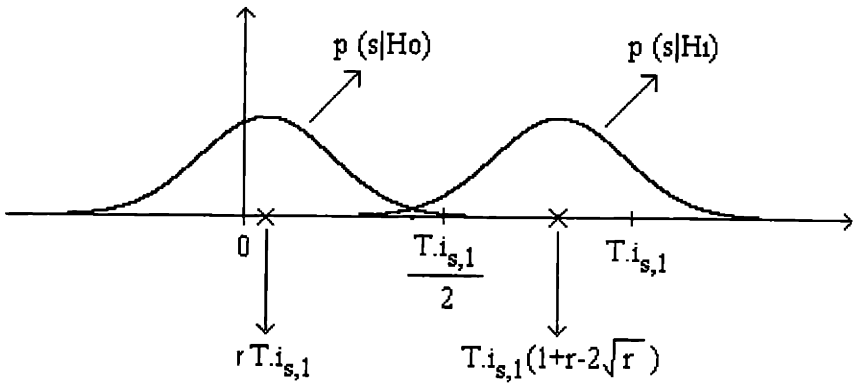

Figure 2-6: Conditional pdf of the sampled signal under worst case crosstalk.

worst case. Let us define

$$r \triangleq \frac{i_{c,1}}{i_{s,1}} = \frac{P_{c,1}}{P_{s,1}} \tag{2.31}$$

The noise statistics were given in section 2.1.1. The detected current at the output of the sampler is

$$i'(kT) = \begin{cases} T\left(i_{s,1} + i_{c,1} - 2\sqrt{i_{s,1} i_{c,1}}\right) + n'(kT) & \text{when signal bit is a 1} \\ T i_{c,1} + n'(kT) & \text{when signal bit is a 0} \end{cases} \tag{2.32}$$

The conditional probability densities of $i'(kT)$ given that the signal is a mark and given that the signal is a space are illustrated in Figure 2.6. When the decision threshold is set to $i_{th} = \frac{T i_{s,1}}{2}(1-x)$ where x is the normalized difference between the threshold and $\frac{T i_{s,1}}{2}$ (the optimum threshold of the crosstalk-free case), the performance becomes

$$P(E) = \frac{1}{2}P(E|H_0) + \frac{1}{2}P(E|H_1)$$

$$= \frac{1}{2}Q\left(\frac{\frac{Ti_{s,1}}{2}(1-x-2r)}{\sigma_{n'(t)}}\right) + \frac{1}{2}Q\left(\frac{\frac{Ti_{s,1}}{2}(2+2r-4\sqrt{r}-1+x)}{\sigma_{n'(t)}}\right)$$

$$= \frac{1}{2}Q\left((1-x-2r)\sqrt{\frac{Ti_{s,1}^2}{2N_0}}\right) + \frac{1}{2}Q\left((1+x-4\sqrt{r}+2r)\sqrt{\frac{Ti_{s,1}^2}{2N_0}}\right) \quad (2.33)$$

If we plug $E_b = \frac{1}{2}Ti_{s,1}^2$ in our BER expression, we get the following.

$$P(E) = \frac{1}{2}Q\left((1-x-2r)\sqrt{\frac{E_b}{N_0}}\right) + \frac{1}{2}Q\left((1+x-4\sqrt{r}+2r)\sqrt{\frac{E_b}{N_0}}\right) \quad (2.34)$$

The two curves $p(s|H_1)$ and $p(s|H_0)$ given in Figure 2.6 have the same variance. Thus, the optimum threshold is located at the mid point of the means of the two. It is straightforward to find the optimum x as follows

$$x_{opt} = 2\sqrt{r} - 2r \quad (2.35)$$

and the optimum performance becomes,

$$P(E) = Q\left((1-2\sqrt{r})\sqrt{\frac{E_b}{N_0}}\right)$$

$$= Q\left(\sqrt{(1-2\sqrt{r})^2\frac{E_b}{N_0}}\right) \quad (2.36)$$

The worst case performances are sketched in Figures 2.7 and 2.8 for crosstalks of -20 dB ($r = 0.01$) and -17 dB ($r = 0.02$) respectively. One can observe from 2.36 that the worst case curve is the scaled version of the baseline with

$$\gamma_p = 10\log\left[(1-2\sqrt{r})^2\right] \text{ dB} \quad (2.37)$$

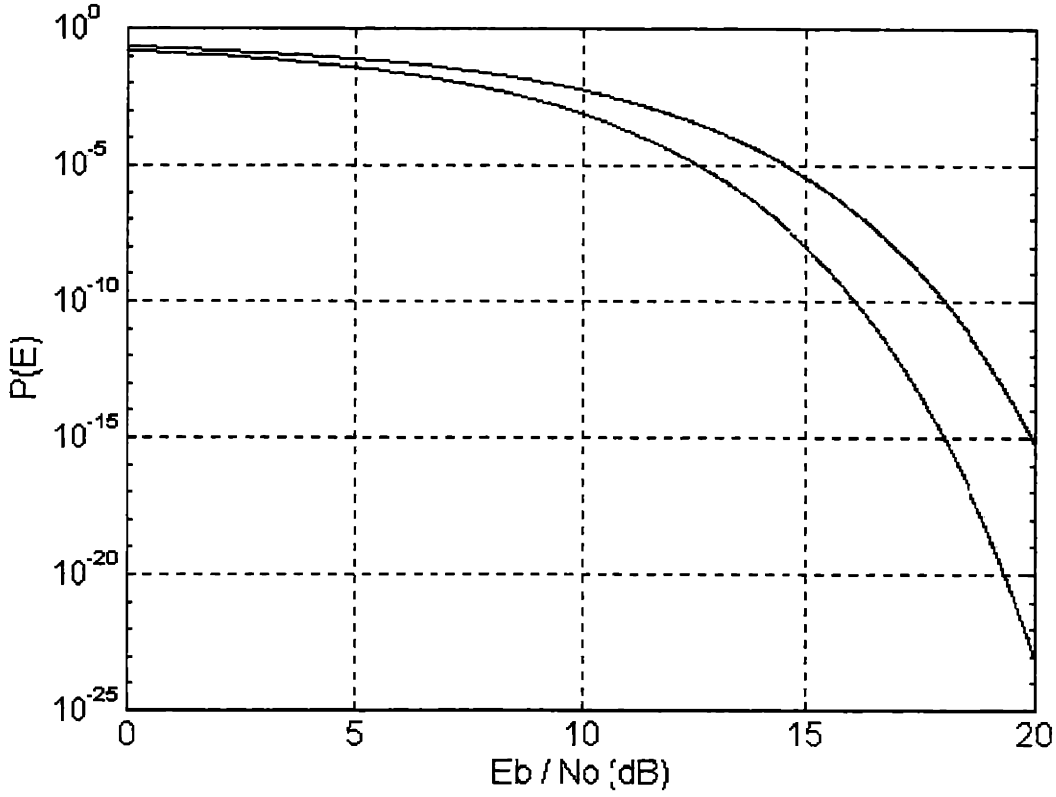

Figure 2-7: Baseline and Worst Case for -20 dB crosstalk. Electrical Power Penalty = 2 dB

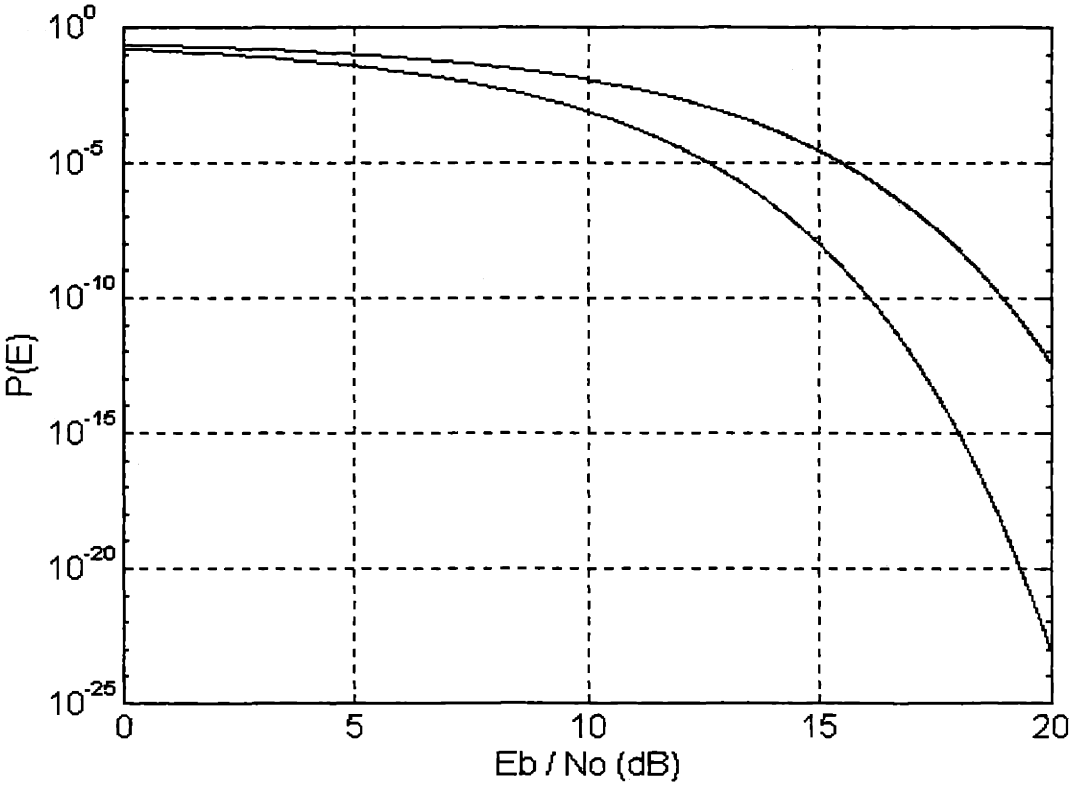

Figure 2-8: Baseline and Worst Case for -17 dB Crosstalk. Electrical Power Penalty = 3 dB

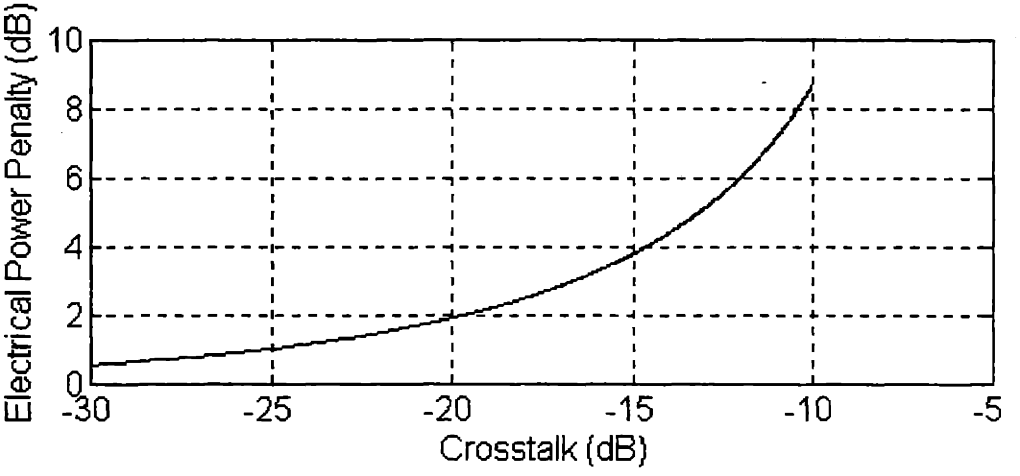

Figure 2-9: Electrical Power Penalty versus Crosstalk. 2 dB and 3 dB penalties due to -20 dB and -17 dB crosstalk respectively.

where γ_p is the power penalty due to the worst case for a crosstalk of $10\log(r)$ dB. It is important to note that this power penalty is electrical. The corresponding optical power penalty is thus,

$$\gamma_{op} = \frac{\gamma_p(dB)}{2} = 10\log\left(1 - 2\sqrt{r}\right) dB \tag{2.38}$$

Electrical power penalty can also be observed from the performance graphs. There is 2 dB electrical power penalty due to -20 dB crosstalk and 3 dB electrical power penalty due to -17 dB crosstalk. Electrical and optical power penalties (γ_p, γ_{op}) versus the crosstalk are sketched in Figures 2.9 and 2.10 respectively.

2.3 Conclusions

In this chapter, we introduced basic crosstalk analysis methods for the two simplest cases which are the 0 crosstalk (baseline) and the worst cases. The most important conclusion of this chapter is that we understood the difference between a fiber-optic system and a

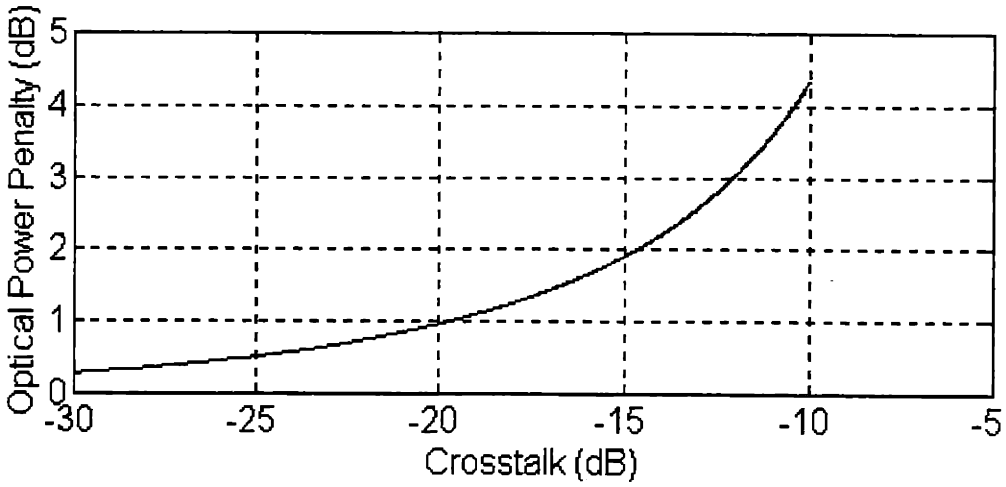

Figure 2-10: Optical Power Penalty versus Crosstalk. 1 dB and 1.5 dB penalties due to -20 dB and -17 dB crosstalk respectively.

non-optical system (wireless, non-optical wired communication systems) in the following sense. In a non-optical system a constant interferer has no impact on the performance since it is deterministic and independent of the signal. However, in an optical system the signal at the output of the detector is proportional to the square of the electric field strength at its input. Thus, the interference portion of the current becomes a function the communication signal due to the signal-interference beat terms. It takes on different values depending on whether the signal bit is a 1 or a 0. Therefore, even though we know everything about the crosstalk in the fiber, we cannot do anything to cancel the interference at the receiver. The following chapters will base on this idea. The results we get for the electrical and the optical power penalties are consistent with those found in [4] and [6]. The optical power penalty curve given in Figure 2.10 is the same as the one sketched for DC-coupled worst case in [6]; and the electrical power penalty curve presented in Figure 2.9 is the same as the one illustrated for the worst case power penalty at optimized decision threshold setting in [4]. The only difference is that the crosstalk-crosstalk beat terms are neglected by [4] and [6]. This only affects the optimum threshold level and not the error probabilities. Thus, the power penalty curves sketched in this

chapter are the same as those illustrated in [4] and [6].

Chapter 3

Crosstalk as a Random Process

In Chapter 3, we analyzed the systems under worst case crosstalk. We made the assumption that the crosstalk is constant for all time. Starting from this chapter, we will model it as a random process.

We generally assume that the coherent crosstalk is formed as a result of the mixing of another communication signal. Therefore, it is composed of binary symbols which are random in each slot. These time slots are not necessarily synchronous with those of the communication signal and even the bit rate of the crosstalk signal may not be equal to that of the desired signal[1]. In the evolution of this chapter, we will assume the phase and the polarization parameters of the crosstalk are at the worst case and remain unchanged throughout the communication. Therefore, we will drop the vector notation along with this chapter and deal only with the amplitudes.

This chapter consists of three sections. First section contains the analysis of the system when the bit slots of the crosstalk are synchronous with those of the signal. Section 2 generalizes the analysis to the case where signal and crosstalk are asynchronous. Each section is separated into two subsections where one of them deals with the case where the crosstalk bit rate is less than that of the signal; and the other deals with greater crosstalk

[1] We assume that the bit rate of the crosstalk is either an integer multiple or an integer factor of that of the signal which is commonly the actual case in practice. The standard optical channels OC-1 to OC-192 have such bit rates and we will pursue the analyses with this assumption.

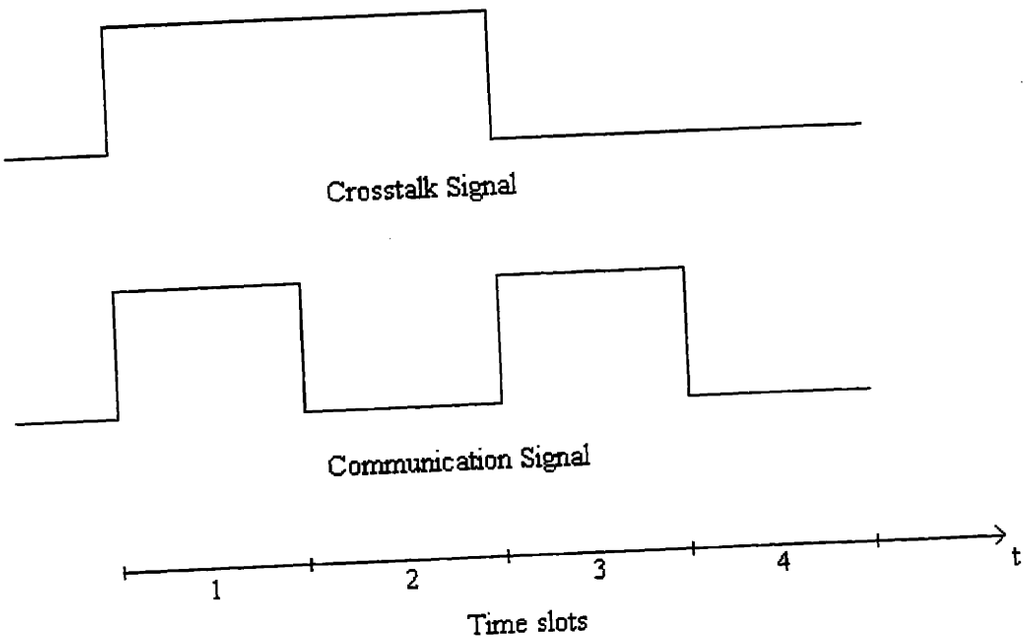

Figure 3-1: Crosstalk Signal, Communication Signal and the time slots. Communication Signal is twice as fast as crosstalk.

bit rates. There is a subsection about AC coupled decision thresholding as well at the end of the first section. The chapter will be finalized with conclusions and remarks.

3.1 Synchronous Bit Slots

3.1.1 Lower Crosstalk Bit Rate

A sample sequence where the crosstalk is synchronous to the signal at a lower bit rate is given in Figure 3.1.

The ratio of the bit rates of the two signals given in Figure 3.1 is $n = 2$. One can observe that the figure illustrates all the possible combinations of signal and crosstalk. In four consecutive time slots, (signal, crosstalk) pair becomes (1,1), (0,1), (1,0), (0,0) in the given order. As indicated before, the matched filter behaves as an integrator with an

integrating interval T where T is the bit period of a signal pulse. We have just illustrated that when the signal and crosstalk are synchronous and crosstalk is at a lower bit rate, in an interval of integration, crosstalk remains constant at $i_{c,1}$ or 0 with probability $\frac{1}{2}$. Consequently, we may write the detected current as in Equation 2.30.

$$i_{\text{det}}(t) = i_s(t) - 2\sqrt{i_s(t)i_c(t)} + i_c(t) \text{ Amps} \tag{3.1}$$

This time $i_c(t)$ is not a constant as it was in Chapter 2. $i_s(t)$ is constant at $i_{s,1}$ and 0 given that the signal bit is a 1 and a 0 respectively. Let us redefine r as follows.

$$r \triangleq \frac{i_{c,1}}{i_{s,1}} = \frac{P_{c,1}}{P_{s,1}} \tag{3.2}$$

The detected current at the output of the sampler $i'(kT)$ is

$$i'(kT) = \begin{cases} T(i_{s,1} + i_{c,1} - 2\sqrt{i_{s,1}i_{c,1}}) + n'(kT) & \text{when the signal and crosstalk are both 1} \\ Ti_{s,1} + n'(kT) & \text{when the signal is a 1 and crosstalk is a 0} \\ Ti_{c,1} + n'(kT) & \text{when the signal is a 0 and crosstalk is a 1} \\ n'(kT) & \text{when the signal and crosstalk are both 0} \end{cases}$$

where $n'(t)$ is the noise portion of the signal at the output of the integrator. The conditional pdfs of $i'(kT)$ given that the signal is a mark and given that the signal is a space are illustrated in Figure 4.2. (Note that the curve $p(s|H_i) = \frac{1}{2}p(s|H_i, i_c = 0) + \frac{1}{2}p(s|H_i, i_c = i_{c,1})$).

When the decision threshold is set to $i_{th} = \frac{Ti_{s,1}}{2}(1-x)$, the error performance becomes,

$$\begin{aligned} P(E) &= \frac{1}{4}P\left(E|H_0, i_c = 0\right) + \frac{1}{4}P\left(E|H_1, i_c = 0\right) \\ &\quad + \frac{1}{4}P\left(E|H_0, i_c = i_{c,1}\right) + \frac{1}{4}P\left(E|H_0, i_c = i_{c,1}\right) \\ &= \frac{1}{4}Q\left(\frac{Ti_{s,1}}{2\sigma_{n'(t)}}(1-x)\right) + \frac{1}{4}Q\left(\frac{Ti_{s,1}}{2\sigma_{n'(t)}}(1+x)\right) + \frac{1}{4}Q\left(\frac{Ti_{s,1}}{2\sigma_{n'(t)}}(1-x-2r)\right) \end{aligned} \tag{3.3}$$

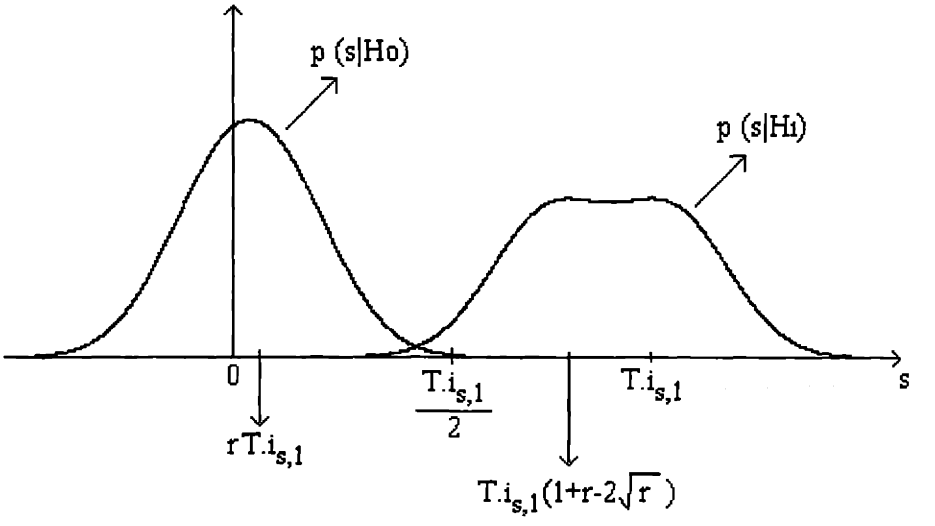

Figure 3-2: The pdf of the detected current conditioned on the transmitted signal.

$$+\frac{1}{4}Q\left(\frac{Ti_{s,1}}{2\sigma_{n'(t)}}\left(2+2r-4\sqrt{r}-1+x\right)\right) \tag{3.4}$$

Rewriting $\frac{Ti_{s,1}}{2\sigma_{n'(t)}}$ as $\sqrt{\frac{(Ti_{s,1})^2}{4\sigma^2_{n'(t)}}}$ and $\sigma^2_{n'(t)}$ as $\frac{N_0}{2}T$, and finally plugging $E_b = \frac{1}{2}Ti_{s,1}{}^2$ simplifies the expression to

$$\begin{aligned} P(E) &= \frac{1}{4}Q\left((1-x)\sqrt{\frac{E_b}{N_o}}\right)+\frac{1}{4}Q\left((1+x)\sqrt{\frac{E_b}{N_o}}\right)+\frac{1}{4}Q\left((1-x-2r)\sqrt{\frac{E_b}{N_o}}\right) \\ &\quad +\frac{1}{4}Q\left(\left(1+x+2r-4\sqrt{r}\right)\sqrt{\frac{E_b}{N_o}}\right) \end{aligned} \tag{3.5}$$

DC Coupled Decision Threshold

If we use DC coupled decision thresholding, x will be set to its optimum value and kept unchanged throughout the communication. To minimize Expression 3.5 to find the optimum static threshold (DC-coupled), we equate the derivative of $P(E)$, which is illustrated below, to 0. Note that the following expression is not the actual value of the

derivative (It is proportional to the exact expression).

$$\frac{dP(E)}{dx} = \exp\left((1-x)^2\frac{E_b}{N_o}\right) - \exp\left((1+x)^2\frac{E_b}{N_o}\right) + \exp\left((1-x-2r)^2\frac{E_b}{N_o}\right) - \exp\left(\left(1+x+2r-4\sqrt{r}\right)^2\frac{E_b}{N_o}\right) \tag{3.6}$$

Figure 3.3 illustrates the derivative of $P(E)$ at $\frac{E_b}{N_o} = 16$ dB versus x and Figure 3.4 presents the three dimensional plot where $\frac{dP(E)}{dx}, \frac{E_b}{N_o}, x$ are the three axes ($\frac{dP(E)}{dx} = 0$ plane is also given in the figure). Note that, given $\frac{E_b}{N_o}$, $\frac{dP(E)}{dx}$ is monotonically increasing over x values. Therefore, $P(E)$ is a convex function of x, and with $x = 2\sqrt{r} - 2r$ which is the only solution to $\frac{dP(E)}{dx} = 0$, the error probability is globally minimized.

If we examine Figures 3.3 and 3.4, we observe that the optimum x ($= x_{opt}$) is very close to $2\sqrt{r} - 2r$ over the range of $\frac{E_b}{N_0}$ values where the error probability is very low ($\sim 10^{-9}$). $x = 2\sqrt{r} - 2r$ makes the arguments of the final two terms equal which are the aposteriori error probabilities given that the crosstalk bit is a 1.

If we plug x_{opt} in Equation 3.4, we get

$$P(E) = \underbrace{\frac{1}{4}Q\left(\left(1-2\sqrt{r}+2r\right)\sqrt{\frac{E_b}{N_o}}\right)}_{(i)} + \underbrace{\frac{1}{4}Q\left(\left(1+2\sqrt{r}-2r\right)\sqrt{\frac{E_b}{N_o}}\right)}_{(ii)} + \underbrace{\frac{1}{2}Q\left(\left(1-2\sqrt{r}\right)\sqrt{\frac{E_b}{N_o}}\right)}_{(iii)} \tag{3.7}$$

These three terms of Equation 3.7 ($(i), (ii), (iii)$), and their sum (i.e., $P(E)$) are illustrated separately in Figure 3.5 for $r = -20$ dB, we observe that the second term ((ii)) is negligible and the exact error probability is almost equal to (iii). The performance curve is upper and lower bounded as given in the following relation.

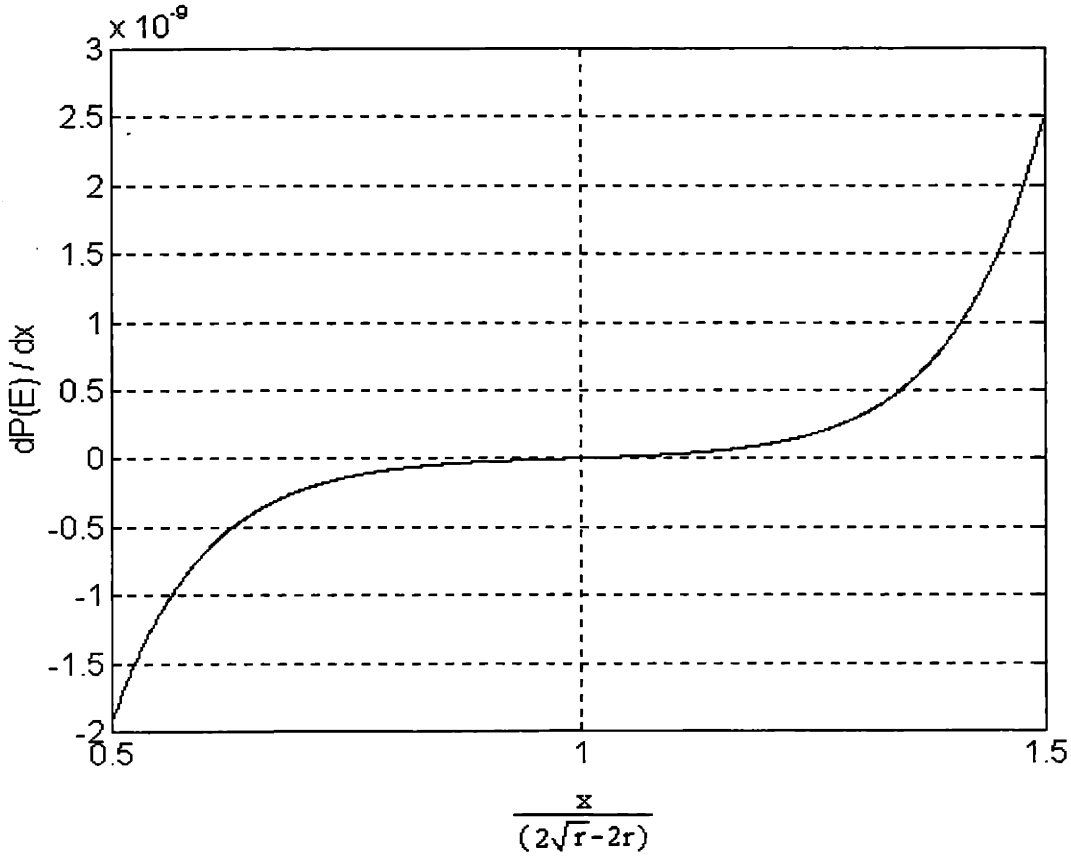

Figure 3-3: The derivative function shows us that there is a global maximum of the performance function when $x = 2\sqrt{r} - 2r$

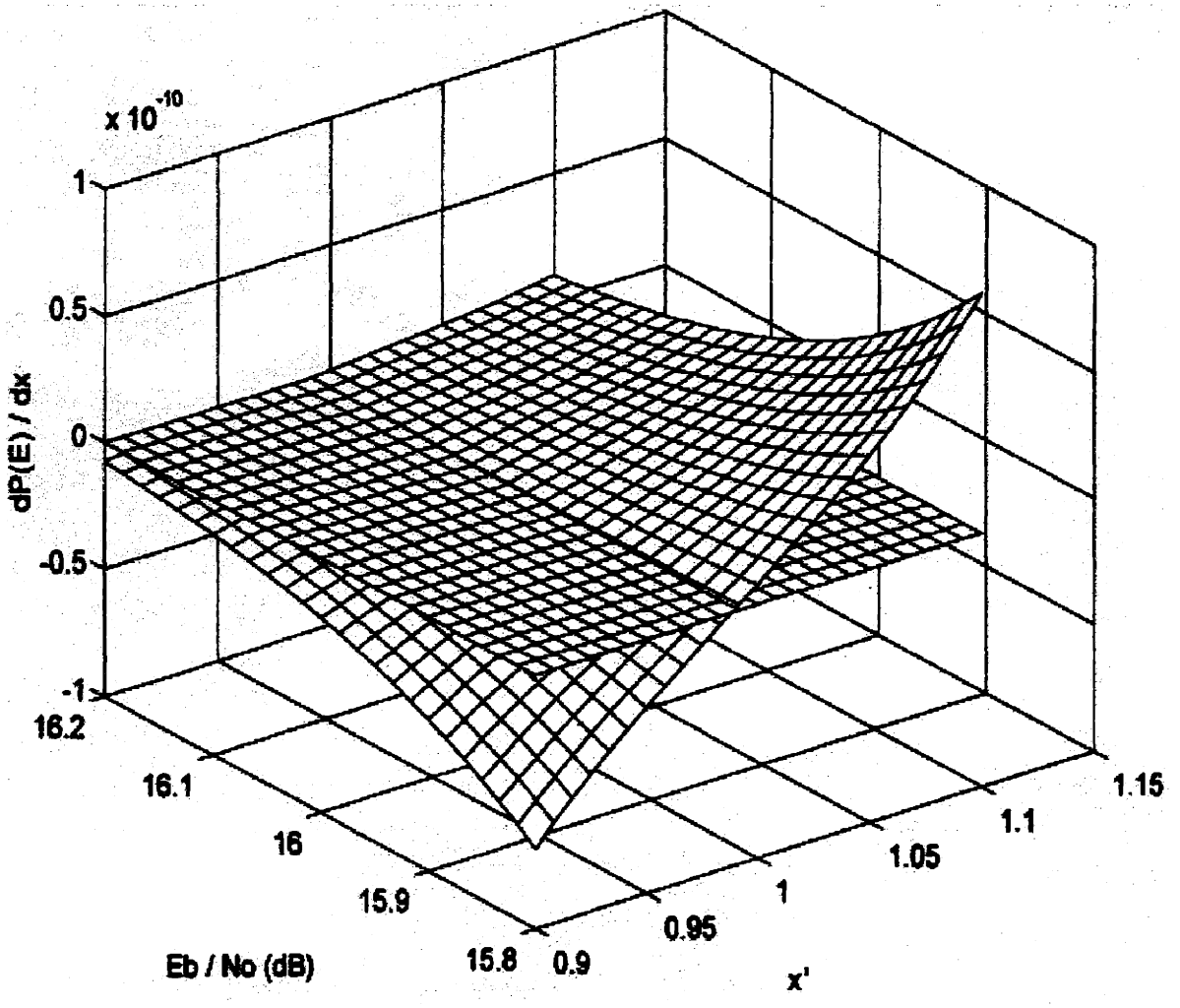

Figure 3-4: It can be seen that $\frac{dP(E)}{dx}$ is monotonically increasing and $x = 2\sqrt{r} - 2r$ is the optimum value over the given range of values of $\frac{E_b}{N_0}$ and x. $\frac{dP(E)}{dx} = 0$ plane is also illustrated.

$$\frac{1}{2}Q\left(\left(1-2\sqrt{r}\right)\sqrt{\frac{E_b}{N_o}}\right) < P(E) < \frac{3}{4}Q\left(\left(1-2\sqrt{r}\right)\sqrt{\frac{E_b}{N_o}}\right) \tag{3.8}$$

These bounds are the same as the expression for error performance of the worst case within a scaling factor. The lower bound and the exact performance curve were illustrated in Figure 3.5. Using these bounds, the optical power penalty can be evaluated as follows.

$$\gamma_{op} \cong -10\log(1-2\sqrt{r})dB \tag{3.9}$$

where γ_{op} was illustrated in Figure 2.10. In Expression 3.9, we ignored the effect of the factor $\frac{3}{4}$. In fact, there is a small effect due to the factor. Let γ_{eff} be the effective electrical power penalty taking the effect of a factor k near the Q function into consideration. The following analysis calculates the impact of that k on the power penalty of the system.

$$kQ\left(\gamma_{op}^{-1}\sqrt{\frac{E_b}{N_o}}\right) = kQ\left(\sqrt{\gamma_p^{-1}\frac{E_b}{N_o}}\right) \tag{3.10}$$

where γ_p and γ_{op} are the electrical and the optical power penalties respectively. Recall that $\gamma_p = \gamma_{op}^2$. Let $y = \sqrt{\gamma_p^{-1}\frac{E_b}{N_o}}$. Then,

$$\begin{aligned} kQ(y) &= \frac{1}{2\pi}\int_y^\infty k\exp\left(-\frac{\sigma^2}{2}\right)d\sigma \qquad (3.11)\\ &= \frac{1}{2\pi}\int_y^\infty \exp\left(-\frac{\sigma^2-\ln(k)}{2}\right)d\sigma \\ &= \frac{1}{2\pi}\int_{\sqrt{y^2-\ln(k)}}^\infty \exp\left(-\frac{\rho^2}{2}\right)d\rho \\ &= Q\left(\sqrt{\gamma_p^{-1}\frac{E_b}{N_o}-\ln(k)}\right) \\ &= Q\left[\left(\gamma_p^{-1}-\frac{\ln(k)}{E_b/N_o}\right)\frac{E_b}{N_o}\right] \qquad (3.12) \end{aligned}$$

Thus,

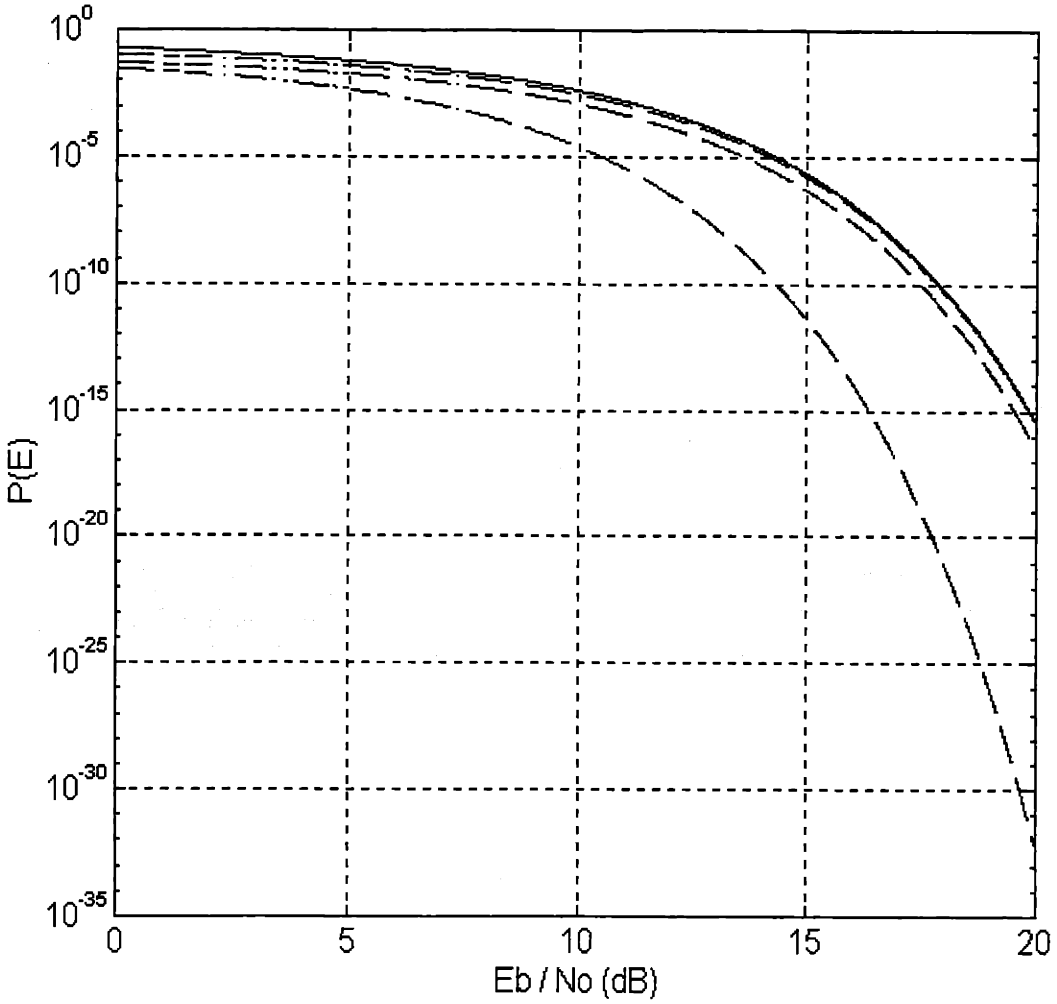

Figure 3-5: The first, second, and third terms of the Expression 3.6 $((i), (ii), (iii))$ are illustrated as dotted curves respectively. The solid curve represents P(E) when $r = -20$ dB. It can be observed that the third term dominates among the three.

$$\gamma_{eff} = \left(\gamma_p^{-1} - \frac{\ln(k)}{E_b/N_o}\right)^{-1} \tag{3.13}$$
$$= -10\log\left(\gamma_p^{-1} - \frac{\ln(k)}{E_b/N_o}\right) \text{ dB}$$

First, let us consider the upper bound, namely when $k = \frac{3}{4}$. For $\frac{E_b}{N_o} \sim 16$ dB, ($P(E) \sim 10^{-9}$), $\gamma_{eff} = 2.94$ dB whereas $\gamma_p = 3$ dB. Therefore, there is only a 0.06 dB difference in power penalty due to the factor $\frac{3}{4}$. Next, if we consider the lower bound, namely $k = \frac{1}{2}$ around the same $\frac{E_b}{N_o}$ values, $\gamma_{eff} = 2.97$ dB which is even closer to γ_p. Therefore, the effective electrical power penalty is between 2.94 and 2.97 dB. We can deduce from this result that the performance of this system is very close to that utilizing worst case parameters where we have a power penalty of exactly 3 dB.

AC Coupled Decision Threshold

In the previous section after evaluating the error performance, we minimized it over the threshold level parameter x to find the optimum performance. Doing that, we assumed that the threshold is static and remained unchanged throughout the communication. In this section we will investigate what happens to the performance when the threshold is dynamic.

In AC coupled decisioning, the threshold varies depending on the detected waveform. Basically, the decision device filters out the average of the discrete waveform at the output of the sampler, i.e., it has a 0 DC response and the threshold is set to 0. This process is equivalent to setting the threshold to the average of the waveform. Note that this averaging should be performed over a large enough number of samples to guarantee that the ratio of the mark signal bits to the space is almost 1. Let q be the ratio of the number of samples that the averaging is performed to n (which is the ratio of the bit rate of the signal to that of the crosstalk). There are three possible cases depending on whether the number of samples that the averaging is performed is much larger than,

comparable with or much less than n ($q \gg 1$, $q \cong 1$ or $q \ll 1$). In all three cases, the expected threshold level is $\frac{Ti_{s,1}}{2}(1 - \frac{x_{opt}}{2})$ where $x_{opt} = 2\sqrt{r} - 2r$. This is the mid point of the optimum thresholds for the worst case ($\frac{Ti_{s,1}}{2}(1 - x_{opt})$) and the crosstalk-free case ($\frac{Ti_{s,1}}{2}$) because, the possible cases are uniformly distributed between these two cases. The dynamics of the threshold around this mean depends on the region of q. In the following three sections, these cases will be examined and corresponding error performances will be analyzed.

Averaging for $q \gg 1$ If $q \gg 1$, then the averaging is performed over a large number of crosstalk bits as well as signal bits. Since the variance of the threshold around its mean is inversely proportional to q, it can be assumed constant at its expected value. Consequently, the error probability is as given in the following expression.

$$\begin{aligned} P(E) &= \frac{1}{4}Q\left(\left(1 - \frac{x_{opt}}{2}\right)\sqrt{\frac{E_b}{N_o}}\right) + \frac{1}{4}Q\left(\left(1 + \frac{x_{opt}}{2}\right)\sqrt{\frac{E_b}{N_o}}\right) \\ &\quad + \frac{1}{4}Q\left(\left(1 - \frac{x_{opt}}{2} - 2r\right)\sqrt{\frac{E_b}{N_o}}\right) \\ &\quad + \frac{1}{4}Q\left(\left(1 + \frac{x_{opt}}{2} + 2r - 4\sqrt{r}\right)\sqrt{\frac{E_b}{N_o}}\right) \qquad (3.14) \\ &= \frac{1}{4}Q\left(\left(1 - \sqrt{r} + r\right)\sqrt{\frac{E_b}{N_o}}\right) + \frac{1}{4}Q\left(\left(1 + \sqrt{r} - r\right)\sqrt{\frac{E_b}{N_o}}\right) \\ &\quad + \frac{1}{4}Q\left(\left(1 - \sqrt{r} - r\right)\sqrt{\frac{E_b}{N_o}}\right) + \frac{1}{4}Q\left(\left(1 + r - 3\sqrt{r}\right)\sqrt{\frac{E_b}{N_o}}\right) \qquad (3.15) \end{aligned}$$

The first two terms and the last two terms of these expressions are found by conditioning on a 0 crosstalk bit and a 1 crosstalk bit respectively. Note that q should be $\gg 1$ if $n \cong 1$ since the averaging should be done over a large number of signal bits.

Averaging for $q \approx 1$ If $q \cong 1$, then the averaging is over a small number of crosstalk bits. This case can occur only for $n \gg 1$ because the operation is performed over a large

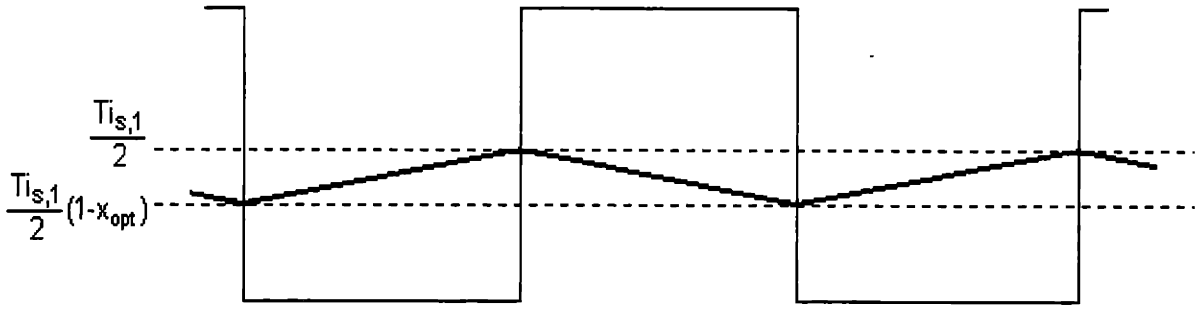

Figure 3-6: The position of the threshold (illustrated with bold solid lines) fluctuates between the two limit points almost linearly since the averaging is performed over $nq \gg 1$ crosstalk bits. The square wave represents the crosstalk bits. Note that the scale is adjusted for clarity.

number of samples and a small number of crosstalk bits.

In this case, the threshold is highly variant. Since the averaging is performed over $nq \gg 1$ samples, it varies slowly but never settles at a level completely. For instance, if $q = 1$, the threshold varies as shown in Figure 3.6. In the figure, the crosstalk bits and the threshold is illustrated simultaneously. Since $n \gg 1$, the threshold varies almost linearly. Since the threshold is variant, so is the error probability. The probability of error in detecting a given bit correctly conditioned on the signal bit being a 0 or a 1 varies in a region enclosed by the worst and the best curves. This region can be defined as follows.

$$Q\left(\left(1+2\sqrt{r}-2r\right)\sqrt{\frac{E_b}{N_o}}\right) \leqslant P(E) \leqslant Q\left(\left(1-4\sqrt{r}+2r\right)\sqrt{\frac{E_b}{N_o}}\right) \tag{3.16}$$

The upper bound represents the error probability given a mark signal at the instant when the threshold is at the optimum value for crosstalk free case. The lower bound represents the error probability given a mark signal bit at the instant when the threshold is at the optimum value for the worst case interference.

However, if we average the error probabilities over all the possible cases, the result will

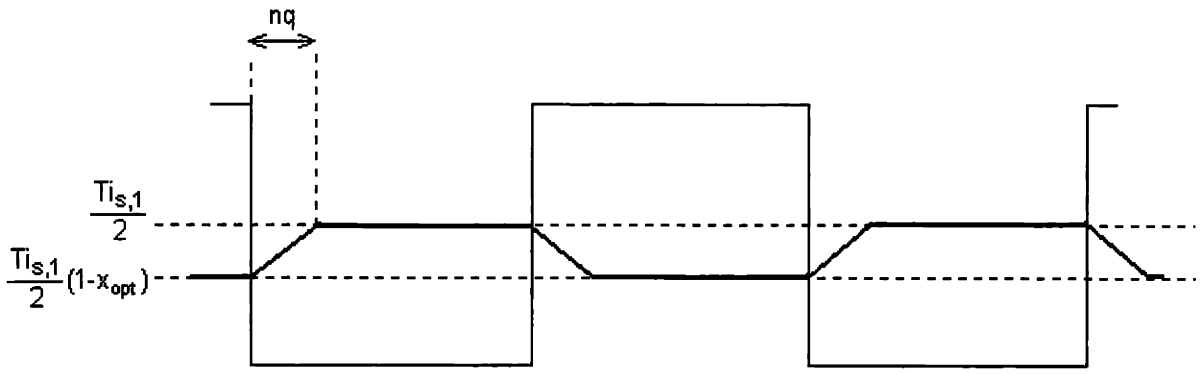

Figure 3-7: The position of the threshold (illustrated with bold solid lines) settles to the optimum value faster this time (nq signal bit periods). The square wave represents the crosstalk bits.

be much closer to the worst case error probability, since the possible cases are uniformly distributed between the worst and the best cases.

Averaging for $q \ll 1$ As explained in the previous section, when $n \gg 1$, if we average over a large number of samples ($nq \gg 1$) then the performance is highly variant and the threshold can hardly settle to the optimum value. This deteriorates the error performance considerably since the worst case is dominant. Thus, for $n \gg 1$, performing the averaging over rather small number of samples (which is still $\gg 1$) by choosing $q \ll 1$ seems to be a better alternative for the threshold to catch the optimum value and settle. The threshold behavior for the same sample of crosstalk bits as in Figure 3.6 is illustrated in Figure 3.7. It can be observed from the figure that the threshold settles to the optimum value faster with a shorter transient. Therefore, the performance remains optimal over a long number of samples. As q approaches 0, the fraction of times that the system achieves optimum performance approaches 1. The performance, thus approaches the following expression asymptotically.

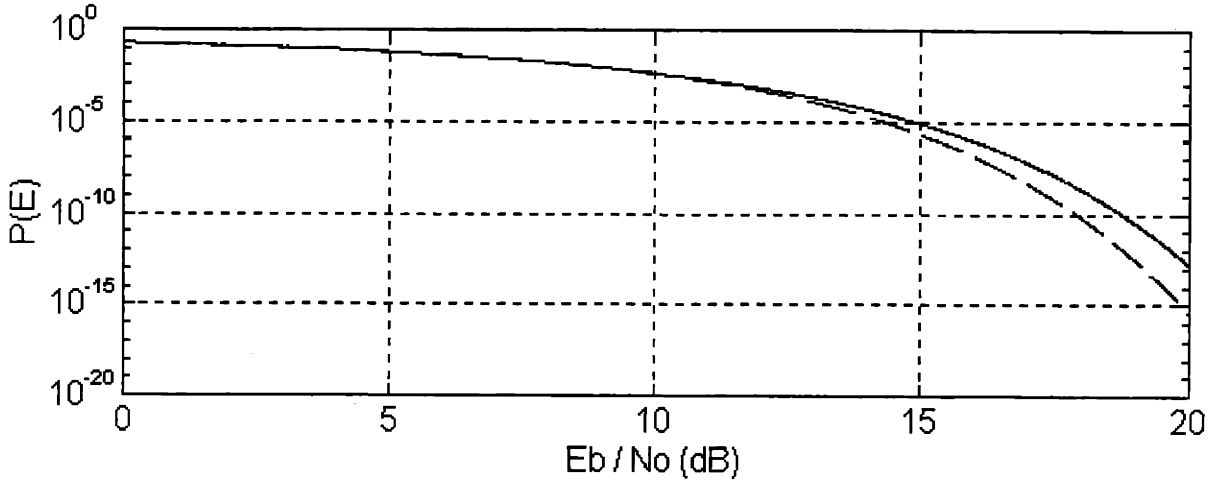

Figure 3-8: The error probabilities for AC thresholding ($q \gg 1$) and optimized static thresholding are illustrated with solid and dashed curves respectively. There is an extra 0.75 dB power penalty for not using static optimized thresholding.

$$P(E) = \frac{1}{2}Q\left(\sqrt{\frac{E_b}{N_o}}\right) + \frac{1}{2}Q\left(\left(1-2\sqrt{r}\right)\sqrt{\frac{E_b}{N_o}}\right) \tag{3.17}$$

where the first term represents the probability of error on a 0 crosstalk bit and the second is on a mark.

The error probability curves corresponding to the cases where $q \gg 1$, $q \ll 1$ and the best and the worst curves for the case $q \cong 1$ are illustrated in Figures 3.8, 3.9 and 3.10 together with the error probability of static threshold at $r = -20$ dB.

In fact, the dynamic thresholding is a method to keep the threshold at its optimum value when the system parameters (e.g., received power, crosstalk power, etc.) are not constant. Also, with dynamic thresholding there is no need for any initial adjustment on the threshold. However, as we proved in the above sections, the performance of the systems can be satisfactory only under some certain conditions with dynamic thresholding. Furthermore, it may not be stable at the optimum value even when the system parameters are constant.

Another very important result can be deduced considering the case where $q \ll 1$

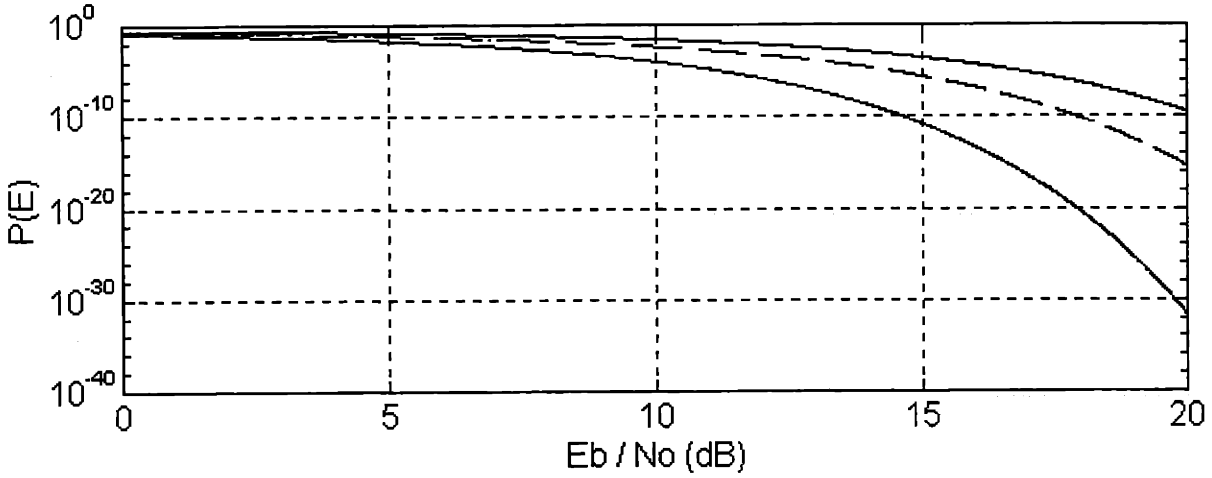

Figure 3-9: The best and worst error probability curves (conditional on signal bit) for AC thresholding are illustrated with solid curves ($q \approx 1$) and the DC coupled best performance is illustrated with dashed curve. The overall performance of the AC coupled case is close to the worst curve.

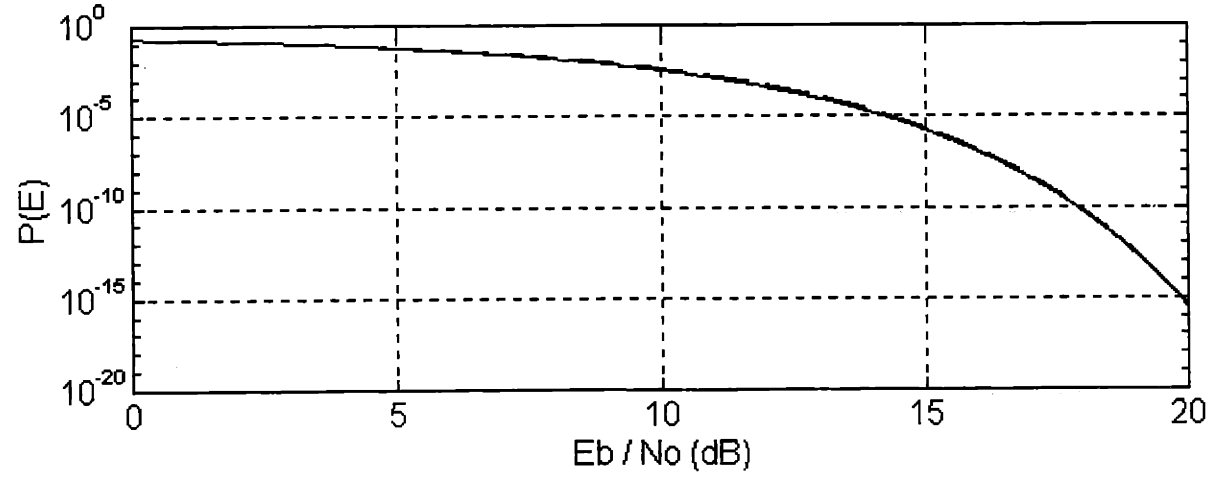

Figure 3-10: The error probabilities for AC thresholding ($q \ll 1$) and optimized static thresholding are illustrated with solid and dashed curves respectively. The peformance of the AC coupled case approaches to the DC coupled case asymptotically.

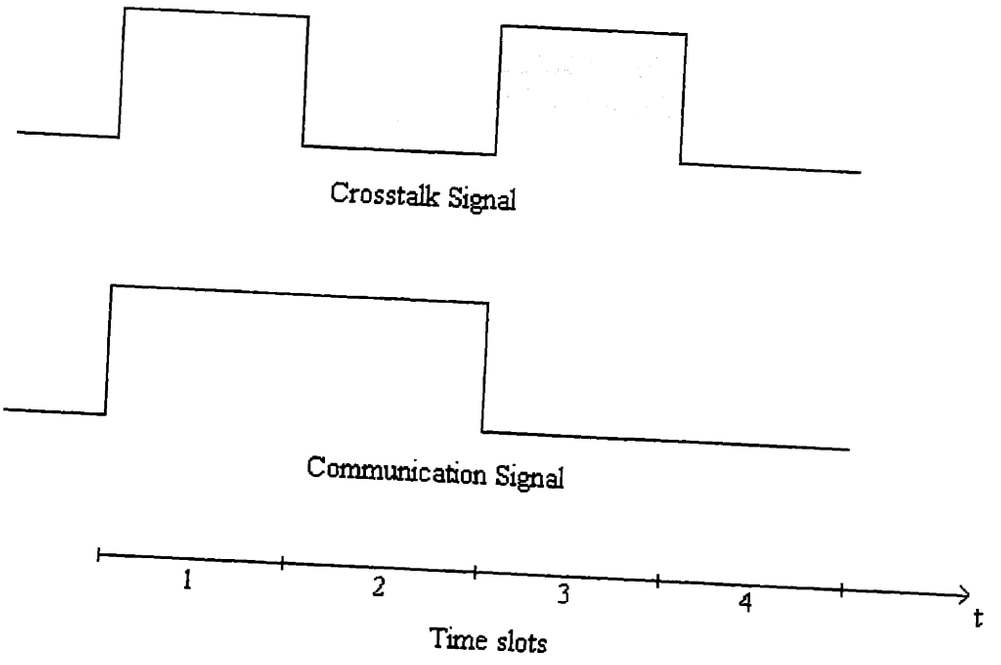

Figure 3-11: Crosstalk Signal, Communication Signal and the time slots. Crosstalk Signal is twice as fast as communication.

noting that Expression 3.17 is also the error probability when the crosstalk bit sequence is known by the receiver. Hence, even the bit sequence of the crosstalk is given, the error performance of the system cannot be improved considerably using that information (as illustrated in Figure 3.10).

3.1.2 Higher Crosstalk Bit Rate

Figure 3.11 illustrates the signal and the crosstalk when the ratio of the bit rate of the crosstalk to that of the signal is $n = 2$, and the signal and the crosstalk are synchronous.

Let us begin with the same detected current as in Expression 3.1 and let us define r similar to Equation 3.2. The interval of integration of the matched filter is a bit period of the signal (i.e., T). This time, in one period, the crosstalk signal may not be constant, because there are n bit periods of crosstalk (i.e., T_c) in T secs. Hence,

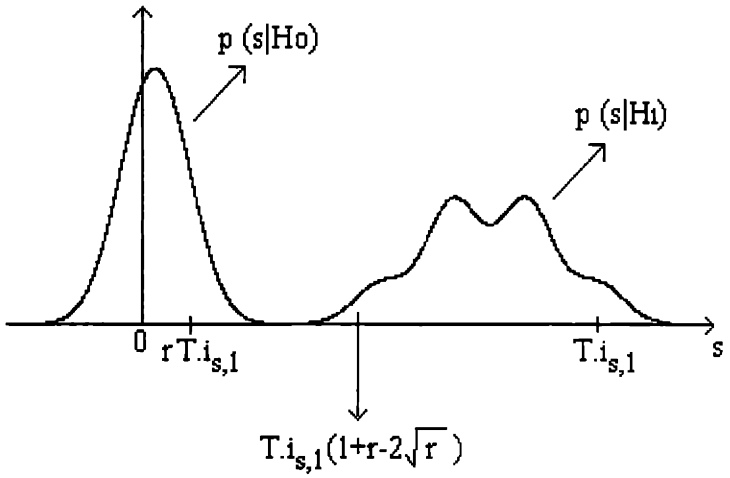

Figure 3-12: The probability density of the detected current conditioned on the signal bit. $n = 3$ for this case.

$$T_c = \frac{T}{n} \tag{3.18}$$

Let us define m such that, m of the n crosstalk bits under a signal bit is 1. Therefore at the output of the sampler, we have

$$i'(kT) = \begin{cases} T\left(i_{s,1} + \frac{m}{n} i_{c,1} - 2\frac{m}{n}\sqrt{i_{s,1} i_{c,1}}\right) + n'(kT) & \text{when the signal bit is a 1.} \\ T\frac{m}{n} i_{c,1} + n'(kT) & \text{when the signal bit is a 0.} \end{cases} \tag{3.19}$$

Since the consecutive bits are independent and 0, 1 are equally likely m has a Binomial distribution over $[0, n]$, which is,

$$P(m = l) = \binom{n}{l}\left(\frac{1}{2}\right)^n \tag{3.20}$$

The pdf of $i'(kT)$ conditioned on the signal bit is illustrated in Figure 3.12. There are $n + 1$ peaks on each curve (the ones over 0 are not distinguishable) due to the Binomial

distribution of crosstalk. The error probability conditioned on m is

$$P(E|m=l) = \frac{1}{2}P(E|m=l,H_1) + \frac{1}{2}P(E|m=l,H_0) \tag{3.21}$$

When the threshold is set to $\frac{TI_{s,1}}{2}(1-x)$, the above probability becomes,

$$P(E|m=l) = \frac{1}{2}Q\left(\left(1-x-2r\frac{l}{n}\right)\sqrt{\frac{E_b}{N_0}}\right) + \frac{1}{2}Q\left(\left(1+x-4\frac{l}{n}\sqrt{r}+2r\frac{l}{n}\right)\sqrt{\frac{E_b}{N_0}}\right) \tag{3.22}$$

The unconditional error probability is thus,

$$\begin{aligned} P(E) &= \sum_{l=0}^{n} P(E|m=l)P(m=l) \\ &= \sum_{l=0}^{n}\binom{n}{l}\left(\frac{1}{2}\right)^{n+1}\left[Q\left(\left(1-x-2r\frac{l}{n}\right)\sqrt{\frac{E_b}{N_0}}\right)\right. \\ &\quad \left. +Q\left(\left(1+x-4\frac{l}{n}\sqrt{r}+2r\frac{l}{n}\right)\sqrt{\frac{E_b}{N_0}}\right)\right] \end{aligned} \tag{3.23}$$

To optimize the threshold, we take the derivative of both sides with respect to x and equate to 0. Differentiating the error probability, we get

$$\begin{aligned} \frac{d}{dx}P(E) &= \sum_{l=0}^{n}\binom{n}{l}\left(\frac{1}{2}\right)^{n+1}\left[-\exp\left(\left(1-x_{opt}-2r\frac{l}{n}\right)\sqrt{\frac{E_b}{N_0}}\right)\right. \\ &\quad \left. +\exp\left(\left(1+x_{opt}-4\frac{l}{n}\sqrt{r}+2r\frac{l}{n}\right)\sqrt{\frac{E_b}{N_0}}\right)\right] \end{aligned} \tag{3.24}$$

This expression is illustrated for $n = 2, 10$ and 100 when $\frac{E_b}{N_0} = 16\ dB$ in Figure 3.13. The three dimensional plot where $\frac{dP(E)}{dx}, \frac{E_b}{N_0}, x$ are the three axes is also given in Figure 3.14 for $n = 10$ together with the plane $\frac{dP(E)}{dx} = 0$. It can be seen from this figure that $x_{opt} \cong 0.75(2\sqrt{r}-2r)$ in the given range of values of $\frac{E_b}{N_0}$ and it increases with increasing

$\frac{E_b}{N_0}$. Note that, given $\frac{E_b}{N_o}$, $\frac{dP(E)}{dx}$ is monotonically increasing over x values. Therefore, $P(E)$ is a convex function of x, and with the x value which is the only solution to $\frac{dP(E)}{dx} = 0$, the error probability is globally minimized.

Finally, the performance of the system for $n = 10$ and $n = 100$ are sketched for the static threshold which is optimized at $\frac{E_b}{N_0} = 16\ dB$ together with the baseline and the worst case performance curves in Figure 3.15 for $r = -20$ dB. One can observe from the figure that at probability of error of 10^{-10}, there is 1.5 dB power penalty when $n = 10$ and 1 dB power penalty when $n = 100$. We can conclude that as the rate of the crosstalk increases, the performance improves.

The reason for this can be explained as follows. The mean and the variance of the crosstalk portion of the sample at the output of the matched filter can be written as follows.

$$\begin{aligned} \text{mean} &= \frac{1}{2}\frac{T_c}{T}nr \\ &= \frac{r}{2} \end{aligned} \tag{3.25}$$

$$\begin{aligned} \text{variance} &= n\left(\frac{1}{2}\frac{T_c}{T}r\right)^2 \\ &= \frac{r^2}{4n} \end{aligned} \tag{3.26}$$

conditioned on a 0 signal bit, and

$$\begin{aligned} \text{mean} &= -\frac{1}{2}\frac{T_c}{T}n2\sqrt{r} + \frac{1}{2}\frac{T_c}{T}nr \\ &= -\sqrt{r} + \frac{r}{2} \end{aligned} \tag{3.27}$$

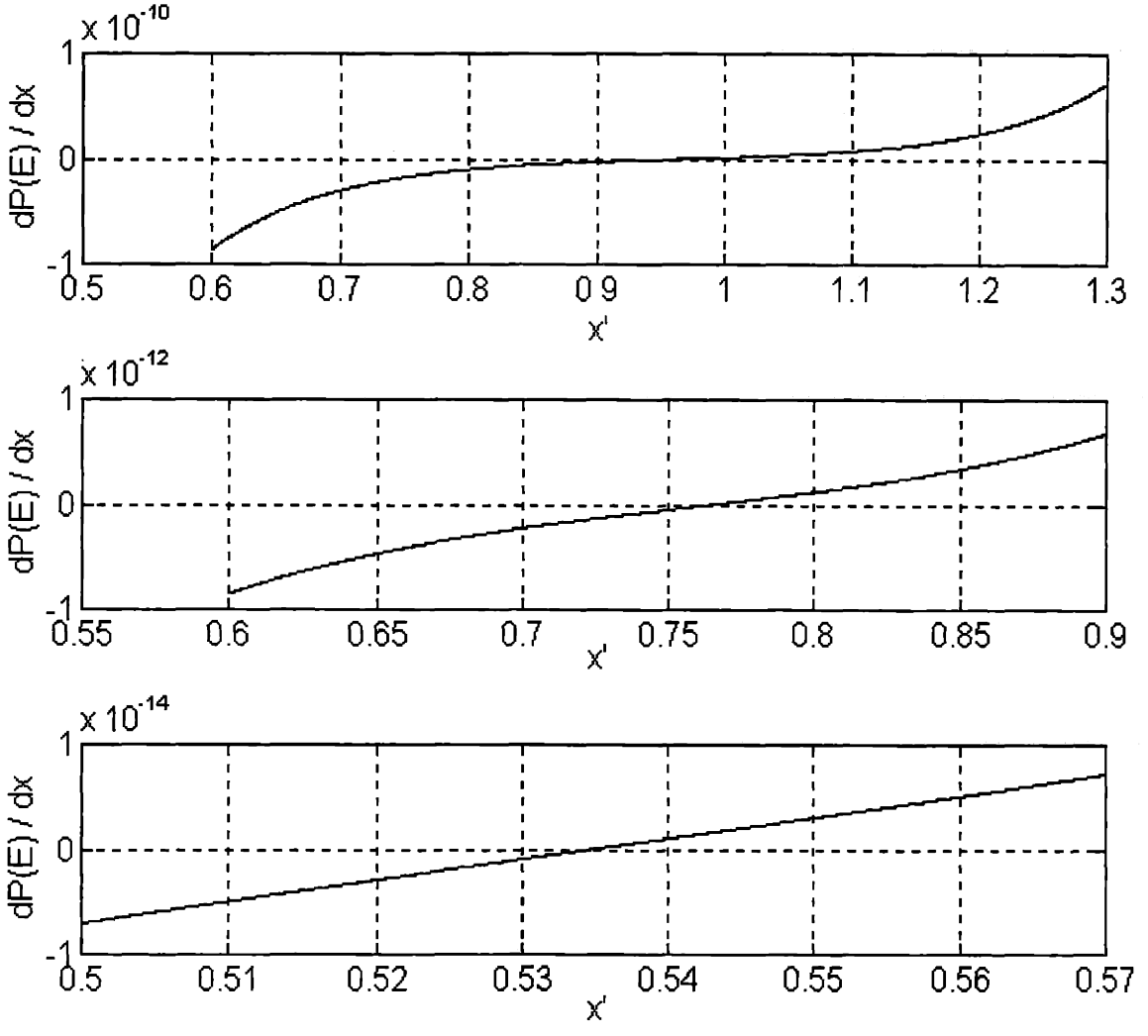

Figure 3-13: The derivative of the probability of error expression for various values of rate ratio. x' denotes normalized x (i.e., $\frac{x}{2\sqrt{r}-2r}$). These sketches show us that x_{opt} is achieved at $2\sqrt{r}-2r$ for n values close to 1, and approaches to $\sqrt{r}-r$ as n increases.

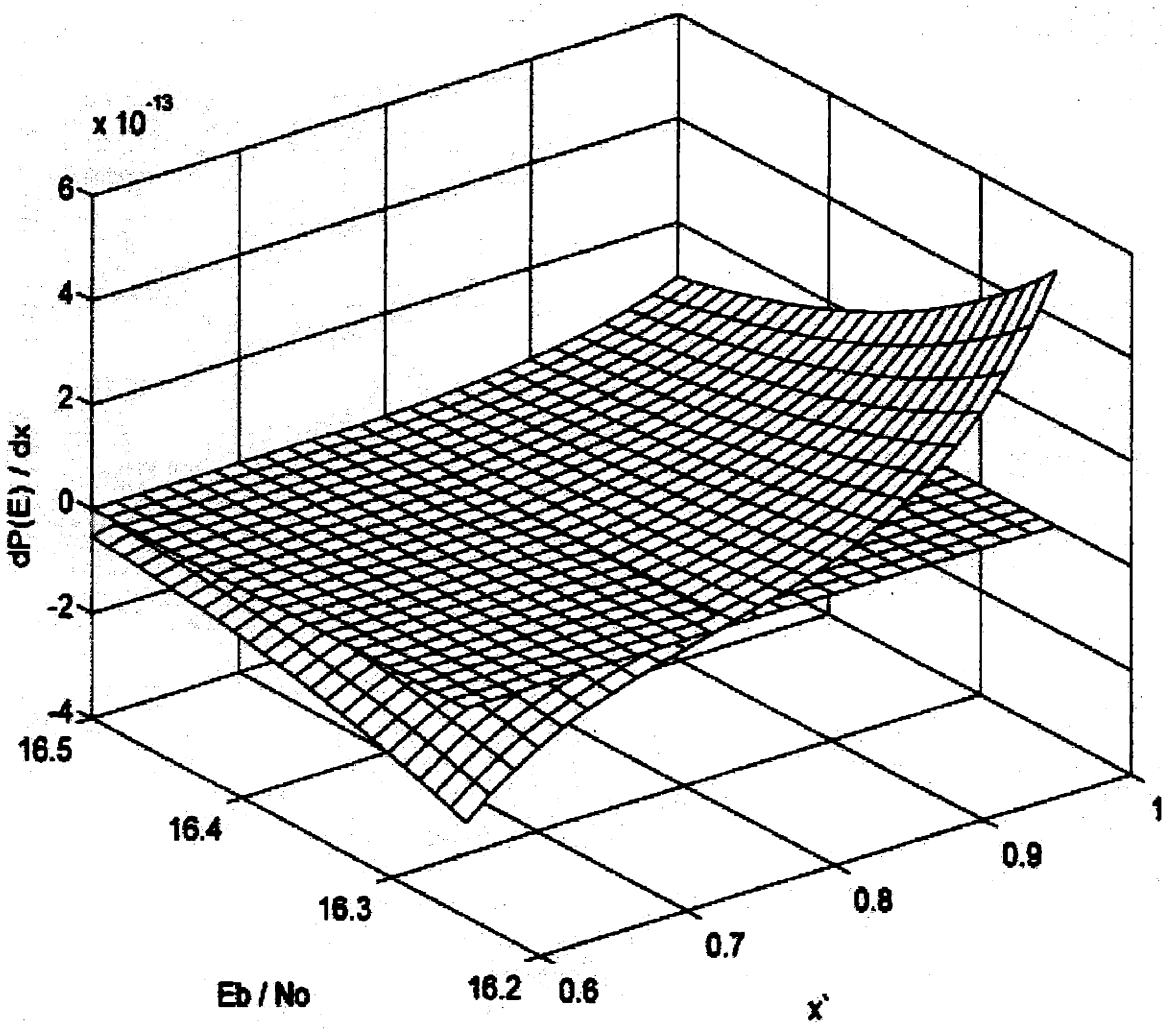

Figure 3-14: It can be seen that $\frac{dP(E)}{dx}$ is monotonically increasing and $x \approx 0.75\,(2\sqrt{r} - 2r)$ is the optimum value over the given range of values of $\frac{E_b}{N_0}$ and x for $n = 10$. $\frac{dP(E)}{dx} = 0$ plane is also illustrated.

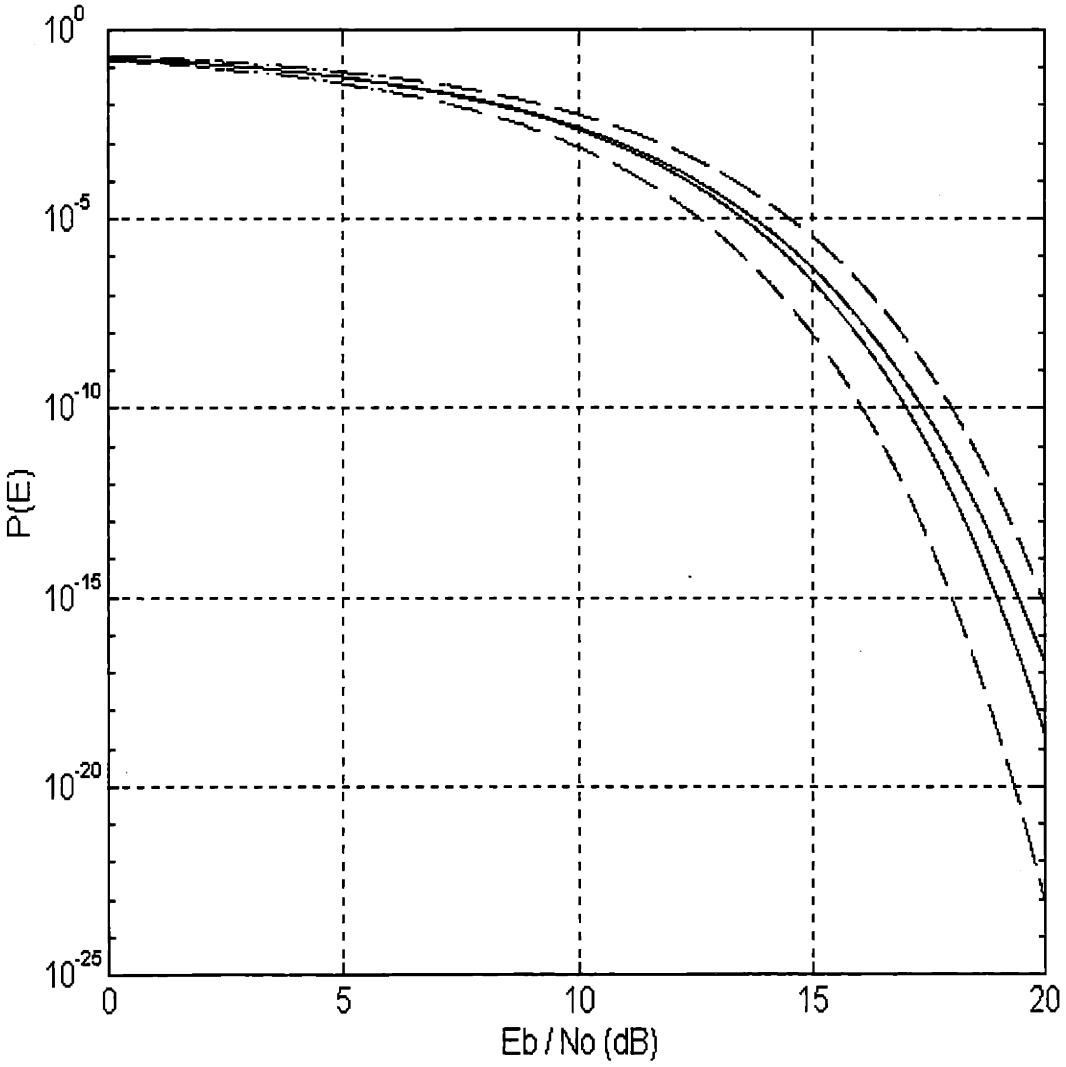

Figure 3-15: Dotted curves represent the baseline and the worst case performances. The solid lines represent optimized static $n = 10$, optimized static $n = 100$ performances. $n = 10$ curve performs 1 dB better than the worst case and 0.35 dB worse than $n = 100$ which performs 0.65 dB worse than the crosstalk-free system.

$$\begin{aligned} \text{variance} &= n\left[\left(\frac{1}{2}\frac{T_c}{T}2\sqrt{r}\right)^2 + \left(\frac{1}{2}\frac{T_c}{T}r\right)^2\right] \\ &= \frac{r - \frac{r^2}{4}}{n} \end{aligned} \tag{3.28}$$

conditioned on a 1 signal bit. The above results show that the mean of the crosstalk sample is constant and the variance decreases inversely with n. Therefore, the error probability decreases with increasing n. As n approaches ∞, the error probability under crosstalk of power r times as much as the signal power approaches to that of the worst case system with crosstalk which has power $\frac{r}{2}$ times the signal power. Also, along with the mean and variance values found above and for large n, we can approximate the distribution of the crosstalk sample as Gaussian.

3.2 Asynchronous Bit Slots

3.2.1 Higher Crosstalk Bit Rate

A sample sequence of the signal and crosstalk is given in Figure 3.16 where the signal is asynchronous with the crosstalk and the crosstalk source is transmitting at a higher bit rate. The ratio of the bit rates of the two signals given in Figure 3.16 is 2.

One can observe from the figure that there are two crosstalk bits during the transmission of which the signal transition occurs. We will call these bits, the "transition bits"[2] and all others, the "non-transition bits". d is the time after the start of the first transition bit before the transition of the signal. It is reasonable to define d as a uniform random variable over $(0, T_c)$ where T_c is the bit period of the crosstalk signal. Note that $T = nT_c$. $T_c - d$ is the time before the end of the second transition bit after the signal

[2]Note that the transition is defined as the instant that one bit ends and the next one begins. These two bits are not necessarily different.

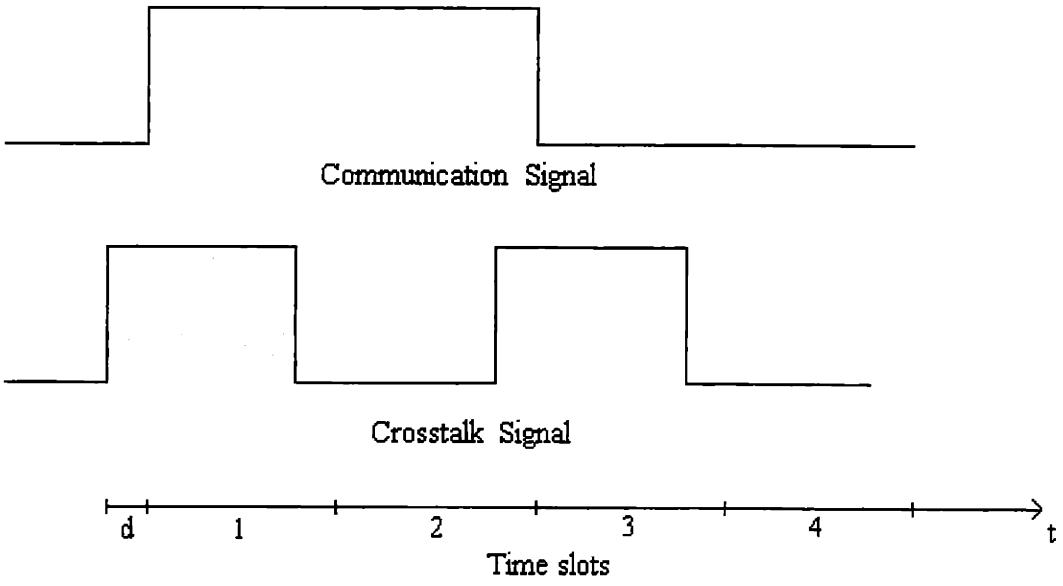

Figure 3-16: Communication and crosstalk signals where n=2. d is the amount of asynchronism between the two.

transition. Let $r_{t,1}$ and $r_{t,2}$ represent the bit values of these two transition bits, namely, 1 if the transition bit is 1 and 0 if it is 0. Therefore $r_{t,1}$ and $r_{t,2}$ are IID Bernoulli random variables. Within a signal bit time, the total duration of transition bits is T_c and that of non-transition bits is $(n-1)T_c$ (i.e., $T_c + (n-1)T_c = T$). Let us define m as the number of non-transition crosstalk bits that are 1. At the output of the sampler we have the following.

$$\begin{aligned} i'(kT) &= Ti_{s,1} + i_{c,1}\left[(n-1)T_c\frac{m}{n-1} + dr_{t,1} + (T_c - d)r_{t,2}\right] \\ &\quad -2\sqrt{i_{s,1}i_{c,1}}\left[(n-1)T_c\frac{m}{n-1} + dr_{t,1} + (T_c - d)r_{t,2}\right] \end{aligned} \tag{3.29}$$

when the signal bit is a 1. Rewriting this with $i_{c,1} = ri_{s,1}$ and $T_c = \frac{T}{n}$, $i'(kT)$ becomes,

$$i'(kT) = Ti_{s,1}\left\{1 + (r - 2\sqrt{r})\left[\frac{m + r_{t,2}}{n} + \frac{d}{T}(r_{t,1} - r_{t,2})\right]\right\} \tag{3.30}$$

Let $g(d, m, n, r_{t,1}, r_{t,2}) \triangleq \left[\frac{m+r_{t,2}}{n} + \frac{d}{T}(r_{t,1} - r_{t,2})\right]$. Then,

$$i'(kT) = Ti_{s,1}\left[1 + (r - 2\sqrt{r})g(d, m, n, r_{t,1}, r_{t,2})\right] \tag{3.31}$$

When the signal bit is a 0, the detected current at the output of the sampler becomes,

$$i'(kT) = Ti_{s,1}rg(d, m, n, r_{t,1}, r_{t,2}) \tag{3.32}$$

When we set the decision threshold to $\frac{i_{s,1}T}{2}(1 - x)$, the probability of error conditioned on $g = g(d, m, n, r_{t,1}, r_{t,2})$ becomes,

$$\begin{aligned} P\left(E|g(d, m, n, r_{t,1}, r_{t,2})\right) &= \frac{1}{2}Q\left[\frac{Ti_{s,1}}{2\sigma_{n'(t)}}\left(1 + x + (2r - 4\sqrt{r})g(d, m, n, r_{t,1}, r_{t,2})\right)\right] \\ &\quad + \frac{1}{2}Q\left[\frac{Ti_{s,1}}{2\sigma_{n'(t)}}\left(1 - x - 2rg(d, m, n, r_{t,1}, r_{t,2})\right)\right] \qquad (3.33) \\ &= \frac{1}{2}Q\left[\sqrt{\frac{E_b}{N_0}}\left(1 + x + (2r - 4\sqrt{r})g(d, m, n, r_{t,1}, r_{t,2})\right)\right] \\ &\quad + \frac{1}{2}Q\left[\sqrt{\frac{E_b}{N_0}}\left(1 - x - 2rg(d, m, n, r_{t,1}, r_{t,2})\right)\right] \qquad (3.34) \end{aligned}$$

Since $d, m, r_{t,1}$ and $r_{t,2}$ are independent, the unconditioned probability of error can be found using total probability theorem as follows.

$$P(E) = \int_0^{T/n} \sum_{m=0}^{n-1} \sum_{r_{t,1}=0}^{1} \sum_{r_{t,2}=0}^{1} P\left(E|g(\tau, m, n, r_{t,1}, r_{t,2})\right) \frac{1}{T}\binom{n-1}{m}\left(\frac{1}{2}\right)^{n-1}\left(\frac{1}{2}\right)^{2} d\tau \tag{3.35}$$

The optimum decision threshold (i.e., optimum x) can be found by solving the following equation.

$$\frac{dP(E)}{dx} = 0 \tag{3.36}$$

where

$$\frac{dP(E)}{dx} = \int_0^{T/n} \sum_{m=0}^{n-1} \sum_{r_{t,1}=0}^{1} \sum_{r_{t,2}=0}^{1} \frac{dP\left(E|g(\tau, m, n, r_{t,1}, r_{t,2})\right)}{dx} \frac{1}{T} \binom{n-1}{m} \left(\frac{1}{2}\right)^{n-1} \left(\frac{1}{2}\right)^{2} d\tau \tag{3.37}$$

The derivative of the probability of error with respect to x versus $x' = \frac{x}{2\sqrt{r}-2r}$ is illustrated in Figure 3.17 for $n = 1$, 2 and 10 at constant $\frac{E_b}{N_0} = 16$ dB. One can observe that when $n = 1$, the optimum x is approximately $2\sqrt{r} - 2r$. As n increases, this optimum value approaches to $\sqrt{r} - r$. Similar to the synchronous system, $\frac{dP(E)}{dx}$ is monotonically increasing and the solution to the equation $\frac{dP(E)}{dx} = 0$ is the global minimum of $P(E)$. Note that the optimal thresholds are very close to that of the synchronous system (See Figure 3.12 for the optimum thresholds corresponding to the synchronous system).

Figure 3.18 illustrates the performance for $n = 1$ and $n = 10$, together with those of the synchronous system. Even with a careful observation, it is very hard to distinguish these two curves for synchronous and asynchronous slots. Also, the difference between the crosstalk penalty of the asynchronous system and that of the synchronous system decreases as n increases since the number of transition bits are $\frac{1}{n}$ of the total number of bits and this ratio decreases as n increases. However, the two performance curves are very close to each other even for $n = 1$. Therefore, the error probability when the bit slots are synchronous is almost equal to that when the bit slots are asynchronous if the bit rate of the interferer is higher than that of the signal.

3.2.2 Lower Crosstalk Bit Rate

A sample sequence of the signal and the crosstalk is illustrated in Figure 3.19. In this figure, the rate of the signal is twice as high as the crosstalk interferer.

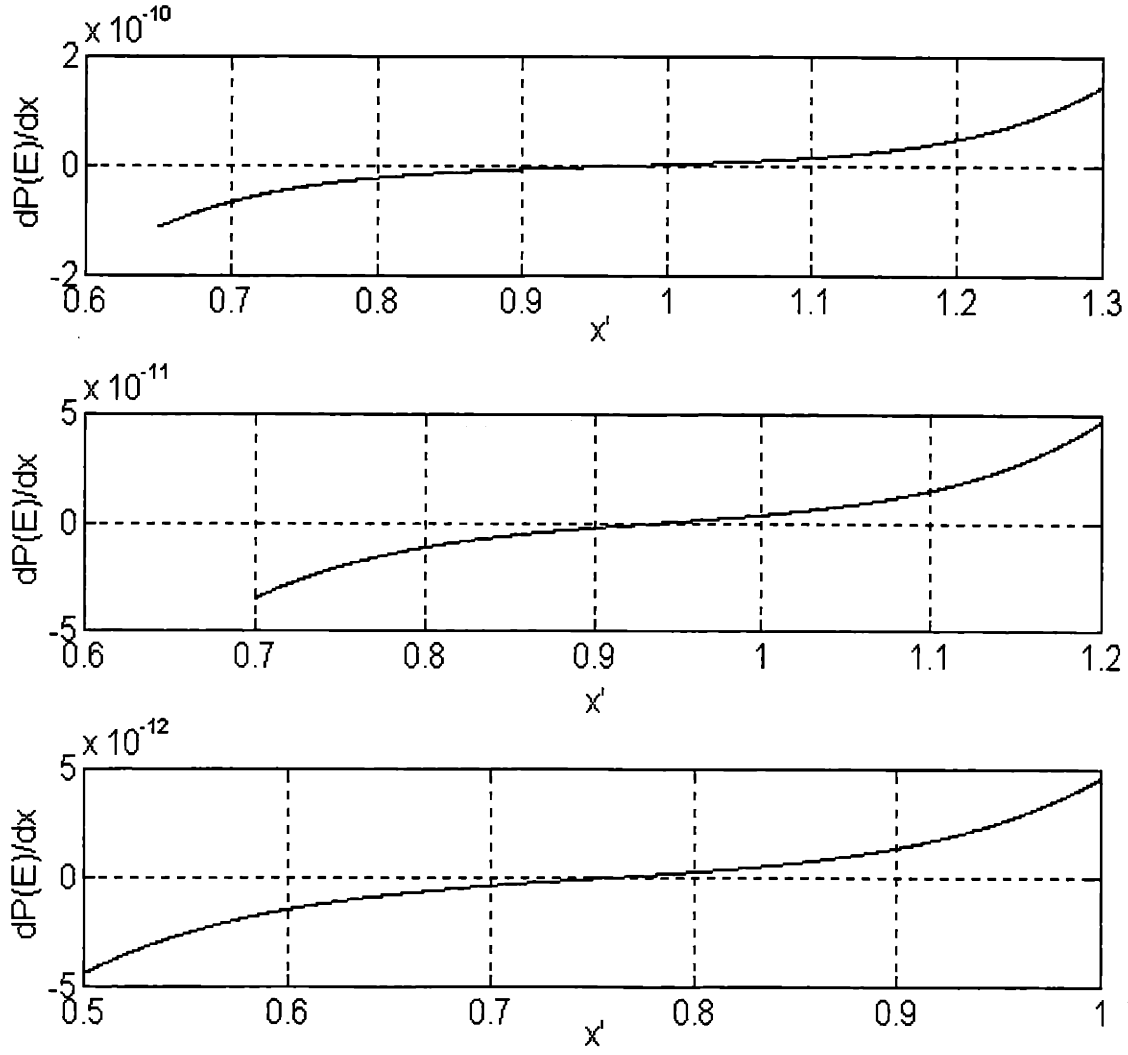

Figure 3-17: $\frac{dP(E)}{dx}$ is illustrated versus $x' = \frac{x}{2\sqrt{r}-2r}$ for $n = 1, 2$ and 10. The threshold levels that minimize error probabilities are very close tothose of the synchronous system.

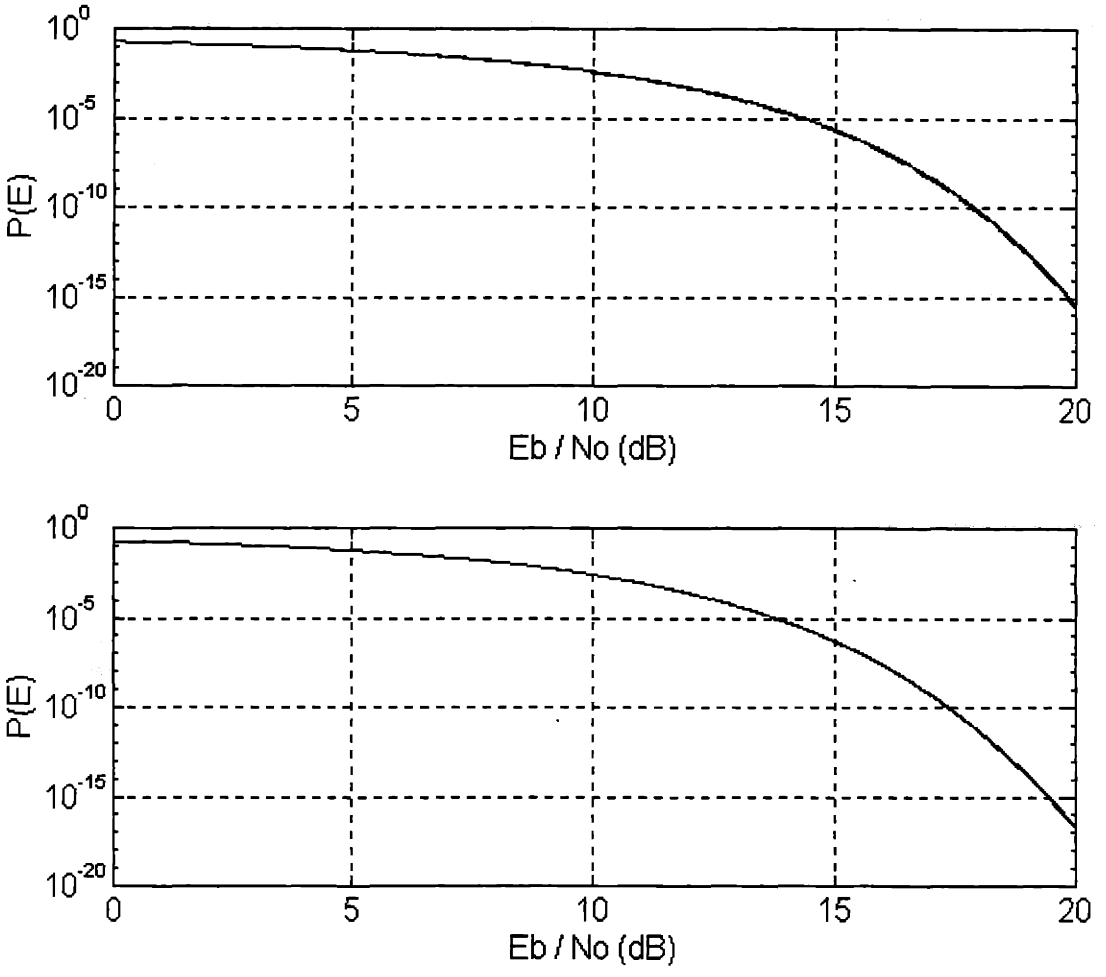

Figure 3-18: The two plots correspond to the error performances for $n = 1$ and $n = 10$. The solid line illustrates the performance of a system where the signal and the crosstalk bits are synchronous and the dotted curve shows the performance where the two are asynchronous.

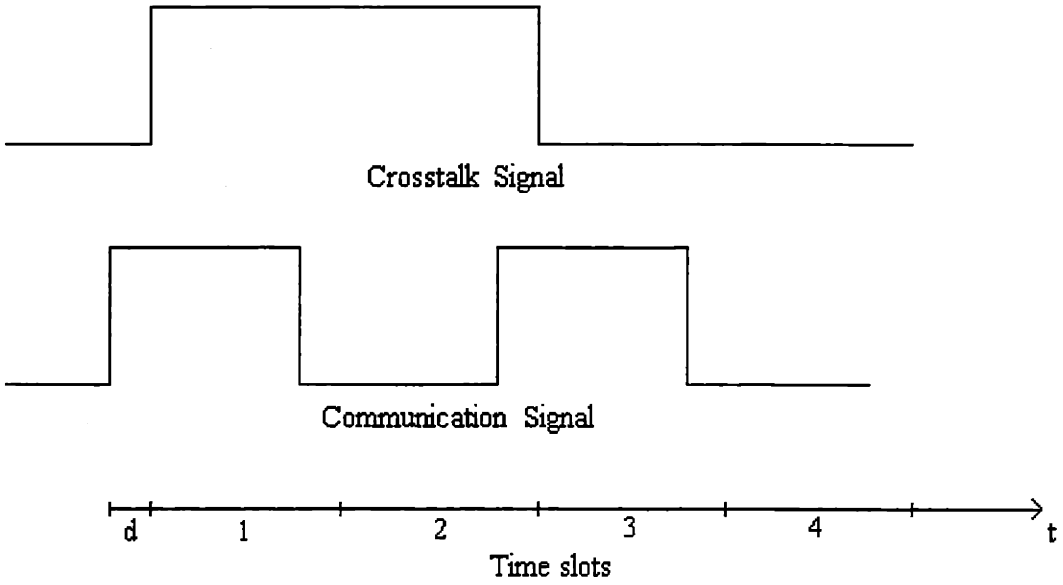

Figure 3-19: Communication and crosstalk signals where n=2. d is the amount of time shift between the two.

In this section, we will define the "transition bits" as the signal bits which occur during the transition of the crosstalk bits. Recall that the transition is defined to be the instant that one bit ends and the next bit starts. d is the amount of the time shift between the signal and the crosstalk sequences. A transition signal bit can be examined as two separate parts as illustrated in Figure 3.20.

Let $r_{t,1}$ be the bit value of the crosstalk signal in the first (d sec) portion of the transition bit and $r_{t,2}$ is that in the second ($T-d$ sec) portion of the transition bit (In Figure 3.20, $r_{t,1}=0, r_{t,2}=1$). $r_{t,1}$ and $r_{t,2}$ are IID Bernoulli random variables. We will pursue the analysis by calculating the probability of error in detection of a transient bit and a non-transient bit separately.

If the bit is non-transient, the analysis is the same as that in section 3.1, where the signal and the crosstalk bits are synchronous. Therefore, the probability of error conditioned on a non-transition bit is given in Equation 3.5 for a threshold of $\frac{Ti_{s,1}}{2}(1-x)$. If the bit is a transient, the current at the sampler becomes,

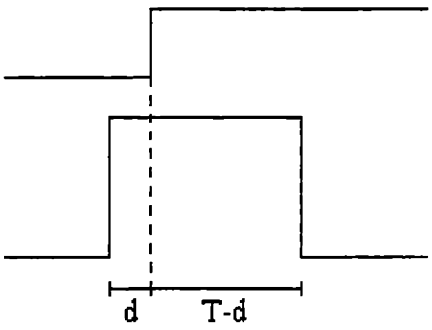

Figure 3-20: A transition signal bit is shown below the crosstalk signal. One crosstalk bit ends and the next one starts during the transmission of the transition bit.

$$i'(kT) = Ti_{s,1} + i_{c,1}\left(dr_{t,1} + (T-d)r_{t,2}\right) + 2\sqrt{i_{s,1}i_{c,1}}\left(dr_{t,1} + (T-d)r_{t,2}\right) \tag{3.38}$$

when the signal bit is a 1. Rewriting this with $i_{c,1} = ri_{s,1}$, $i'(kT)$ becomes,

$$i'(kT) = Ti_{s,1}\left[1 + (r - 2\sqrt{r})g(d, m=0, n=1, r_{t,1}, r_{t,2})\right] \tag{3.39}$$

where $g(d, m, n, r_{t,1}, r_{t,2})$ was defined in section 3.2.1. When the signal bit is a 0, the detected current at the output of the sampler for a transition bit becomes,

$$i'(kT) = Ti_{s,1}rg(d, m=0, n=1, r_{t,1}, r_{t,2}) \tag{3.40}$$

Thus, the probability of error for a transition bit, if we set the threshold to $\frac{Ti_{s,1}}{2}(1-x)$ conditioned on $g = g(d, m=0, n=1, r_{t,1}, r_{t,2})$ is,

$$P\left(E|g(d, m=0, n=1, r_{t,1}, r_{t,2})\right) = \frac{1}{2}Q\left[\sqrt{\frac{E_b}{N_0}}\left(1 + x + (2r - 4\sqrt{r})g\right)\right]$$

$$+\frac{1}{2}Q\left[\sqrt{\frac{E_b}{N_0}}(1-x-2rg)\right] \tag{3.41}$$

Let us recall that the ratio of the bit rate of the crosstalk source to that of the communication signal is $n = \frac{T}{T_c}$. It is obvious that $\frac{1}{n}$ of the signal bits are transient and the rest ($\frac{n-1}{n}$ of them) are non-transient bits. With the above argument, the probability of error conditioned on $g = g(d, m = 0, n = 1, r_{t,1}, r_{t,2})$ can be written as,

$$P\left(E|g(d,0,1,r_{t,1},r_{t,2})\right) = \frac{1}{n}P(E|\text{transition bits}, g) + \frac{n-1}{n}P(E|\text{non-transition bits}, g) \tag{3.42}$$

$$\begin{aligned} &= \left(\frac{n-1}{n}\right)\left\{\frac{1}{4}Q\left(\sqrt{\frac{E_b}{N_0}}(1-x)\right) + \frac{1}{4}Q\left(\sqrt{\frac{E_b}{N_0}}(1-x)\right)\right. \\ &\quad \left. + \frac{1}{4}Q\left(\sqrt{\frac{E_b}{N_0}}(1-x-2r)\right) + \frac{1}{4}Q\left(\sqrt{\frac{E_b}{N_0}}(1+x+2r-4\sqrt{r})\right)\right\} \\ &\quad + \left(\frac{1}{n}\right)\left\{\frac{1}{2}Q\left[\sqrt{\frac{E_b}{N_0}}\left(1+x+(2r-4\sqrt{r})g\right)\right]\right. \\ &\quad \left. + \frac{1}{2}Q\left[\sqrt{\frac{E_b}{N_0}}(1-x-2rg)\right]\right\} \end{aligned} \tag{3.43}$$

The unconditioned error probability $P(E)$ can be written as follows.

$$P(E) = \int_0^T \sum_{r_{t,1}=0}^{1}\sum_{r_{t,2}=0}^{1} P\left(E|g(\tau, m=0, n=1, r_{t,1}, r_{t,2})\right)\frac{1}{T}\frac{1}{4}d\tau \tag{3.44}$$

To find the optimum decision threshold (i.e., optimum x), we take the derivative of $P(E)$ with respect to x and equate to 0. The derivative of the probability of error versus $x' = \frac{x}{2\sqrt{r}-2r}$ is illustrated in Figure 3.21 for $n = 1, 2$ and 10 at constant $\frac{E_b}{N_0} = 18$ dB. Similarly, the x value that makes the derivative 0 is the global optimum value of the point of the error probability. One can observe that the optimum x is approximately $2\sqrt{r} - 2r$ for any n which is also the optimum value for the synchronous system.

Figure 3.21 illustrates the performance for $n = 1$ and $n = 10$ together with those of the synchronous system. The difference between the crosstalk penalty of the asynchronous

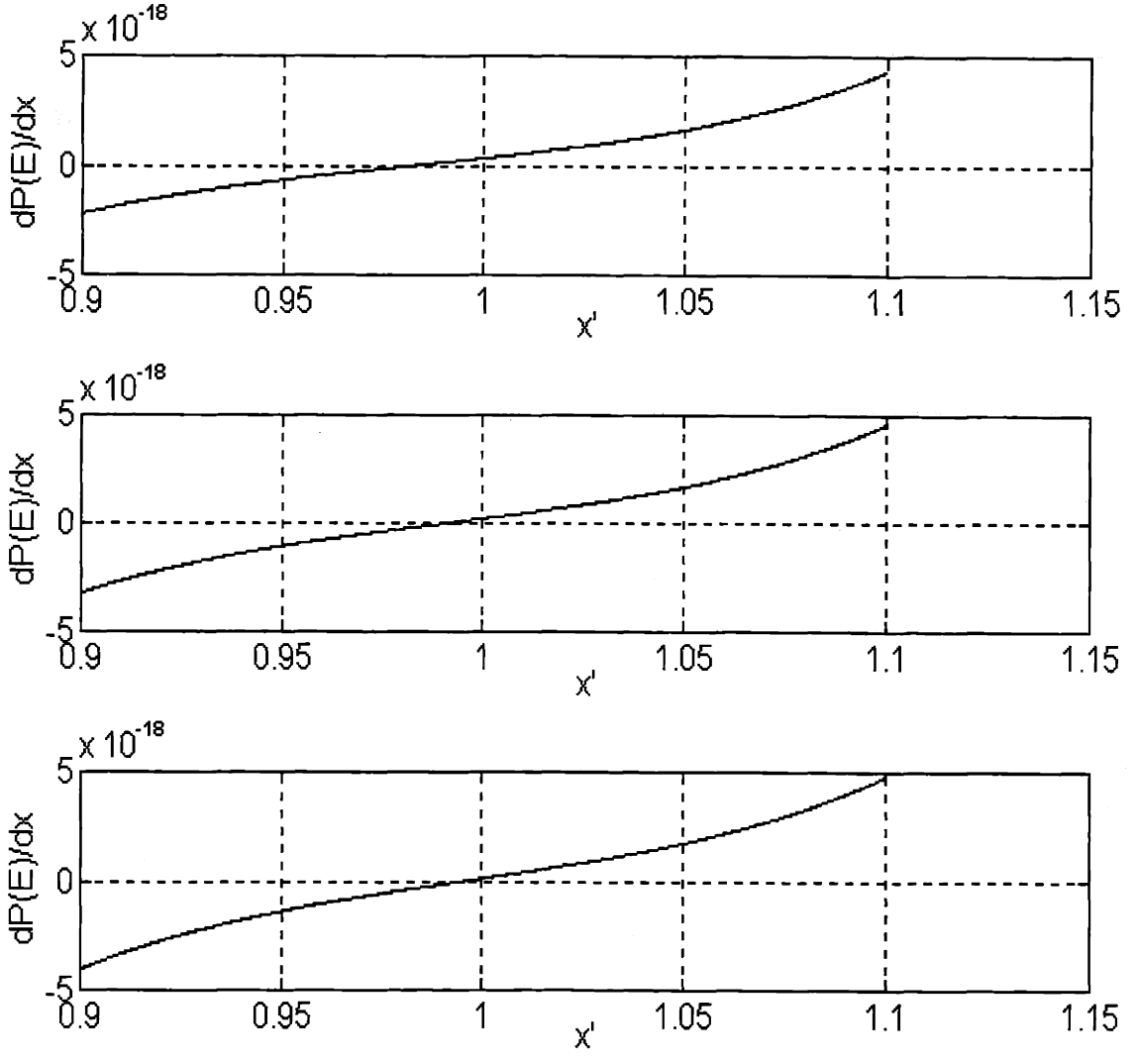

Figure 3-21: $\frac{dP(E)}{dx}$ versus x' at $\frac{E_b}{N_0} = 18$ dB for $n = 1, 2$ and 10. $x' \approx 1$ for all n. The threshold levels that minimize $P(E)$ are very close to that of the synchronous system.

system and that of the synchronous system decreases as n increases since the number of the transition bits are $\frac{1}{n}$ of that of the total number of bits, and this ratio decreases inversely with n. However, even for $n = 1$, this difference is almost negligible. Therefore the probability of error can be assumed to be equal for the two systems (synchronous and asynchronous) when signal has a higher bit rate as well as when it has lower bit rate. Another important observation is that for $n = 1$, the performance is equal to that of the section 4.3 with $n = 1$ (because $g(d, m, n, r_{t,1}, r_{t,2}) = g(d, m = 0, n = 1, r_{t,1}, r_{t,2})$ for $n = 1$ in section 4.3) which verifies the correctness of the analyses in some sense.

3.3 Conclusions

The major conclusions drawn from this chapter can be summarized as follows.

If the signal has a bit rate higher than that of the crosstalk, then the power penalty is very close to that of the worst case. In fact, we found out that the difference between the two cases is no more than 0.05 dB at the error probabilities close to 10^{-9} for an interferer of power 20 dB below that of the signal. We also considered the effects of dynamic thresholding within this case and argued that, with dynamic thresholding the performance could be no better than that with optimum static threshold most of the times (equally well only under some certain conditions). It may be advantageous if the received signal power and the crosstalk power are not constant throughout the communication. Note that these results are consistent with found in [4] and [6] for both AC and DC coupled thresholding except that in [4] and [6], the crosstalk-crosstalk beat terms are neglected.

Another neat result is that even if the bit sequence of the crosstalk is known by the receiver, the error performance of the system cannot be improved considerably using that information.

Next, we considered the case where the bit rate of the signal is lower than that of the crosstalk. We deduced that if the ratio of the rates is small, namely, the rates are

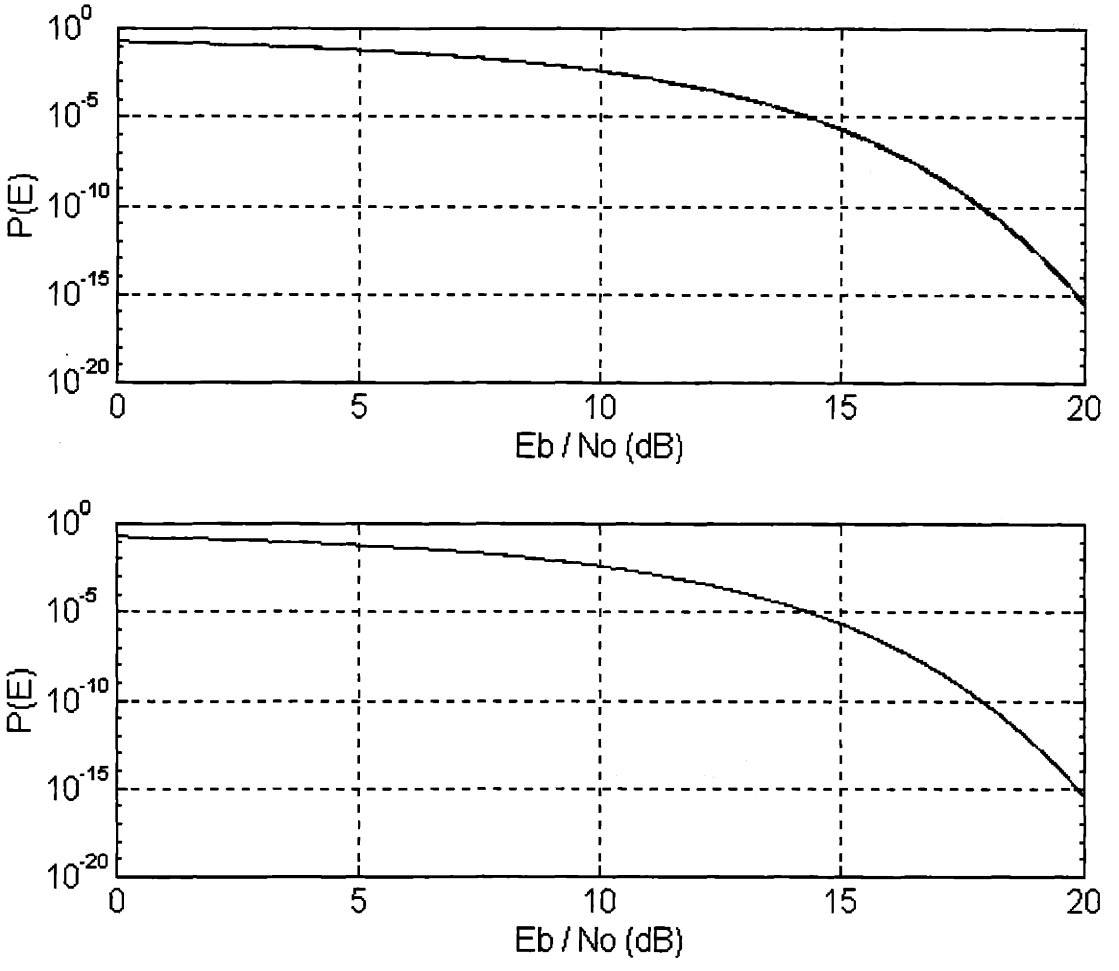

Figure 3-22: The two plots correspond to the error performances for $n = 1$ and $n = 10$. The solid line illustrates the performance of a system where the signal and the crosstalk bits are synchronous and the dotted curve shows the performance where the two are asynchronous.

close to each other, the performance is close to the worst case and the error probability is a decreasing function of this ratio. As n gets larger and larger, the probability of error approaches that of the worst case with a crosstalk power equal to half the original.

Finally we considered the case where the bit slots of the signal and the crosstalk are asynchronous for two subcases when the bit rate of the crosstalk is higher and the converse. We presented that, if the bit rates of the two are equal, the optimum threshold and the error probabilities of the asynchronous system is almost equal to those of the synchronous system. Indeed, they get even closer as the ratio of the rates increase. Therefore, it is reasonable to assume that the bit slots are synchronous to simplify analyses.

Chapter 4

Crosstalk with Random Phase and Polarization

In Chapters 2 and 3, we assumed that the relative phase and the polarization of the crosstalk is always opposite to that of the signal. With this assumption, we dropped the vector notation to simplify the expressions for the received electric field.

In this chapter, we will generalize the analysis done for constant phase and polarization of the crosstalk source to one for random phase and polarization. In Section 4.1, we will present the crosstalk model and using that model in Section 4.2, we will analyze the performance of our system.

4.1 Crosstalk Model

In this chapter, we will assume that, the polarization of the optical wave inserted into the fiber by the laser is arbitrary and this state is not necessarily maintained as the signal propagates. Thus, the electric field at the output of the transmitter can be modeled by a vector whose direction is random and the amplitude is OOK modulated. Hence, we can represent this signal as follows.

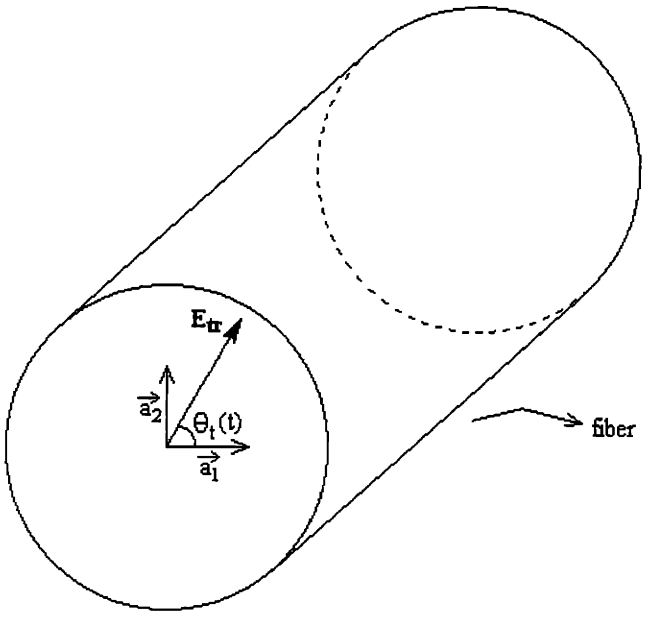

Figure 4-1: The direction of $\mathbf{E}_{tr}$ is illustrated as it is initially injected in the fiber.

$$\mathbf{E}_{tr} = \mathrm{Re}\left\{E_{amp}(t)e^{j[2\pi f_c t+\phi_t(t)]}\right\}\left[\cos\left(\theta_t(t)\right)\overrightarrow{a_1} + \sin\left(\theta_t(t)\right)\overrightarrow{a_2}\right] \tag{4.1}$$

or equivalently,

$$\mathbf{E}_{tr} = E_{amp}(t)\begin{bmatrix} \cos\left(\theta_t(t)\right)\cos\left(2\pi f_c t + \phi_t(t)\right) \\ \sin\left(\theta_t(t)\right)\cos\left(2\pi f_c t + \phi_t(t)\right) \end{bmatrix} \tag{4.2}$$

where $E_{amp}(t)$ is the amplitude (OOK modulated), $\theta_t(t)$ is the initial value of polarization, which may vary in time, f_c is the optical frequency, $\phi_t(t)$ is the initial phase of the wave and $\overrightarrow{a_1}$ and $\overrightarrow{a_2}$ are the unit vectors as shown in Figure 4.1. The phase of the field is a function of time because of the non-coherent characteristics of the laser.

As the field propagates in the fiber, due to birefringence, the state of polarization is not maintained and hence it varies with time. Namely, if we insert a linearly polarized pulse into the fiber, both the amplitude and the phase of the pulse changes as it propagates,

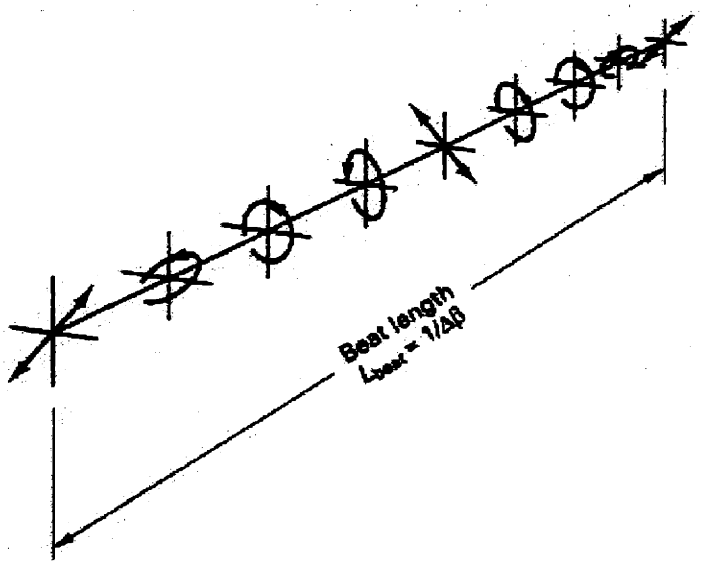

Figure 4-2: Showing one evolution of the polarization state along a fiber. The light traverses a distance L_{beat} before returning to the original polarization state.

thus the state of polarization is not maintained. This change occurs with a periodic nature (with a large period) as illustrated in Figure 4.2. Note that the fluctuations in optical phases are rapid ($\sim$ MHz) compared to the fluctuation in the polarization state ($\sim$ Hz). Thus, we will assume that the polarization state is constant for a time much longer than one bit period.

This phenomena can be modeled by an extra parameter $\Psi(t)$ which appears only in one of the components of the vector. The overall field at the input of the detector together with the crosstalk signal which has similar characteristics is the following.

$$\begin{aligned}\mathbf{E}_{\text{det}} &= E_s(t)\begin{bmatrix}\cos[\theta_s(t)]\cos[2\pi f_c t+\phi_s(t)]\\ \sin[\theta_s(t)]\cos[2\pi f_c t+\phi_s(t)+\Psi_s(t)]\end{bmatrix}\\ &\quad +E_x(t)\begin{bmatrix}\cos[\theta_x(t)]\cos[2\pi f_c t+\phi_x(t)]\\ \sin[\theta_x(t)]\cos[2\pi f_c t+\phi_x(t)+\Psi_x(t)]\end{bmatrix}\end{aligned} \tag{4.3}$$

This time, the parameters are those of the received electric field. It is reasonable to assume that at an instant $t = t^*$, $\theta_s(t^*), \theta_x(t^*), \phi_s(t^*), \phi_x(t^*), \Psi_s(t^*)$ and $\Psi_x(t^*)$ are all independent and uniformly distributed in $(0, 2\pi)$. $E_s(t)$ and $E_x(t)$ are OOK modulated amplitudes of the signal and the crosstalk components respectively; thus, samples of $E_s(t)$ and $E_x(t)$ at $t = t^*$ are Bernoulli random variables with two equiprobable values $E_{s,1}$ and $E_{x,1}$ respectively and 0. Note that, as we mentioned at the end of Chapter 3, we will assume that the crosstalk bit slots are synchronous with those of the signal (i.e., there are no transition bits).

With these definitions, the stochastic modeling of the detected field is completed.

4.2 System Performance

In the previous section, we modeled the crosstalk and the signal in terms of their random amplitude, phase and polarization statistics. In this section, we will use that expression to derive an expression for the detected current and the probability of error. Throughout the section, to simplify the notation, we will use the parameters which are functions of time without the argument (t) (i.e., $f(t) \rightarrow f$).

The detected current is proportional to the detected optical power, i.e.,

$$i_{\text{det}} = \Re P_{\text{det}} \tag{4.4}$$

where $\Re$ is the detector's responsivity. The instantaneous detected power is proportional to $\mathbf{E}_{\text{det}}^T \mathbf{E}_{\text{det}}$. The constant of proportionality is $\epsilon/2$ where ϵ $(= \epsilon_r \epsilon_o)$ is the dielectric constant of the fiber. Therefore,

$$i_{\text{det}} = \frac{1}{2}\Re\epsilon \mathbf{E}_{\text{det}}^T \mathbf{E}_{\text{det}} \tag{4.5}$$

$$\begin{aligned} = \frac{1}{2}\Re\epsilon \Big\{ & E_s^2 \left[\cos^2(\theta_s)\cos^2(2\pi f_c t + \phi_s) + \sin^2(\theta_s)\cos^2(2\pi f_c t + \phi_s + \Psi_s)\right] \\ & + 2E_s E_x \left[\cos(\theta_s)\cos(\theta_x)\cos(2\pi f_c t + \phi_s)\cos(2\pi f_c t + \phi_x)\right. \\ & \left. + \sin(\theta_s)\sin(\theta_x)\cos(2\pi f_c t + \phi_s + \Psi_s)\cos(2\pi f_c t + \phi_x + \Psi_x)\right] \end{aligned} \tag{4.6}$$

$$
\begin{aligned}
&+E_x^2\left[\cos^2(\theta_x)\cos^2(2\pi f_c t+\phi_x)+\sin^2(\theta_x)\cos^2(2\pi f_c t+\phi_x+\Psi_x)\right]\Big\}\\
=\;&\frac{1}{2}\Re\epsilon\left\{E_s^2\left[\cos^2(\theta_s)\frac{1+\cos(4\pi f_c t+2\phi_s)}{2}+\sin^2(\theta_s)\frac{1+\cos(4\pi f_c t+2\phi_s+2\Psi_s)}{2}\right]\right.\\
&+E_sE_x\left[\cos(\theta_s)\cos(\theta_x)\left(\cos(4\pi f_c t+\phi_s+\phi_x)+\cos(\phi_s-\phi_x)\right)\right. \qquad (4.7)\\
&+\sin(\theta_s)\sin(\theta_x)\left(\cos(4\pi f_c t+\phi_s+\phi_x+\Psi_s+\Psi_x)+\cos(\phi_s-\phi_x+\Psi_s-\Psi_x)\right)\Big]\\
&\left.+E_x^2\left[\cos^2(\theta_x)\frac{1+\cos(4\pi f_c t+2\phi_x)}{2}+\sin^2(\theta_x)\frac{1+\cos(4\pi f_c t+2\phi_x+2\Psi_x)}{2}\right]\right\}
\end{aligned}
$$

The detector will not respond to the double frequency terms. Hence,

$$
\begin{aligned}
i_{\text{det}} \;=\;&\frac{1}{2}\Re\epsilon\left\{\frac{1}{2}E_s^2+\frac{1}{2}E_c^2+E_sE_x\left[\cos(\theta_s)\cos(\theta_x)\cos(\phi_s-\phi_x)\right.\right.\\
&\left.\left.+\sin(\theta_s)\sin(\theta_x)\cos(\phi_s-\phi_x+\Psi_s-\Psi_x)\right]\right\} \qquad (4.8)
\end{aligned}
$$

Let us define $P_s \triangleq \frac{1}{2}\epsilon E_s^2$ and $P_x \triangleq \frac{1}{2}\epsilon E_x^2$. The detected current becomes,

$$
\begin{aligned}
i_{\text{det}} \;=\;&\Re P_s+\Re P_x+2\Re\sqrt{P_sP_x} \qquad (4.9)\\
&\times\underbrace{\left[\cos(\theta_s)\cos(\theta_x)\cos(\phi_s-\phi_x)+\sin(\theta_s)\sin(\theta_x)\cos(\phi_s-\phi_x+\Psi_s-\Psi_x)\right]}_{\zeta}
\end{aligned}
$$

We defined the terms in big bracket as ζ. Let us rewrite ζ as follows.

$$
\begin{aligned}
\zeta \;=\;&\cos(\theta_s)\cos(\theta_x)\cos(\phi_s-\phi_x)+\sin(\theta_s)\sin(\theta_x)\cos(\phi_s-\phi_x)\cos(\Psi_s-\Psi_x)\\
&-\sin(\theta_s)\sin(\theta_x)\sin(\phi_s-\phi_x)\sin(\Psi_s-\Psi_x) \qquad (4.10)\\
=\;&\left[\cos(\theta_s)\cos(\theta_x)+\sin(\theta_s)\sin(\theta_x)\cos(\Psi_s-\Psi_x)\right]\cos(\phi_s-\phi_x)\\
&-\left[\sin(\theta_s)\sin(\theta_x)\sin(\Psi_s-\Psi_x)\right]\sin(\phi_s-\phi_x) \qquad (4.11)\\
=\;&\left\{\left[\cos(\theta_s)\cos(\theta_x)+\sin(\theta_s)\sin(\theta_x)\cos(\Psi_s-\Psi_x)\right]^2\right.\\
&\left.+\left[\sin(\theta_s)\sin(\theta_x)\sin(\Psi_s-\Psi_x)\right]^2\right\}^{1/2}\cos(\phi_s-\phi_x+\gamma) \qquad (4.12)
\end{aligned}
$$

where $\gamma=\tan^{-1}\left(\frac{\sin(\theta_s)\sin(\theta_x)\sin(\Psi_s-\Psi_x)}{\cos(\theta_s)\cos(\theta_x)+\sin(\theta_s)\sin(\theta_x)\cos(\Psi_s-\Psi_x)}\right)$.

$$
\zeta \;=\; \left[\cos^2(\theta_s)\cos^2(\theta_x)+\sin^2(\theta_s)\sin^2(\theta_x)\cos^2(\Psi_s-\Psi_x)\right.
$$

$$
\begin{aligned}
&+\sin^2(\theta_s)\sin^2(\theta_x)\sin^2(\Psi_s-\Psi_x) \\
&+2\cos(\theta_s)\cos(\theta_x)\sin(\theta_s)\sin(\theta_x)\cos(\Psi_s-\Psi_x)]^{1/2}\cos(\phi_s-\phi_x+\gamma) \qquad (4.13)\\
= \;& \left[\left(\frac{1+\cos(2\theta_s)}{2}\right)\left(\frac{1+\cos(2\theta_x)}{2}\right)+\left(\frac{1-\cos(2\theta_s)}{2}\right)\left(\frac{1-\cos(2\theta_x)}{2}\right)\right. \\
&\left.+2\cos(\Psi_s-\Psi_x)\frac{1}{4}\sin(2\theta_s)\sin(2\theta_x)\right]^{1/2}\cos(\phi_s-\phi_x+\gamma) \qquad (4.14)\\
= \;& \left[\frac{1}{4}\left(1+\cos(2\theta_s)+\cos(2\theta_x)+\frac{1}{2}\cos(2\theta_s+2\theta_x)+\frac{1}{2}\cos(2\theta_s-2\theta_x)\right)\right. \\
&+\frac{1}{4}\left(1-\cos(2\theta_s)-\cos(2\theta_x)+\frac{1}{2}\cos(2\theta_s+2\theta_x)+\frac{1}{2}\cos(2\theta_s-2\theta_x)\right) \\
&\left.+\frac{1}{2}\cos(\Psi_s-\Psi_x)\frac{1}{2}\left(\cos(2\theta_s-2\theta_x)-\cos(2\theta_s+2\theta_x)\right)\right]^{1/2} \qquad (4.15)\\
&\cdot\cos(\phi_s-\phi_x+\gamma) \\
= \;& \left[\frac{1}{2}+\frac{1}{4}\cos(2\theta_s+2\theta_x)+\frac{1}{4}\cos(2\theta_s-2\theta_x)+\frac{1}{4}\cos(\Psi_s-\Psi_x)\cos(2\theta_s-2\theta_x)\right. \\
&\left.-\frac{1}{4}\cos(\Psi_s-\Psi_x)\cos(2\theta_s+2\theta_x)\right]^{1/2}\cos(\phi_s-\phi_x+\gamma) \qquad (4.16)\\
= \;& \frac{1}{2}\left[2+\cos(2\theta_s-2\theta_x)\left[1+\cos(\Psi_s-\Psi_x)\right]\right. \\
&\left.+\cos(2\theta_s+2\theta_x)\left[1-\cos(\Psi_s-\Psi_x)\right]\right]^{1/2}\cos(\phi_s-\phi_x+\gamma) \qquad (4.17)
\end{aligned}
$$

Let us define $\phi_r = \phi_s - \phi_x$, $\Psi_r = \Psi_s - \Psi_x$. Both ϕ_r and Ψ_r are uniform in $(0, 2\pi)$. Since γ is independent of ϕ_r, $\cos(\phi_r + \gamma)$ has the same distribution as $\cos(\phi_r)$. Let us rewrite ζ as

$$
\begin{aligned}
\zeta \;=\; & \zeta(\phi_r, \Psi_r, \theta_s, \theta_x) = \frac{1}{2}\left[2+\cos(2\theta_s-2\theta_x)\left[1+\cos(\Psi_s-\Psi_x)\right]\right. \\
&\left.+\cos(2\theta_s+2\theta_x)\left[1-\cos(\Psi_s-\Psi_x)\right]\right]^{1/2}\cos(\phi_s-\phi_x+\gamma) \qquad (4.18)
\end{aligned}
$$

and let $i_s = \Re P_s$ and $i_c = \Re P_c$. Along with these definitions, the detected current becomes,

$$
i_{\text{det}} = i_s + i_c + 2\sqrt{i_s i_c}\,\zeta(\phi_r, \Psi_r, \theta_s, \theta_x) \qquad (4.19)
$$

After this point, the analysis is pretty much the same as the analysis given in Chapter 4 for synchronous bit slots. The only difference is that we have an extra factor $\zeta(\phi_r, \Psi_r, \theta_s, \theta_x)$ near $\sqrt{r}$ (where $r = \frac{i_{c,1}}{i_{s,1}}$) since the phase and the polarization is random. We will evaluate the error probability for two separate cases where in the first case the crosstalk, and in the second case the signal is at a higher rate.

4.2.1 Higher Crosstalk Bit Rate

Rewriting 3.19 with phase and polarization parameters, the detected current at the output of the sampler becomes

$$i'(kT) = Ti_{s,1}\left[1 + \frac{m}{n}r - 2\frac{m}{n}\sqrt{r}\zeta(\phi_r, \Psi_r, \theta_s, \theta_x)\right] \tag{4.20}$$

if the k^{th} signal bit is a 1,

$$i'(kT) = Ti_{s,1}\frac{m}{n}r \tag{4.21}$$

if the k^{th} signal bit is a 0 where m of the n crosstalk bits are 1. Hence, for a threshold of $\frac{Ti_{s,1}}{2}(1-x)$, the probability of error conditioned on $\zeta = \zeta(\phi_r, \Psi_r, \theta_s, \theta_x)$ is the following.

$$P(E|\zeta, m=l) = \frac{1}{2}Q\left(\sqrt{\frac{E_b}{N_0}}\left(1 + x + 2r\frac{l}{n} - 4\frac{l}{n}\sqrt{r}\zeta\right)\right) + \frac{1}{2}Q\left(\sqrt{\frac{E_b}{N_0}}\left(1 - x - 2r\frac{l}{n}\right)\right) \tag{4.22}$$

and, thus the unconditioned probability of error is

$$P(E) = \int_0^{2\pi}\int_0^{2\pi}\int_0^{2\pi}\int_0^{2\pi}\sum_{l=0}^{n} P(E|\zeta, m=l)\binom{n}{l}\left(\frac{1}{2}\right)^n\left(\frac{1}{2\pi}\right)^4 d\phi_r d\Psi_r d\theta_s d\theta_x \tag{4.23}$$

To find the optimal threshold, we apply a similar approach to Chapter 3, i.e., solve $\frac{dP(E)}{dx} = 0$. $\frac{dP(E)}{dx}$ is illustrated for $n = 1$ and 10 in Figure 4.3, versus $x' = \frac{x}{2\sqrt{r}-2r}$ at $E_b/N_0 = 16$ dB. Note that, since $\frac{dP(E)}{dx}$ is monotonically increasing, the solution to the

equation $\frac{dP(E)}{dx} = 0$ is unique and the corresponding x value minimizes $P(E)$ globally. The optimum threshold parameters for $n = 1$ and $n = 10$ are $x' = 0.81$ and $x' = 0.59$ respectively. Due to random polarization and phase values, at the given value of E_b/N_0, the optimum threshold is now higher than that with worst case parameters.

Figure 4.4 illustrates the performance for $n = 1$ and 10 for $r = -20$ dB when the threshold is set to its optimum value, together with those with the worst case polarization and phase statistics. If we compare the optimum threshold and performance curves illustrated in 4.3 and 4.4 with those with worst case phase and polarizations, we observe that the optimal thresholds with all random parameters are closer to $\frac{Ti_{s,1}}{2}$ (i.e., the signal mark level) and achieve 0.3-0.4 dB superior performances at $r = -20$ dB. The increase in the threshold level is expected since the effects of the interferer are less severe with random parameters than the worst case even though the improvement in the performance is very minor.

4.2.2 Lower Crosstalk Bit Rate

In this section, we will repeat the derivation introduced in Section 3.1.1 for random polarization and phase. The error probability conditioned on the phase and polarization parameters ($\zeta = \zeta(\phi_r, \Psi_r, \theta_s, \theta_x)$) can be written as follows.

$$\begin{aligned} P(E|\text{non-transition}, \zeta) &= \frac{1}{4}Q\left(\sqrt{\frac{E_b}{N_0}}(1-x)\right) + \frac{1}{4}Q\left(\sqrt{\frac{E_b}{N_0}}(1+x)\right) \\ &\quad + \frac{1}{4}Q\left(\sqrt{\frac{E_b}{N_0}}(1-x-2r)\right) \\ &\quad + \frac{1}{4}Q\left(\sqrt{\frac{E_b}{N_0}}(1+x+2r-4\sqrt{r}\zeta)\right) \end{aligned} \tag{4.24}$$

The unconditioned error rate is thus,

$$P(E) = \int_0^{2\pi}\int_0^{2\pi}\int_0^{2\pi}\int_0^{2\pi} P(E|\zeta)\left(\frac{1}{2\pi}\right)^4 d\tau d\phi_r d\Psi_r d\theta_s d\theta_x \tag{4.25}$$

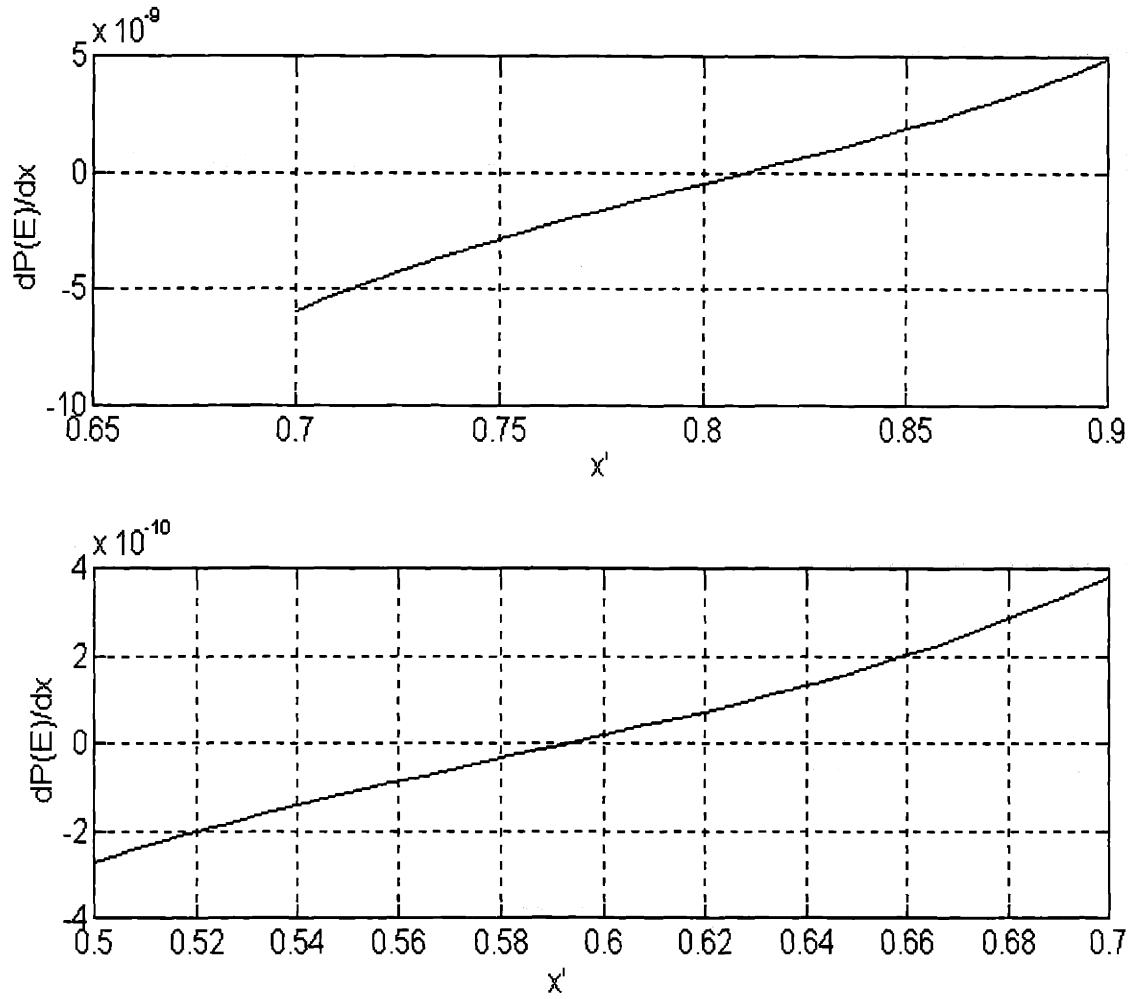

Figure 4-3: The derivative of the error probability versus $x' = \frac{x}{2\sqrt{r-2r}}$ is illustrated in the figure. The above figure is for $n = 1$ and the below figure is for $n = 10$. The optimal thresholds are lower than those utilizing worst case parameters.

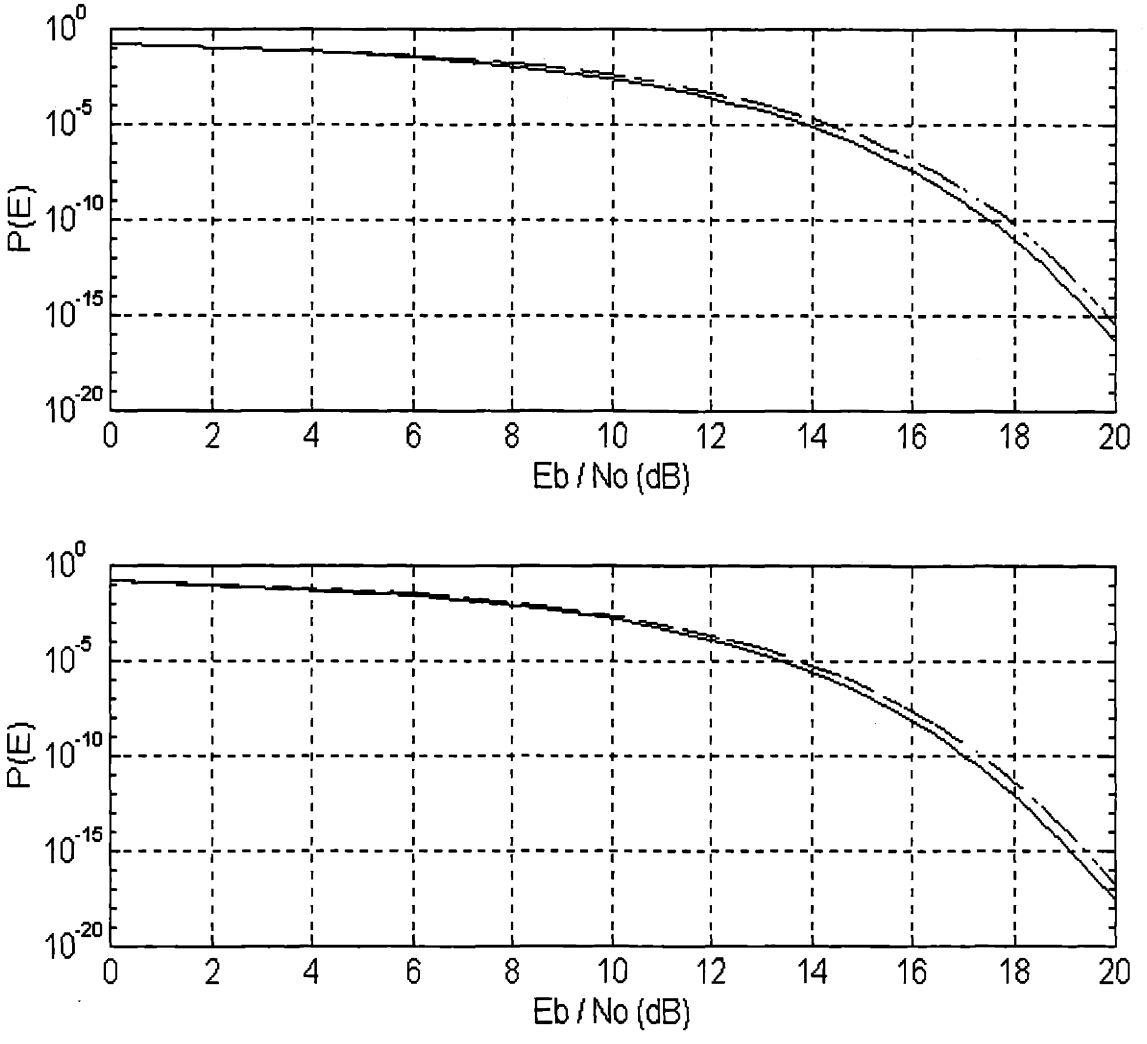

Figure 4-4: The performance curves at the optimum threshold for $n = 1$ and $n = 10$. The curves for $n = 1$ and $n = 10$ are almost 0.4 dB and 0.3 dB superior compared to those with worst case polarization & phase parameters (which are illustrated with dashed lines) respectively at $E_b/N_0 = 16$ dB.

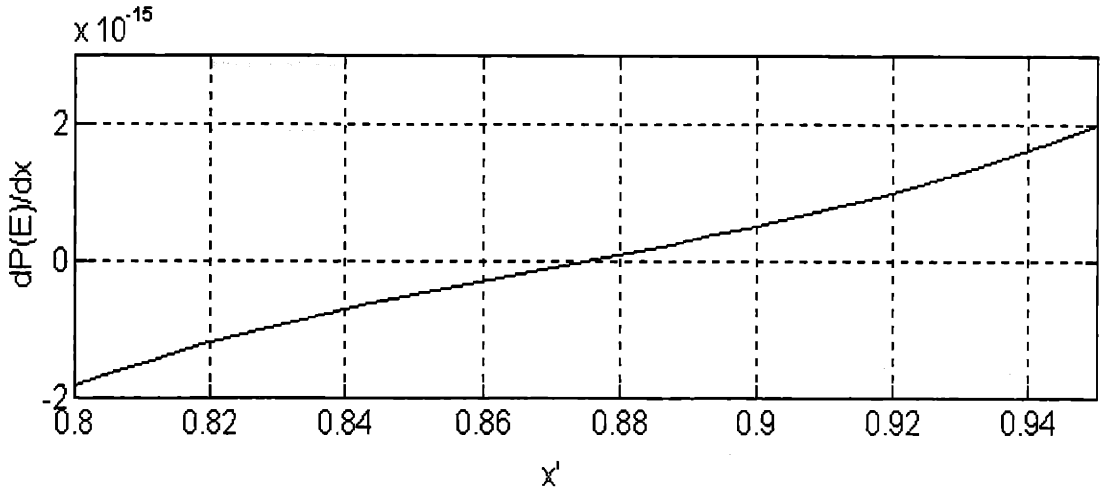

Figure 4-5: The derivative of the error probability versus $x' = \frac{x}{2\sqrt{r}-2r}$ is illustrated in the figure.

The derivative of the probability of error versus x' is illustrated in Figure 4.5 at $E_b/N_0 = 18$ dB. Since $\frac{dP(E)}{dx}$ is monotonically increasing, the solution to the equation $\frac{dP(E)}{dx} = 0$ is unique and the corresponding x value minimizes $P(E)$ globally. Figure 4.6 illustrates the performance of the optimal detector together with the worst case curve. Note that if the bit rate of the signal is higher, than this optimal value is valid regardless of the rate of the crosstalk. Similar to the previous section where the crosstalk bit rate is higher, the optimum threshold level when the signal bit is at a higher rate is increased compared to the worst case. Also there is a 0.4 dB improvement in the performance at $r = -20$ dB which is very minor.

4.3 Conclusions

In this chapter, the analysis done for the worst case phases and polarizations are generalized to those for random phases and polarizations. We expressed the detected field as a vector employing four extra parameters $(\phi_r, \Psi_r, \theta_s, \theta_x)$ to represent the randomness

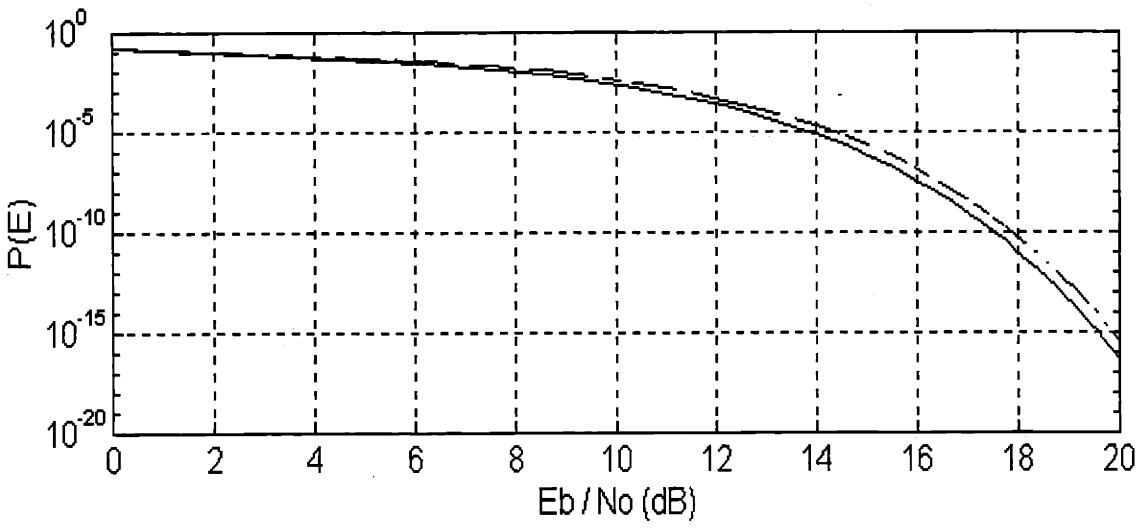

Figure 4-6: The optimum performance curves for random phase and polarization (solid line) and worst case phase and polarization (dashed line). The curve for random phase and polarization is 0.4 dB superior to that with worst case polarization & phase parameters at $E_b/N_0 = 18$ dB.

in the phases and the polarizations. This model which was introduced by [6] handles all the states of polarizations (e.g., circular, elliptic, linear, etc.) and all the possible relative directions of the crosstalk with respect to the signal from the worst case of matched signal and crosstalk polarizations to orthogonal polarizations. Even with such a detailed representation, the expression for the detected current is fairly simple. It is almost equal to that with worst case parameters except that there is an additional factor which is a function of ϕ_r, Ψ_r, θ_s and θ_x.

Next, we analyzed the error probability of the optimum receiver along with the model. As expected, the optimum threshold level is increased compared to the worst case and gets closer to $\frac{Ti_{s,1}}{2}$ which is the optimum threshold level for the crosstalk-free case both when the bit rate of the signal is higher and vice-versa. Regardless of the rates of the signal and the crosstalk relative to each other, the performance of the system is very close to the worst case which justifies the conclusions drawn by [9], namely, systems with randomly polarized fields display a statistical preference for near-worst case operation (a

substantial likelihood of operation within a few dB of the worst case).

Chapter 5

Multiple Crosstalk Sources

Upto this chapter, we dealt with the performances of the systems where there is one intruder. In this chapter, we are going to generalize the analysis to the case where there is more than one interferer. Current waveforms observed at the output of the optical detector were simulated for 10 and 100 crosstalk sources in Figures 1.15 and 1.16 respectively.

In this chapter, we will deal with the case where all the intruders are synchronous, the polarization states are aligned and the intruders and the signal are out of phase with π rads. In the first section, starting from Equation 1.3 for the received electric field, we will model the current at the output of the integrator with Bernoulli processes. Next, we will specify a region where neglecting the crosstalk-crosstalk beat terms is not reasonable and we will introduce a linear approximation for these terms. In the next section, we will switch to the transform domain and use the Chernoff bound to determine an upper bound for the error probability, and then optimize this bound over the threshold level and the transform parameter s. The following section presents three practical examples and illustrates the bound found in the second section for these examples. We end the chapter with conclusions and a brief summary.

5.1 Modeling the Process

5.1.1 Definitions

We dealt with the special case of this in Section 4.1 and 4.2 for single intruder. In the former, the interferer had a lower rate, and in the latter, the signal and the interferer were at the same rate or the interferer is at a higher rate.

In this section, we will combine 4.1 and 4.2 for $N-1$ intruders l of which are at a higher rate than the signal[1]. Since all the electric field vectors are in the same direction and out of phase with the signal field, we can start with Equation 1.3 and rewrite it as follows.

$$E_{\text{det}}(t) = \left(E_s(t) - \sum_{i=1}^{N-1} E_{ci}(t) \right) \cos\left(2\pi f_c t\right) \tag{5.1}$$

where f_c is the carrier frequency of the optical waves, E_s is the amplitude of the signal and E_{ci} is the amplitude of the i^{th} interferer. E_s and E_{ci} are OOK modulated. Let the interferers be in the descending order of rates from $i = 1$ to $N-1$ so that $E_{c1}, \ldots, E_{cl}$ are the components which are modulated at a higher rate than the signal. Thus, the received optical power can be found similar to Equation 3.28 as follows.

$$P_{\text{det}}(t) = P_s(t) + \sum_{i=1}^{N-1} P_{ci}(t) - 2\sum_{i=1}^{N-1} \sqrt{P_s(t)P_{ci}(t)} + 2\sum_{i=1}^{N-2}\sum_{j=i+1}^{N-1} \sqrt{P_{ci}(t)P_{cj}(t)} \tag{5.2}$$

where

$$\begin{aligned} P_s(t) &= \frac{1}{2}\left[E_s(t)\right]^2 \\ P_{ci}(t) &= \frac{1}{2}\left[E_{ci}(t)\right]^2 \end{aligned} \tag{5.3}$$

[1] We will assume that the bit rate of the interferers are either integer multiples or integer factors of that of the signal.

The photodetector current is,

$$i_{\text{det}}(t) = i_s(t) + \sum_{i=1}^{N-1} i_{ci}(t) - 2\sum_{i=1}^{N-1}\sqrt{i_s(t)i_{ci}(t)} + 2\sum_{i=1}^{N-2}\sum_{j=i+1}^{N-1}\sqrt{i_{ci}(t)i_{cj}(t)} \tag{5.4}$$

where

$$\begin{aligned} i_{\text{det}}(t) &= \Re P_{\text{det}}(t) \\ i_s(t) &= \Re P_s(t) \\ i_{ci}(t) &= \Re P_{ci}(t) \end{aligned} \tag{5.5}$$

Since $i_s(t)$ is OOK modulated, it is constant at $i_{s,1}$ given that the signal is mark and 0 given that the signal is a space. Also, $i_{ci}(t)$ varies between $i_{ci,1}$ and 0 depending on whether the i^{th} intruder is a mark or a space. Let us define

$$\begin{aligned} r_i &\triangleq \frac{i_{ci,1}}{i_{s,1}} \\ &= \frac{P_{ci,1}}{P_{s,1}} \end{aligned} \tag{5.6}$$

We will make a simplifying assumption at this point and assume $r_i = r$ for all i where r is a constant. This means that all the intruders have equal power[2]. Along with this assumption, we can rewrite the detected current as follows.

$$i_{\text{det}}(t) = i_s(t)\left[1 + \sum_{i=1}^{N-1}\rho_i(t) - 2\sum_{i=1}^{N-1}\sqrt{\sigma_i(t)} + 2\sum_{i=1}^{N-2}\sum_{j=i+1}^{N-1}\sqrt{\rho_i(t)\rho_j(t)}\right] \tag{5.7}$$

where

[2]In a real system, this assumption may not be 100% precise. In general, it may be reasonable to take r as the ratio of average interferer power to the power of the signal.

$$\rho_i(t) = \begin{cases} r_i & \text{when } i_{c,i}(t) > 0 \\ 0 & \text{when } i_{c,i}(t) = 0 \end{cases} \tag{5.8}$$

and

$$\sigma_i(t) = \begin{cases} r_i & \text{when } i_s(t), i_{c,i}(t) > 0 \\ 0 & \text{otherwise} \end{cases} \tag{5.9}$$

After defining the photodetector current, we will now find the samples at the output of the matched filter. Let $n_i : i = 1, \ldots, l$ be the ratio of the rate of the i^{th} interferer to that of the signal and $n_i = 1$ for $i = l+1, \ldots, N-1$. In other words, there are n_i bit periods of the i^{th} intruder $(i = 1, \ldots, l)$ in T secs where T is the bit period of the signal. Indeed, let us define $T_{ci} = \frac{T}{n_i}$, where T_{ci} is the bit period of the i^{th} intruder $(i = 1, \ldots, l)$, and let $T_{ci} = 1$ for $i = l+1, \ldots, N-1$.

Let k_i be the ratio of the duration that the i^{th} interferer is mark to the bit period of the signal (T) for a signal bit. Thus, k_i is a Binomial random variable whose probability mass function is as follows.

$$P\left(k_i = k\frac{T_{ci}}{T}\right) = \binom{n_i}{k}\left(\frac{1}{2}\right)^{n_i} \tag{5.10}$$

Note that

$$\begin{aligned} E[k_i] &= \frac{1}{2}\frac{T_{ci}}{T}n_i \\ &= \frac{1}{2} \end{aligned} \tag{5.11}$$

and

$$\text{var}(k_i) = \left(\frac{1}{2}\frac{T_{ci}}{T}\right)^2 n_i \tag{5.12}$$

$$= \frac{1}{4}\frac{T_{ci}}{T}$$

For small values of $\frac{T_{ci}}{T}$, the i^{th} crosstalk component is mark during almost half of the bit period of the signal. Before writing an expression for the detected current at the output of the matched filter, we first discuss the relation between the variable k_i and the process $\rho_i(t)$. Since $\rho_i(t)$ is constant (r) when the i^{th} interferer is a mark and 0 otherwise, for the signal bit which starts at time τ, k_i can be defined as

$$k_i = \frac{1}{T}\int_{\tau}^{\tau+T} \frac{\rho_i(t)}{r}\, dt \tag{5.13}$$

$$rTk_i = \int_{\tau}^{\tau+T} \rho_i(t)\, dt \tag{5.14}$$

Similarly, rewriting Expression 5.13 in a different form, we get

$$k_i = \frac{1}{T}\int_{\tau}^{\tau+T} \sqrt{\frac{\rho_i(t)}{r}}\, dt \tag{5.15}$$

$$\sqrt{r}Tk_i = \int_{\tau}^{\tau+T} \sqrt{\rho_i(t)}\, dt \tag{5.16}$$

At this point, we have enough tools to write the expression for a sample of the current at the output of the matched filter. Since the shape of the pulses are rectangular, the matched filter is equivalent to an integrator of duration T. Therefore, if the signal bit is a 1, the output of the sampler will be

$$i'(cT) = \int_{cT}^{(c+1)T} i_{s,1}\left(1 + \sum_{i=1}^{N-1}\rho_i(t) - 2\sum_{i=1}^{N-1}\sqrt{\rho_i(t)} + 2\sum_{i=1}^{N-2}\sum_{j=i+1}^{N-1}\sqrt{\rho_i(t)\rho_j(t)}\right) dt \tag{5.17}$$

$$= i_{s,1}\int_{cT}^{(c+1)T} dt + \sum_{i=1}^{N-1}\int_{cT}^{(c+1)T} \rho_i(t)\, dt - 2\sum_{i=1}^{N-1}\int_{cT}^{(c+1)T} \sqrt{\rho_i(t)}\, dt$$
$$+2\sum_{i=1}^{N-2}\sum_{j=i+1}^{N-1}\int_{cT}^{(c+1)T} \sqrt{\rho_i(t)}\sqrt{\rho_j(t)}\, dt \qquad (5.18)$$

The final term in Equation 5.18 is very complicated to deal with as itself since it involves the sum of the integral of the product of two different rate Bernoulli processes (namely, the number of trials per second (bit rate) differs for different processes) and the terms to be added are not independent. We are going to introduce an approximation for this term to make it simpler.

5.1.2 Crosstalk-Crosstalk Beat Terms

In this part, we will identify the region of parameters in which the approximation we are going to make in the next section is worth using, namely, where it improves the accuracy of the results considerably without neglecting the crosstalk-crosstalk beat terms at all.

Conditioned on the signal being a mark, the variance of the sample is

$$\mathrm{var}\left[\frac{i'(cT)}{i_{s,1}}\right] = \mathrm{var}\left[2\sum_{i=1}^{N-2}\sum_{j=i+1}^{N-1}\int_{cT}^{(c+1)T} \sqrt{\rho_i(t)}\sqrt{\rho_j(t)}\, dt \right.$$
$$\left. -\sum_{i=1}^{N-1}\int_{cT}^{(c+1)T} \left(\rho_i(t) - 2\sqrt{\rho_i(t)}\right)\, dt\right] \qquad (5.19)$$

Since the two terms of the above expression are negatively correlated, the variance of the sum of them is less than or equal to the sum of the individual variances. Also, in the first term the variance of the integral of the product of two processes is less than or equal to the variance of the integral of the square of the process with lower rate (i.e., $\sqrt{\rho_i(t)}$). Thus, an upper bound for the expression can be written as follows.

$$\mathrm{var}\left[\frac{i'(cT)}{i_{s,1}}\right] \leqslant 4\mathrm{var}\left[\sum_{i=1}^{N-2}\sum_{j=i+1}^{N-1}\int_{cT}^{(c+1)T} \rho_i(t)\, dt\right]$$

$$
\begin{aligned}
&+\text{var}\left[\sum_{i=1}^{N-1}\int_{cT}^{(c+1)T}\left(\rho_i(t)-2\sqrt{\rho_i(t)}\right)\,dt\right] \\
&= 4r^2\text{var}\left[\sum_{i=1}^{N-2}\sum_{j=i+1}^{N-1}k_i\right]+\left(r-2\sqrt{r}\right)^2\text{var}\left[\sum_{i=1}^{N-1}k_i\right] \qquad (5.20)\\
&= 4r^2\sum_{i=1}^{N-2}(N-i-1)^2\,\text{var}\left[k_i\right]+\left(r-2\sqrt{r}\right)^2\sum_{i=1}^{N-1}\text{var}\left[k_i\right]
\end{aligned}
$$

Noting that since the process k_i is Binomial which takes n_i possible values from 0 to 1, the variance of k_i can be found as

$$
\begin{aligned}
\text{var}\left[k_i\right] &= \left(\frac{1}{n_i}\right)^2 n_i\left(\frac{1}{2}\right)^2 \\
&= \frac{1}{4n_i} \qquad (5.21)
\end{aligned}
$$

Rewriting the bound with the variance calculated for k_i, we get

$$
\begin{aligned}
\text{var}\left[\frac{i'(cT)}{i_{s,1}}\right] &\leqslant 4r^2\sum_{i=1}^{N-2}(N-i-1)^2\frac{1}{4n_i}+\left(r-2\sqrt{r}\right)^2\sum_{i=1}^{N-1}\frac{1}{4n_i} \qquad (5.22)\\
&\leqslant \frac{1}{6}r^2(N-2)(N-1)(2N-3)+r(N-1) \qquad (5.23)
\end{aligned}
$$

The second inequality follows from $n_i \geqslant 1$, $\left(r-2\sqrt{r}\right)^2 \geqslant 4r$. The first term in the expression is due to crosstalk-crosstalk beat and the second is due to the signal-crosstalk beat. The percentage contribution of the first term is sketched as a function of N when $r=-30$ dB and $r=-40$ dB in Figures 5.1 and 5.2 respectively.

We can conclude from the two graphs that crosstalk-crosstalk beat variance becomes increasingly important since it increases as $O\left(N^3\right)$ whereas the signal-crosstalk variance increases as $O\left(N\right)$ and has an important contribution on the total interference process. Therefore, neglecting these terms becomes more and more unreasonable as N increases.

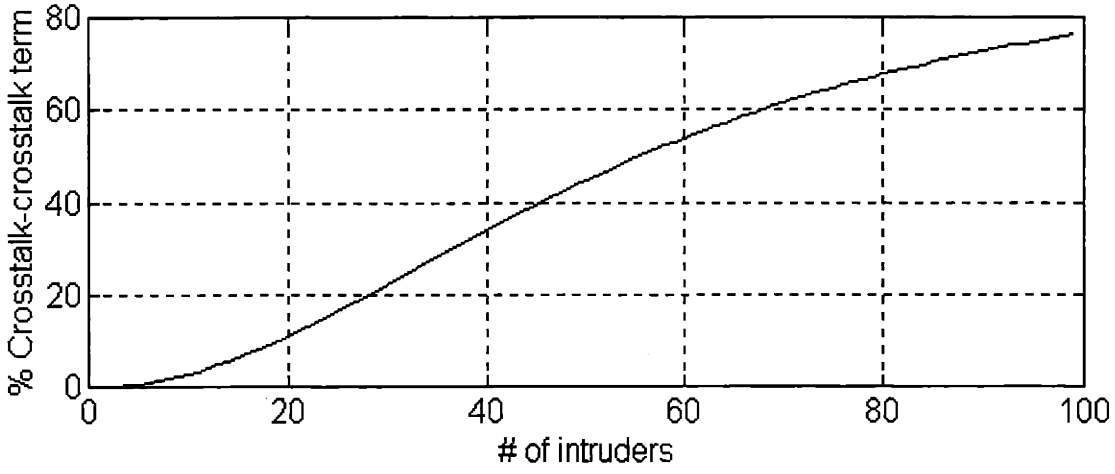

Figure 5-1: The percentage of the variance of the crosstalk-crosstalk interferer versus $N-1$ for $r=-30$ dB. As the number of interferers exceeds 50, the crosstalk-crosstalk variance starts to dominate.

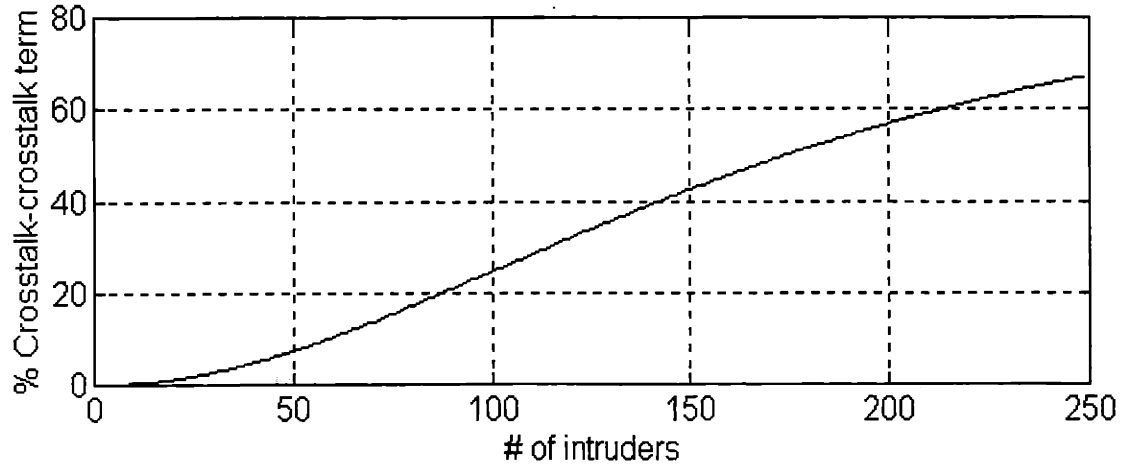

Figure 5-2: The percentage of the variance of the crosstalk-crosstalk interferer versus $N-1$ for $r=-40$ dB. As the number of interferers exceeds 150, the crosstalk-crosstalk variance starts to dominate.

5.1.3 The Linear Approximation

In Equation 5.18, the rate of the second process inside the integral ($\sqrt{\rho_j(t)}$) is higher than that of the first one ($\sqrt{\rho_i(t)}$). The below inequalities are valid for all $\rho_i(t), \rho_j(t)$ pairs at all times.

$$0 \leqslant \sqrt{\rho_i(t)}\sqrt{\rho_j(t)} \leqslant \rho_i(t) \tag{5.24}$$

$$0 \leqslant \sqrt{\rho_i(t)}\sqrt{\rho_j(t)} \leqslant \rho_j(t) \tag{5.25}$$

These two inequalities lead us to employ the linear approximation of the form $a_1\rho_i(t) + a_2\rho_j(t) + a_3$ to represent $\sqrt{\rho_i(t)}\sqrt{\rho_j(t)}$. Evaluation of the three parameters a_1, a_2 and a_3 can be viewed as a linear estimation problem. We will find the process of the form $a_1\rho_i(t) + a_2\rho_j(t) + a_3$ which is unbiased and minimizes the mean square error. Next, we will indicate the important observations to develop the tools to solve the problem.

1. Let $b(t)$ be the random binary wave. Namely, the value of $b(t)$ between times cT and $(c+1)T$ can be evaluated by a toss of a fair coin for an integer c. If the outcome of the toss is "H", the value is 1 and otherwise it is 0. One can make the following observations.

$$\rho_i(t) = rb_i(t) \tag{5.26}$$

$$\sqrt{\rho_i(t)} = \sqrt{r}b_i(t) \tag{5.27}$$

   where $b_i(t)$ is the normalized version of $\rho_i(t)$.

2. The autocorrelation function of the random binary wave $b_i(t)$ can be evaluated as follows by straightforward manipulations on [22].

$$R_b(\tau) = \begin{cases} \frac{1}{4}\left(2 - \frac{\tau}{T_{ci}}\right) & , |\tau| < T \\ \frac{1}{4} & , \ |\tau| \geqslant T \end{cases} \tag{5.28}$$

Let us return to the main problem and define the error process whose power is to be minimized (to minimize the mean square error).

$$e(t) \triangleq \sqrt{\rho_i(t)}\sqrt{\rho_j(t)} - \left[a_1\rho_i(t) + a_2\rho_j(t) + a_3\right] \tag{5.29}$$

For the estimation to be unbiased, the mean of $e(t)$ should be 0.

$$\begin{aligned} E[e(t)] &= E\left[\sqrt{\rho_i(t)}\sqrt{\rho_j(t)} - \left[a_1\rho_i(t) + a_2\rho_j(t) + a_3\right]\right] \\ &= E\left[\sqrt{\rho_i(t)}\right] E\left[\sqrt{\rho_j(t)}\right] - a_1 E[\rho_i(t)] - a_2 E[\rho_j(t)] - a_3 \\ &= \frac{\sqrt{r}}{2}\frac{\sqrt{r}}{2} - a_1\frac{r}{2} - a_2\frac{r}{2} - a_3 \end{aligned} \tag{5.30}$$

This leads to the first relation between a_1, a_2 and a_3.

$$\frac{r}{4} - \frac{r}{2}(a_1 + a_2) - a_3 = 0 \tag{5.31}$$

The covariance function of the error process can be found as follows.

$$\begin{aligned} K_e(\tau) &= E[e(t+\tau)\, e(t)] \qquad (5.32) \\ &= E\Big\{\sqrt{\rho_i(t+\tau)}\sqrt{\rho_i(t)}\sqrt{\rho_j(t+\tau)}\sqrt{\rho_j(t)} \\ &\quad -2\left[a_1\sqrt{\rho_i(t+\tau)}\sqrt{\rho_j(t+\tau)}\rho_i(t) + a_2\sqrt{\rho_j(t+\tau)}\sqrt{\rho_i(t+\tau)}\rho_j(t)\right] \\ &\quad +a_1^2\rho_i(t+\tau)\rho_i(t) + a_1a_2\rho_i(t+\tau)\rho_j(t) + a_1a_2\rho_i(t)\rho_j(t+\tau) + a_2^2\rho_j(t+\tau)\rho_j(t)\Big\} \\ &\quad -2a_3E\left[\sqrt{\rho_i(t+\tau)}\sqrt{\rho_j(t)} - a_1\rho_i(t) - a_2\rho_j(t)\right] + a_3^2 \\ &= E[rb_i(t+\tau)\, b_i(t)]\, E[rb_j(t+\tau)\, b_j(t)] \\ &\quad -2E\left[a_1r^{3/2}b_i(t+\tau)\, b_i(t)\right] E\left[\sqrt{r}b_j(t+\tau)\right] \\ &\quad -2E\left[a_2r^{3/2}b_j(t+\tau)\, b_j(t)\right] E\left[\sqrt{r}b_i(t+\tau)\right] + E\left[a_1^2r^2b_i(t+\tau)\, b_i(t)\right] \\ &\quad +E[a_1rb_i(t+\tau)]\, E[a_2rb_j(t)] + E[a_1rb_i(t)]\, E[a_2rb_j(t+\tau)] \\ &\quad +E\left[a_2^2r^2b_j(t+\tau)\, b_j(t)\right] - 2a_3^2 + a_3^2 \end{aligned}$$

$$
\begin{aligned}
&= r^2 R_{b_i}(\tau) R_{b_j}(\tau) - a_1 r^2 R_{b_i}(\tau) - a_2 r^2 R_{b_j}(\tau) + a_1 r^2 R_{b_i}(\tau) + \frac{1}{2} a_1 a_2 r^2 \\
&\quad + a_2 r^2 R_{b_j}(\tau) - a_3^2 \\
&= r^2 \left[R_{b_i}(\tau) R_{b_j}(\tau) + \frac{1}{2} a_1 a_2 + \left(a_1^2 - a_1\right) R_{b_i}(\tau) + \left(a_2^2 - a_2\right) R_{b_j}(\tau) \right] - a_3^2 \quad (5.33)
\end{aligned}
$$

The mean square error is the variance of a sample of the error process, $e(t)$. Thus, the MSE can be found as

$$
\begin{aligned}
\sigma_e^2 &= K_e(0) \\
&= \frac{1}{4} r^2 \left[1 + 2a_1 a_2 + 2\left(a_1^2 - a_1\right) + 2\left(a_2^2 - a_2\right)\right] - a_3^2
\end{aligned} \quad (5.34)
$$

Next, we will minimize this quantity together with the constraint $\frac{r}{4} - \frac{r}{2}(a_1 + a_2) - a_3 = 0$. Let us define the objective function $D(a_1, a_2, a_3, \lambda)$ as follows.

$$
\begin{aligned}
D(a_1, a_2, a_3, \lambda) &= \frac{1}{4} r^2 \left[1 + 2a_1 a_2 + 2\left(a_1^2 - a_1\right) + 2\left(a_2^2 - a_2\right)\right] - a_3^2 \\
&\quad - \lambda \left[\frac{r}{4} - \frac{r}{2}(a_1 + a_2) - a_3\right]
\end{aligned} \quad (5.35)
$$

where λ is the Lagrange multiplier. Taking the derivative of $D(a_1, a_2, a_3, \lambda)$ with respect to a_1, a_2, and a_3 yield

$$
\frac{\partial D(a_1, a_2, a_3, \lambda)}{\partial a_1} = \frac{1}{4} r^2 (2a_2 + 4a_1 - 2) + \lambda \frac{r}{2} \quad (5.36)
$$

$$
\frac{\partial D(a_1, a_2, a_3, \lambda)}{\partial a_2} = \frac{1}{4} r^2 (2a_1 + 4a_2 - 2) + \lambda \frac{r}{2} \quad (5.37)
$$

$$
\frac{\partial D(a_1, a_2, a_3, \lambda)}{\partial a_3} = -2a_3 + \lambda \quad (5.38)
$$

Note that in the expression for σ_e^2, if we plug in $a_3 = \frac{r}{4} - \frac{r}{2}(a_1 + a_2)$ (which is the equation of the constraint surface), $\frac{\partial \sigma_e^2}{\partial a_1} = \frac{\partial \sigma_e^2}{\partial a_2} = \frac{r^2}{2} > 0$. Therefore, the error variance is a convex function over the plane $\frac{r}{4} - \frac{r}{2}(a_1 + a_2) - a_3 = 0$, and it has an global minima at the point where $\frac{\partial D(a_1, a_2, a_3, \lambda)}{\partial a_1} = \frac{\partial D(a_1, a_2, a_3, \lambda)}{\partial a_2} = \frac{\partial D(a_1, a_2, a_3, \lambda)}{\partial a_3} = 0$. Solving the three equations

simultaneously on the constraint plane gives us that the minima occurs at $a_1 = a_2 = \frac{1}{2}$, $a_3 = -\frac{r}{4}$. The corresponding Lagrange Multiplier is $\lambda = -\frac{1}{2}r$. The minimum mean square error (MMSE) is thus,

$$\begin{aligned} \sigma^2_{e-MMSE} &= \frac{1}{4}r^2\left(\frac{1}{2}\right) - \frac{r^2}{16} \\ &= \frac{1}{16}r^2 \end{aligned} \tag{5.39}$$

Hence,

$$\sigma_{e-MMSE} = \frac{1}{4}r \tag{5.40}$$

Note that, the variance of a sample of the process $\sqrt{\rho_i(t)}\sqrt{\rho_j(t)}$ is $\frac{3}{16}r^2$ which is the variance of the error process increased by a factor 3. Also, the variance of a sample of the process $\frac{1}{2}\left(\rho_i(t) + \rho_j(t)\right) - \frac{r}{4}$ is $\frac{1}{8}r^2$.

5.2 Evaluating the Error Probability

Rewriting the sample value conditioned on the signal bit being a 1 along with the approximation, we get

$$\begin{aligned} i'(cT) &= i_{s,1}\int_{cT}^{(c+1)T} dt + \sum_{i=1}^{N-1}\int_{cT}^{(c+1)T}\left(\rho_i(t) - 2\sqrt{\rho_i(t)}\right)\, dt \\ &\quad +2\sum_{i=1}^{N-2}\sum_{j=i+1}^{N-1}\int_{cT}^{(c+1)T}\frac{1}{2}\left[\rho_i(t) + \rho_j(t) - \frac{r}{2}\right]\, dt \\ &= Ti_{s,1}\left[1 + \left(r - 2\sqrt{r}\right)\sum_{i=1}^{N-1}k_i + r\sum_{i=1}^{N-2}\sum_{j=i+1}^{N-1}\left(k_i + k_j - \frac{r}{2}\right)\right] \end{aligned} \tag{5.41}$$

The last term in the above equation can be rewritten as follows.

$$\begin{aligned} r\sum_{i=1}^{N-2}\sum_{j=i+1}^{N-1}\left(k_i+k_j-\frac{r}{2}\right) &= r\left[\sum_{i=1}^{N-2}\sum_{j=i+1}^{N-1}k_i+\sum_{i=1}^{N-2}\sum_{j=i+1}^{N-1}k_j-\frac{r}{2}\sum_{i=1}^{N-2}\sum_{j=i+1}^{N-1}1\right] \\ &= r\left[\sum_{i=1}^{N-2}(N-i-1)\,k_i+\sum_{i=2}^{N-1}(i-1)\,k_i-\frac{r}{2}\sum_{i=1}^{N-2}(N-i-1)\right] \\ &= r\,(N-2)\left[\sum_{i=1}^{N-1}k_i-\frac{N-1}{2}\right] \end{aligned} \tag{5.42}$$

Plugging this back in the main expression together with the thermal noise, the sample value of the current at the c^{th} instant becomes

$$\begin{aligned} i'(cT) &= Ti_{s,1}\left[1+\left(r\,(N-1)-2\sqrt{r}\right)\sum_{i=1}^{N-1}k_i-\frac{r\,(N-2)\,(N-1)}{2}\right]+n'(cT) \\ &= Ti_{s,1}\left[1-\frac{r}{2}\,(N-2)\,(N-1)\right] \\ &\quad +Ti_{s,1}\left[r\,(N-1)-2\sqrt{r}\right]\sum_{i=1}^{N-1}k_i+n'(cT) \end{aligned} \tag{5.43}$$

Similarly, when the signal bit is a 0, the sample value of the current is in the following form.

$$i'(cT) = -Ti_{s,1}\frac{r}{2}\,(N-2)\,(N-1)+Ti_{s,1}r\,(N-1)\sum_{i=1}^{N-1}k_i+n'(cT) \tag{5.44}$$

The constant term, $-Ti_{s,1}\frac{r}{2}\,(N-2)\,(N-1)$, is always present in the current expressions regardless of the signal bit value. Thus, it has no effect on the performance of the system. We will ignore the term after this point for simplicity. The total interference and noise that perturbs the signal is

$$Z_1 = Ti_{s,1}\left[r\,(N-1)-2\sqrt{r}\right]\sum_{i=1}^{N-1}k_i+n'(cT) \tag{5.45}$$

when the signal bit is a 1, and

$$Z_0 = Ti_{s,1}r\,(N-1) \sum_{i=1}^{N-1} k_i + n'\,(cT) \tag{5.46}$$

when the signal bit is a space. Let $\mu_0 = Ti_{s,1}r\,(N-1)$ and $\mu_1 = Ti_{s,1}\left[r\,(N-1) - 2\sqrt{r}\right]$. The transforms of the densities of Z_0 and Z_1 can be found as

$$\begin{aligned} M_{Z_j}(s) &= E\left[\exp\left(sZ_j\right)\right] \\ &= \prod_{i=1}^{N-1}\left[\frac{1}{2} + \frac{1}{2}\exp\left(\frac{\mu_j}{n_i}s\right)\right]^{n_i} \exp\left(\frac{1}{2}s^2\sigma_{n'}^2\right) \end{aligned} \tag{5.47}$$

where $j \in \{0,1\}$ and $\sigma_{n'}^2 = \frac{N_0}{2}T$ is the variance of the Gaussian noise samples at the output of the matched filter. If the decision threshold is set to $\beta = \frac{Ti_{s,1}}{2}(1-x)$, the Chernoff bound can now be used to provide a tight upper bound on the BER.

$$P(E) \leqslant \frac{1}{2}M_{Z_0}(s)\exp\left(-s\beta\right) + \frac{1}{2}M_{Z_1}(-s)\exp\left(-s\beta'\right) \tag{5.48}$$

where $\beta' = Ti_{s,1} - \beta$ and $s > 0$. Note that the Chernoff bound has been found to be very tight (exponentially) for the error probabilities we have been dealing with and it is reasonable to assume that it is equal to the exact error probability. We will now minimize the error probability over x and s.

It is obvious that when the threshold is set to its optimum value (i.e., $x = x_{opt}$), the two terms of the expression will be equal, namely the error probability conditioned on a mark signal bit is equal to that conditioned on a space. This is intuitively reasonable if we observe the pdf of the sample conditioned on the signal which is illustrated in Figure 5.3. The effect of the ripples located around 0 and $Ti_{s,1}$ will disappear at the tails of the distribution (which is perfectly valid at $\sim 10^{-10}$ BER if we assume $\mu_j \ll 1$; the region in which this assumption is valid will be specified later). The optimal threshold is the point where the two curves intersect. Hence,

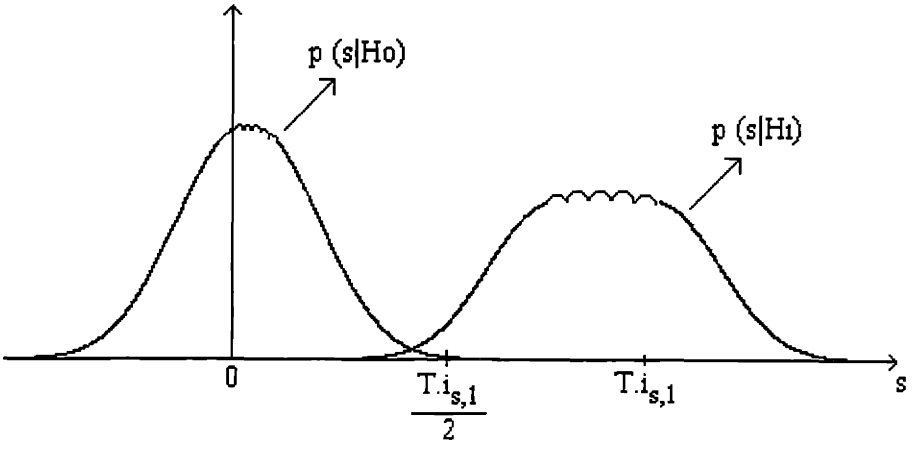

Figure 5-3: The impacts of the ripples of the sample density becomes negligable at the tails.

$$M_{Z_0}(s)\exp\left(-s\beta_{opt}\right) = M_{Z_1}(-s)\exp\left(-s\beta'_{opt}\right) \tag{5.49}$$

where $\beta_{opt} = \frac{Ti_{s,1}}{2}(1 - x_{opt})$ and $\beta'_{opt} = \frac{Ti_{s,1}}{2}(1 + x_{opt})$. To simplify the calculations, we are going to make the following approximation for $M_{Z_j}(s)$.

$$\begin{aligned}
M_{Z_j}(s) &= \prod_{i=1}^{N-1}\left[\frac{1}{2} + \frac{1}{2}\exp\left(\frac{\mu_j}{n_i}s\right)\right]^{n_i}\exp\left(\frac{1}{2}s^2\sigma_{n'}^2\right) \\
&\cong \prod_{i=1}^{N-1}\left(1 + \frac{1}{2}\frac{\mu_j}{n_i}s\right)^{n_i}\exp\left(\frac{1}{2}s^2\sigma_{n'}^2\right) &(5.50)\\
&\cong \prod_{i=1}^{N-1}\left(1 + \binom{n_i}{1}\frac{1}{2}\frac{\mu_j}{n_i}s\right)\exp\left(\frac{1}{2}s^2\sigma_{n'}^2\right) &(5.51)\\
&= \left(1 + \frac{1}{2}\mu_j s\right)^{N-1}\exp\left(\frac{1}{2}s^2\sigma_{n'}^2\right) &(5.52)
\end{aligned}$$

where 5.50 follows from the series expansion of $\exp\left(\frac{\mu_j}{n_i}s\right)$. μ_j is very close to 0 and we assume at this point that $\left|\frac{1}{2}\mu_j s\right| \ll 1$ (which is valid in some certain range of values and that range will be specified later). Therefore, in the series expansion we neglected the second and higher order terms. Relation 5.51 follows from the Binomial expansion of

$\left(1+\frac{1}{2}\frac{\mu_j}{n_i}s\right)^{n_i}$ and similarly neglecting the higher order terms with the assumption that $\left|\frac{1}{2}\mu_j s\right| \ll 1$. Along with these approximations, 5.49 can be modified as follows.

$$\begin{aligned} Ti_{s,1}sx &= (N-1)\ln\left[\frac{1-\frac{1}{2}\mu_1 s}{1+\frac{1}{2}\mu_0 s}\right] && (5.53)\\ &= (N-1)\ln\left[1+\frac{\frac{1}{2}(-\mu_1-\mu_0)s}{1+\frac{1}{2}\mu_0 s}\right] \\ &\cong (N-1)\frac{\frac{1}{2}(-\mu_1-\mu_0)s}{1+\frac{1}{2}\mu_0 s} && (5.54)\end{aligned}$$

where 5.54 follows from the series expansion of $\ln\left[1+\frac{\frac{1}{2}(-\mu_1-\mu_0)s}{1+\frac{1}{2}\mu_0 s}\right]$ and assuming that $\frac{\frac{1}{2}(-\mu_1-\mu_0)s}{1+\frac{1}{2}\mu_0 s}$ is close to 0. The optimum x as a function of s can be found as follows.

$$x_{opt} = (N-1)\frac{\sqrt{r}-(N-1)r}{1+\frac{1}{2}\mu_0 s} \qquad (5.55)$$

Next, we are going to find out the optimum s value as a function of x and solve it together with 5.55. When the threshold is set to its optimum value, the error probability conditioned on the transmission of a mark is equal to that conditioned on the transmission of a space. Using Equation 5.52, the error probability can be written as

$$\begin{aligned} P(E) &= \exp\left[(N-1)\ln\left(1+\frac{1}{2}\mu_0 s\right)+\frac{1}{2}s^2\sigma_{n'}^2 - s\beta\right] && (5.56)\\ &= \exp\left\{(N-1)\underbrace{\left[\ln\left(1+\frac{1}{2}\mu_0 s\right)+\frac{1}{2(N-1)}s^2\sigma_{n'}^2\right]}_{\gamma(s)} - s\beta\right\} \\ &= \exp\left[(N-1)\gamma(s) - s\beta\right] && (5.57)\end{aligned}$$

The optimum value of s (the value of s which makes the Chernoff bound tightest) can be found by solving the below equation.

$$\gamma'(s) = \frac{\beta}{N-1} \qquad (5.58)$$

$$\frac{\frac{1}{2}\mu_0}{1+\frac{1}{2}\mu_0 s}+\frac{1}{N-1} = \frac{\beta}{N-1}$$

where $\beta = \beta_{opt} = \frac{Ti_{s,1}}{2}(1-x_{opt})$. We will use the assumption that $\left|\frac{1}{2}\mu_0 s\right| \ll 1$ one more time to derive the optimal bound expression as follows.

$$s_{opt} \cong \frac{\beta_{opt} - \frac{1}{2}\mu_0 (N-1)}{\sigma^2_{n'}} \tag{5.59}$$

Plugging this back in expression 5.55 after rewriting β_{opt} with the optimum x value, we get a complicated expression for x_{opt} once we solve the equation with MAPLE[3]. That expression could be approximated as $(N-1)\sqrt{r}-(N-1)^2 r$ (i.e., the numerator of 5.55) since $\left|\frac{1}{2}\mu_0 s\right| \ll 1$.

Before we go on and evaluate the performance, we will identify the region that all our approximations for finding out the optimal threshold (x_{opt}) and the optimal bound parameter (s_{opt}) are reasonable. However, the only assumption we made was that $\left|\frac{1}{2}\mu_0 s\right| \ll 1$. Indeed,

$$\begin{aligned}
\frac{1}{2}\mu_0 s_{opt} &= \frac{1}{2} Ti_{s,1} r (N-1) \frac{Ti_{s,1}}{2\sigma^2_{n'}} \left[1 - x_{opt} - r(N-1)^2\right] \\
&= \frac{Ti^2_{s,1}}{2N_0} r (N-1)\left[1-\sqrt{r}(N-1)\right] \\
&= \frac{E_b}{N_0} r (N-1)\left[1-\sqrt{r}(N-1)\right]
\end{aligned} \tag{5.60}$$

Figures 5.4, 5.5, 5.6 illustrate the absolute value of the Expression 5.60 ($\left|\frac{1}{2}\mu_0 s_{opt}\right|$) versus $N-1$ for $r = -25, -30$, and -40 dB respectively at $\frac{E_b}{N_0} = 16$ dB. We can deduce from these curves that the expressions we get for optimum x and s values are valid only under some certain conditions which generally impose a limit on the maximum number users that can be supported by the network. For instance, if the crosstalk per user is -30 dB, Expressions 5.61 and 5.62 give very accurate estimates of the optimum x value and the

[3]Version 5, Release 4. © Copyright 1981-1998 Waterloo Maple Inc.

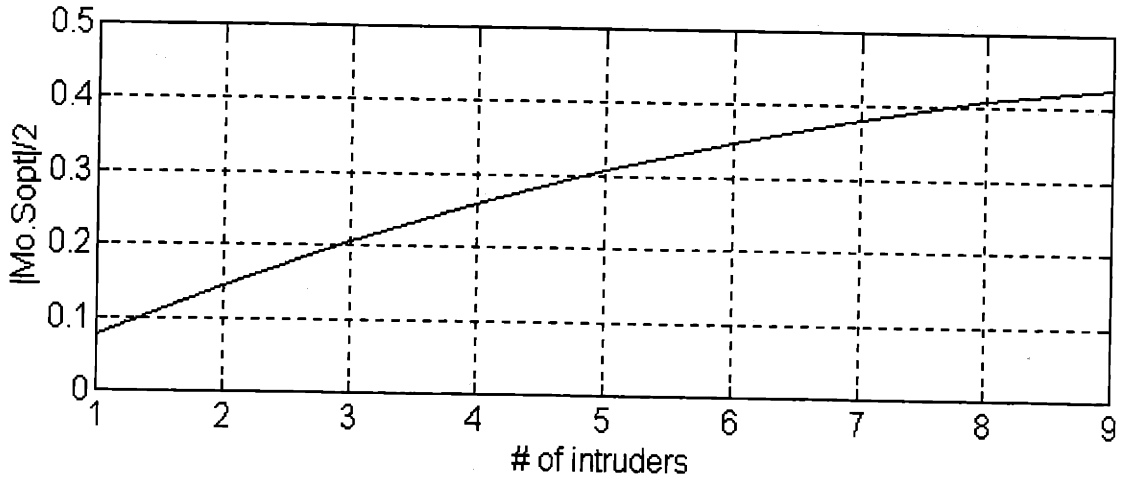

Figure 5-4: Illustration of 5.60 versus $N-1$ for constant $\frac{E_b}{N_o} = 16$ dB, $r = -25$ dB. One can observe that the approximations are good if $N \leqslant 5$ (the curve stays below 0.25).

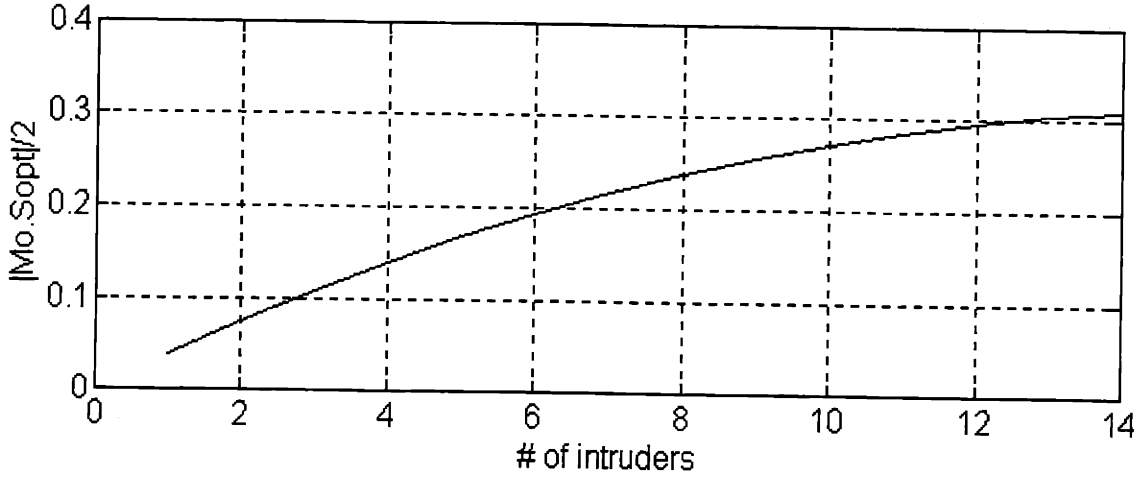

Figure 5-5: Illustration of 5.60 versus $N-1$ for constant $\frac{E_b}{N_o} = 16$ dB, $r = -30$ dB. One can observe that the approximations are good if $N \leqslant 10$ (the curve stays below 0.25).

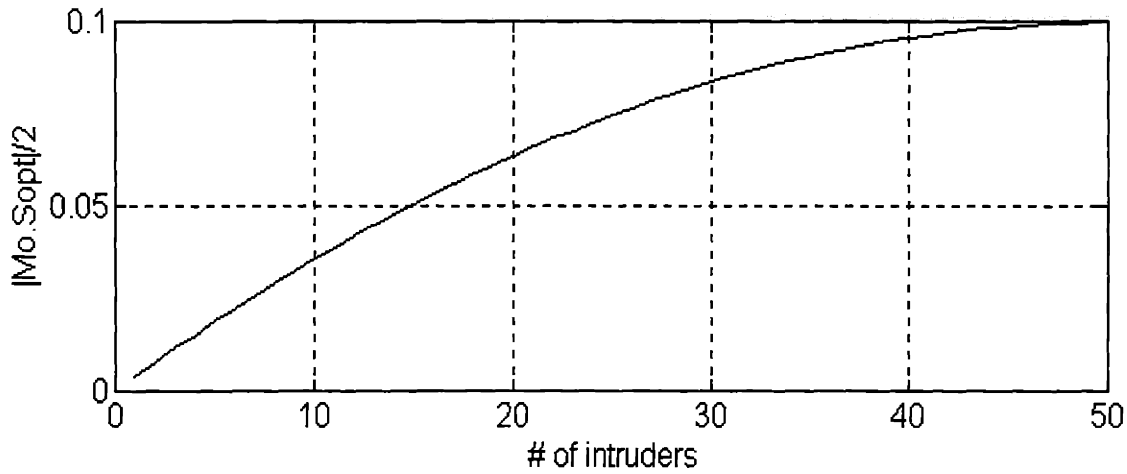

Figure 5-6: Illustration of 5.60 versus $N-1$ for constant $\frac{E_b}{N_o} = 16$ dB, $r = -40$ dB. One can observe that the approximations are good if $N \leqslant 50$ (the curve stays below 0.1).

optimum s value respectively iff $N \leqslant 10$ (i.e., $\left|\frac{1}{2}\mu_0 s\right| \leqslant 0.25$).

Now, we will turn back and plug the optimum values to the error probability expressions to find the tightest bound on the error probability. The optimal parameters are

$$x_{opt} \cong (N-1)\sqrt{r} - (N-1)^2 r \tag{5.61}$$

$$s_{opt} \cong \frac{Ti_{s,1}^2}{2\sigma_{n'}^2}\left[1 - \sqrt{r}\,(N-1)\right] \tag{5.62}$$

and the tightest bound on the BER is thus,

$$P(E) \leqslant M_{Z_0}(s_{opt}) \exp\left(-s_{opt}\beta_{opt}\right) \tag{5.63}$$

$$= \prod_{i=1}^{N-1}\left[\frac{1}{2} + \frac{1}{2}\exp\left(\frac{1}{n_i}\mu_0 s_{opt}\right)\right]^{n_i} \exp\left(-s_{opt}\beta_{opt}\right)$$

$$= \prod_{i=1}^{N-1}\left\{\frac{1}{2} + \frac{1}{2}\exp\left(\frac{1}{n_i} r\,(N-1)\left[1 - \sqrt{r}\,(N-1)\right]\frac{2E_b}{N_0}\right)\right\}^{n_i} \tag{5.64}$$

$$\exp\left(-\left[1-2\sqrt{r}\,(N-1)+2r\,(N-1)^2-r^{3/2}\,(N-1)^3\right]\frac{E_b}{N_0}\right)$$

5.3 Examples

In this section, we will examine three systems and use Expression 5.64 to determine their error probability curves.

As the first example, consider a 32×32 wavelength router which can support 32 users that are always active. -40 dB of the power of a channel leaks to every other port. All the users communicate at the same constant rate ($n_i = 1, \forall i$).

First of all, let us check whether $\frac{1}{2}\mu_0 s_{opt}$ is sufficiently small so that 5.61 and 5.62 are reasonably close to the optimal values.

$$\begin{aligned}\frac{1}{2}\mu_0 s_{opt} &= \frac{E_b}{N_0}10^{-4}\left[31\left(1-31\times 10^{-2}\right)\right]\\ &= 2.14\times 10^{-3}\frac{E_b}{N_0}\end{aligned} \tag{5.65}$$

Thus, $\left|\frac{1}{2}\mu_0 s_{opt}\right| \leqslant 0.2$ if $\frac{E_b}{N_0} < 20$ dB. The BER of a channel versus $\frac{E_b}{N_0}$ is illustrated in Figure 5.7 together with the baseline. Note that if $\frac{E_b}{N_0}$ exceeds 20 dB, the performance found by 5.64 will no longer be optimal. Examining the figure, we observe that the power penalty at 10^{-10} error probability is ~ 4 dB.

The second example is Lucent 000371695 Wavelength Grating Router. It has 8 ports and it has been experimentally determined that the average crosstalk is -30 dB. If all the users communicate all the time at the same rate through the router, the minimum error probability can be found by 5.64 iff

$$\begin{aligned}\frac{1}{2}\mu_0 s_{opt} &= \frac{E_b}{N_0}10^{-3}\left[7\left(1-7\times 0.032\right)\right]\\ &= 5.43\times 10^{-3}\frac{E_b}{N_0}\end{aligned} \tag{5.66}$$

is sufficiently small. Thus, the error probability curve illustrated in Figure 5.8 is the

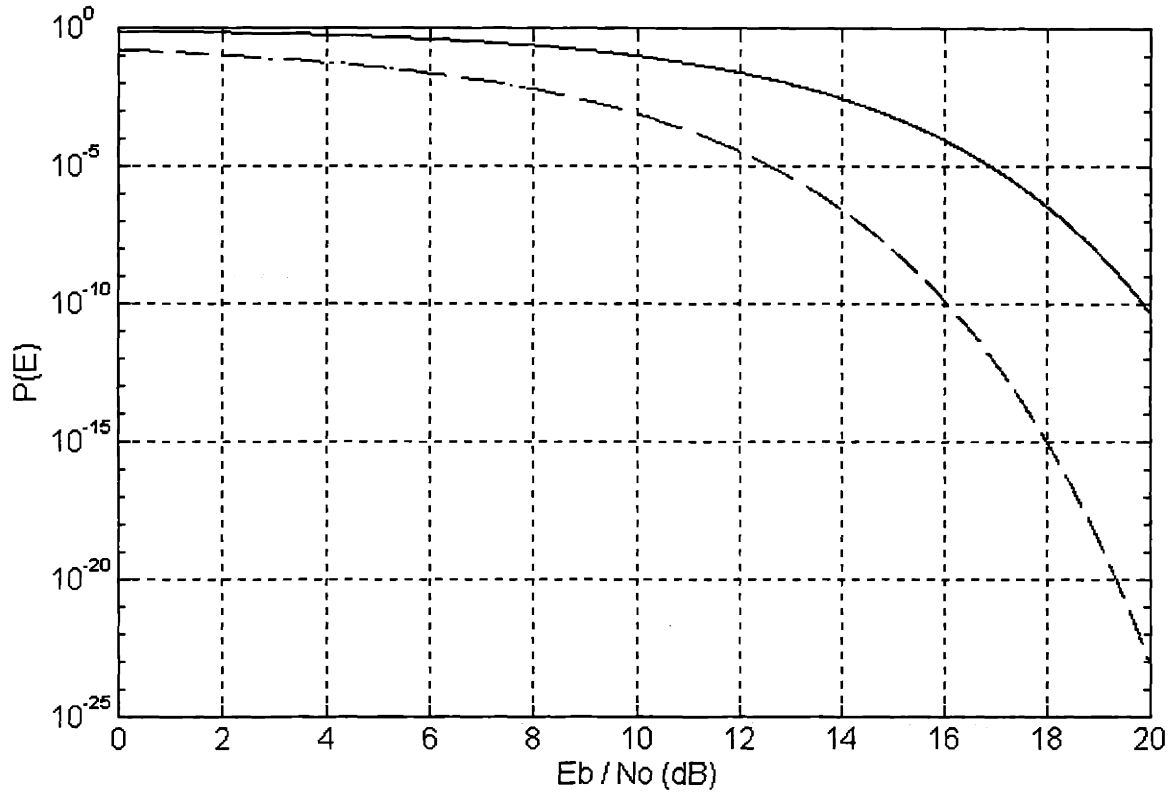

Figure 5-7: The perfromance curve of the system with a 32×32 wavelength router (solid curve) and the baseline (dashed curve). The power penalty is 4 dB when the error probability is $\sim 10^{-10}$. Note that the solid curve gives the tightest bound for the error probability of the system in the give region.

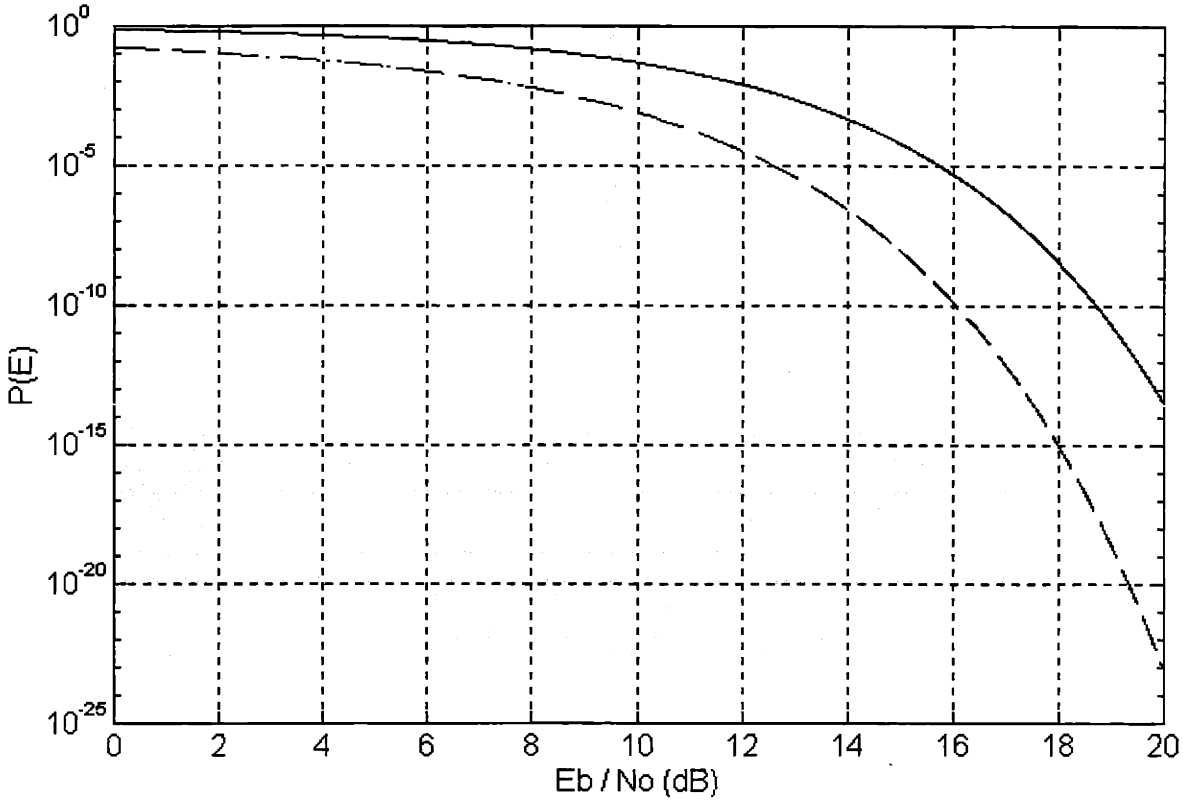

Figure 5-8: The perfromance curve of the system with Lucent 000371695 wavelength router (solid curve) and the baseline (dashed curve). The power penalty is 2.8 dB when the error probability is $\sim 10^{-10}$. Note that the solid curve gives the tightest bound for the error probability of the system for $\frac{E_b}{N_0} \leqslant 19$ dB.

optimal curve until $\frac{E_b}{N_0} \sim 18 - 19$ dB. The power penalty at 10^{-9} error probability is 2.7 dB.

The above two examples are examined in [25] in which crosstalk-crosstalk terms were neglected. At optimum threshold, the power penalty was found to be ~ 1 dB for the first example where $N = 32$, and ~ 1.5 dB for the second example where $N = 8$. One can observe that the power penalty found by [25] for 8 intruders is 1.2 dB less than that found using 5.64 and this difference becomes 3 dB for 32 intruders. This proves that neglecting crosstalk-crosstalk beat terms become increasingly inappropriate with increasing N.

Finally, let us consider a communication system at rate 2.488 Gb/s. Let there be 5

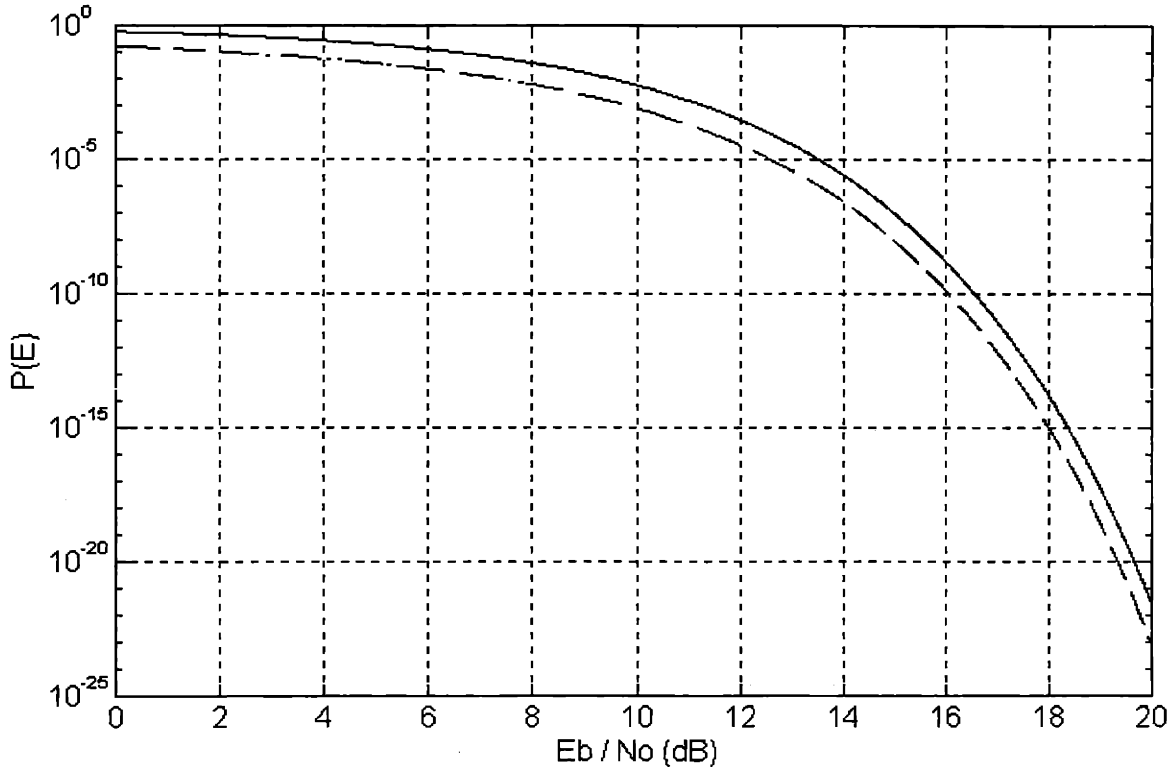

Figure 5-9: The perfromance curve of the system with 5 intruders all at different rates (solid curve) and the baseline (dashed curve). The power penalty is 0.5 dB when the error probability is $\sim 10^{-10}$. Note that the solid curve gives the tightest bound for the error probability of the system for $\frac{E_b}{N_0} \leqslant 19$ dB ($P(E) \geqslant 10^{-18}$).

interferers, two at 9.95 Gb/s and the others at 2.488 Gb/s, 622 Mb/s and 155 Mb/s each with power -30 dB. Then the condition of optimality for 5.64 is that

$$\begin{aligned} \frac{1}{2}\mu_0 s_{opt} &= \frac{E_b}{N_0} 10^{-3} \left[5\left(1 - 5 \times 0.032\right)\right] \\ &= 4.2 \times 10^{-3} \frac{E_b}{N_0} \end{aligned} \tag{5.67}$$

should be sufficiently small. The error probability curve is illustrated in Figure 5.9 and it is optimal for $\frac{E_b}{N_0} \leqslant 18 - 19$ dB. The power penalty at 10^{-9} BER is 0.5 dB.

5.4 Summary and Conclusions

In this chapter, we presented a worst case approach for the case where there is more than one intruder. We claimed that neglecting the crosstalk-crosstalk beat terms is not always reasonable even when the crosstalk is low and we proved our claim by illustrating the range of parameters that these terms are not negligible. Instead of neglecting them, we introduced a linear MMSE approximation for the crosstalk-crosstalk beat terms. Next, we employed a minimum Chernoff bound approach to determine the optimum threshold and find the most strict bound on the error probability. Finally we analyzed three practical examples to illustrate the results.

Some of the most significant results of this chapter can be listed as follows. In all the past work encountered on the issue of crosstalk analysis of multiple interferers, the crosstalk-crosstalk beat terms have been neglected. We presented a region where that approximation is valid and the error probabilities found following that approximation are precise. We found an approximate optimum threshold, specified the region where it is close to the real optimum value, performed a very precise analysis without neglecting the crosstalk-crosstalk beat terms, and covered a very general case where the rates at which the signals transmit are arbitrary. We compared our results with those deduced in the past work in which crosstalk-crosstalk beat terms had been neglected and found that there is a considerable gap between the power penalties which increases as the number of the interferers increases. This proves that neglecting those terms may be inappropriate for many cases and may not yield accurate results.

Chapter 6

Conclusions

In this thesis, we presented rigorous crosstalk analysis techniques for an optical communication system. We specified a number of different cases and identified our goals step by step. Our analysis strategy was to begin from the simplest case and extend the ideas and combine them with the new ones and those of the previous work to solve harder cases. In all these steps, we were very accurate and did not make any assumptions without making sure that they are reasonable. We verified some of the past results and showed their weaknesses if their results are inaccurate.

In the first chapter, we introduced our models and system structures. We mentioned that our motivation for this work was the approximations and assumptions made in the past work which we find doubtful. We specified the steps of the analysis and indicated the models and system parameters we used.

In the second chapter, we introduced basic crosstalk analysis methods for the two simplest cases which are 0 crosstalk (baseline) and the worst cases. We showed that even a deterministic optical interferer may harm the system since, due to the square-law nature of the optical detector, any wave propagating beside the signal is multiplied with the signal in the electrical domain. Thus, the interference portion of the current becomes a function the communication signal due to the signal-interference beat terms. It takes on different values depending on whether the signal bit is a 1 or a 0. This sets up the

basic idea for the following chapters. We showed that even an interferer of power 20 dB lower than that of the signal can cause 2 dB of crosstalk. We found out that the results we get for the electrical and the optical power penalties are consistent with those found in [4] and [6], only more accurate since we did not neglect the crosstalk-crosstalk beat terms.

We divided Chapter 3 into two sections one of which consists of the analysis for synchronous signal and crosstalk bit streams and the other generalizes this for asynchronous streams. In the first section, we found out that if the signal has a bit rate higher than that of the crosstalk, then the power penalty is very close to that of the worst case. In fact, we determined that the difference between the two cases is no more than 0.05 dB at the error probabilities close to 10^{-9} for an interferer of power 20 dB below that of the signal. We also considered the effects of dynamic thresholding within this case and argued that, with dynamic thresholding the performance could be no better than that with optimum static threshold most of the times (equally well only under some certain conditions). It may be advantageous if the received signal power and the crosstalk power are not constant throughout the communication. We also showed that even the bit sequence of the crosstalk is known by the receiver, the error performance of the system cannot be improved considerably. Next, we considered the case where the bit rate of the signal is lower than that of the crosstalk. We deduced that if the ratio of the rates is small, namely, the rates are close to each other, the performance is close to the worst case and the error probability is a decreasing function of this ratio. As n gets larger and larger, the probability of error approaches to that of the worst case with crosstalk power equal to half the original. In the next section, we proved that the optimum threshold and the error probabilities of the asynchronous system is almost equal to those of the synchronous. Hence, assuming that the bit streams are synchronous is perfectly reasonable and it simplifies analyses enormously.

In the fourth chapter, the analysis done for the worst case phases and polarizations are generalized to those for random phases and polarizations for single interferer. We

used the model which was introduced by [6]. All the states of polarizations (e.g., circular, elliptic, linear, etc.) and all the possible relative directions of the crosstalk with respect to the signal from the worst case of matched signal and crosstalk polarizations to orthogonal polarizations can be represented with this model. The expression for the detected current is fairly simple even with such a detailed representation. As expected, the optimum threshold level is increased compared to the worst case and gets closer to $\frac{Ti_{s,1}}{2}$ which is the optimum threshold level for the crosstalk-free case both when the bit rate of the signal is higher and vice-versa. Regardless of the rates of the signal and the crosstalk relative to each other, the performance of the system is very close to the worst case which justifies the conclusions drawn by [9], namely, systems with randomly polarized fields display a statistical preference for near-worst case operation (a substantial likelihood of operation within a few dB of the worst case).

Finally in Chapter 5, we presented a worst case approach for the case where there are more than one intruder. In all the past work encountered on the issue of crosstalk analysis of multiple interferers, the crosstalk-crosstalk beat terms had been neglected. We presented a region where that approximation is valid and the error probabilities found following that approximation are precise. We found an approximate optimum threshold, specified the region where it is close to the real optimum value, performed a very precise analysis without neglecting the crosstalk-crosstalk beat terms, and covered a very general case where the rates at which the signals transmit are arbitrary. We compared our results with those deduced in the past work in which crosstalk-crosstalk beat terms had been neglected and found that there is a considerable gap between the power penalties which increases as the number of the interferers increases. This proves that neglecting those terms may be inappropriate for many cases and may not yield accurate results.

The future work can proceed in different directions. First, it is necessary to find a method to combine the ideas of Chapters 4 and 5 in order to get an expression for the error probability of the most general case, multiple crosstalk sources all with random phase and polarizations. In addition, it is more realistic in some cases to assume that the

sources are not active all the times; in particular, a statistical model can be developed for the number of users (e.g., Binomial) and the system can be analyzed with that statistics. As a next step, methods to improve the crosstalk performance can be sought. For instance, the results found and techniques used in this thesis can be modified to analyze fiber-optic CDMA systems employing optical orthogonal codes. It can be proved that, due to the orthogonal nature of CDMA codewords, such systems perform much better compared to other multiple accessing schemes. It can be shown that instead of using a WDM system with a large wavelength router, using CDMA over a rather small router suppresses crosstalk drastically. However, more work needs to be done to determine the ability of CDMA to suppress crosstalk.

Bibliography

[1] B. R. Hemenway, M. L. Stevens, R. A. Barry, C. E. Koksal and E. A. Swanson, "Demonstration of a Re-Configurable Wavelength-Routed Network at 1.14 Tbps", Optical Fiber Communication Conference '97, Postdeadline Papers 26 (1997)

[2] B. R. Hemenway, M. L. Stevens, R. A. Barry and E. A. Swanson, "20-Channel Wavelength-Routed Tbps Capacity All-Optical MAN Test-beds" (1997)

[3] I. P. Kaminow, et. al., "A Wideband All-Optical WDM Network", IEEE Journal on Selected Areas of Communications, Vol.14, No. 5, 780-799 (1996)

[4] H. Takahashi, K. Oda and H. Toba, "Impact of Crosstalk in an Arrayed-Waveguide Multiplexer on NxN Optical Interconnection", Journal of Lightwave Technology, Vol. 14, No. 6, 1097-1104 (1996)

[5] D. J. Blumenthal, P. Granestrand and L. Thylen, "BER Floors due to Heterodyne Coherent Crosstalk in Space Photonic Switches for WDM Networks", IEEE Photonics Technology Letters, Vol. 8, No. 2, 284-286 (1996)

[6] E. L. Goldstein, L. Eskildsen and A. F. Elrefaie, "Performance Implications of Component Crosstalk in Transparent Lightwave Networks", IEEE Photonics Technology Letters, Vol. 6, No. 5, 657-660 (1994)

[7] E. L. Goldstein and L. Eskildsen, "Scaling Limitations in Transparent Optical Networks Due to Low-Level Crosstalk", IEEE Photonics Technology Letters, Vol. 7, No. 1, 93-94 (1995)

[8] C. Li and F. Tong, "Crosstalk and Interference Penalty in All-Optical Networks Using Static Wavelength Routers", Journal of Lightwave Technology, Vol. 14, No. 6, 1120-1126 (1996)

[9] E. L. Goldstein, L. Eskildsen, C. Lin and Y. Silberberg "Polarization Statistics of Crosstalk-Induced Noise in Transparent Lightwave Networks", IEEE Photonics Technology Letters, Vol. 7, No. 11, 1345-1347 (1995)

[10] C. Saxtorf and P. Chidgey, "Error Rate Degradation Due to Switch Crosstalk in Largew Modulator Switched Optical Networks", IEEE Photonics Technology Letters, Vol. 5, No. 7, 828-831 (1993)

[11] K. Inoue, "Crosstalk and Its Power Penalty in Multichannel Transmission Due to Gain Saturation in a Semiconductor Laser Amplifier", Journal of Lightwave Technology, Vol. 7, No. 7, 1118-1123 (1989)

[12] G. Jeong and J. W. Goodman, "Analysis of Crosstalk in Photonic Crossbar Switches Based on On/Off Gates", Journal of Lightwave Technology, Vol. 14, No. 3, 359-364 (1996)

[13] P. E. Green, "Fiber Optic Networks", Prentice Hall, New Jersey (1995)

[14] R. G. Gallager, "Discrete Stochastic Processes", Kluwer Academic Publishers, Massachusetts (1995)

[15] J. Zhou, R. Cadeddu, E. Casaccia, C. Cavazzoni and M. J. O'Mahony, "Crosstalk in Multiwavelength Optical Cross-Connect Networks", Journal of Lightwave Technology, Vol. 14, No. 6, 1423-1435 (1996)

[16] M. Tur and E. L. Goldstein, "Dependence of Error Rate on Signal to Noise Ratio in Fiber Optic Communication Systems with Phase-Induced Intensity Noise", Journal of Lightwave Technology, Vol. 7, No. 12, 2055-2057 (1989)

[17] M. Tur and E. L. Goldstein, "Probability Distribution of Phase-Induced Intensity Noise Generated by Distributed Feedback Lasers", Optics Letters, Vol. 15, No. 1, 1-3 (1990)

[18] P. S. Kumar and S. Roy, "Optimization for Crosstalk Suppression with Noncoordinating Users", IEEE Transactions on Communications, Vol. 44, No. 7, 894-905 (1996)

[19] Y. Sanada and Q. Wang, "A Co-Channel Interference Technique Using Orthogonal Convolutional Codes", IEEE Transactions on Communications, Vol. 44, No. 5, 549-556 (1996)

[20] Y. Sanada and M. Nakagawa, "A Multiuser Interference Technique Utilizing Convolutional Codes and Orthogonal Multicarrier Modulation for Wireless Indoor Communications", IEEE Journals on Selected Areas in Communications, Vol. 14, No. 8, 1500-1509 (1996)

[21] M. L. Honig, P. Crespo and K. Steiglitz, "Suppression of Near and Far End Crosstalk by Linear Pre and Post Filtering", IEEE Journals on Selected Areas in Communications, Vol. 10, No. 3, 614-628 (1992)

[22] S. Haykin, "Communication Systems", third edition, John Wiley & Sons, Inc. (1994), (4.71), 247

[23] G. Keiser, "Optical Fiber Communication", second edition, Mcgraw-Hill Inc. (1991), (6.17), 247

[24] D. Forney, "Lecture Notes of Principles of Communication"

[25] L. Moura, N. Karafolas, P. Lane, A. Hill and J. O'Reilly, "Modelling of Interferometric Crosstalk in Optical Networks", GLOBECOM 96, 333 (1996)